

RESEARCH REPORT

IDAHO TRANSPORTATION DEPARTMENT



**Your Safety • Your Mobility  
Your Economic Opportunity**

**RP 266**

## **Evaluation of Skid Resistance of Idaho Pavements at Different Speeds**

By  
Emad Kassem  
Richard Nielsen  
Simpson Lamichhane  
Mohammad Al-Assi

University of Idaho

Prepared for  
Idaho Transportation Department  
Research Program, Contracting Services  
Highways Construction and Operations

August 2019

### **Standard Disclaimer**

This document is disseminated under the sponsorship of the Idaho Transportation Department and the United States Department of Transportation in the interest of information exchange. The State of Idaho and the United States Government assume no liability of its contents or use thereof.

The contents of this report reflect the view of the authors, who are responsible for the facts and accuracy of the data presented herein. The contents do not necessarily reflect the official policies of the Idaho Transportation Department or the United States Department of Transportation.

The State of Idaho and the United States Government do not endorse products or manufacturers.

Trademarks or manufacturers' names appear herein only because they are considered essential to the object of this document.

***This report does not constitute a standard, specification or regulation***

1. Report No. FHWA-ID-19-266	2. Government Accession No.	3. Recipient's Catalog No.	
4. Title and Subtitle  Evaluation of Skid Resistance of Idaho Pavements at Different Speeds		5. Report Date August 2019	6. Performing Organization Code
7. Author(s) (LIST ALL AUTHORS- erase this phrase before final) Emad Kassem, Richard Nielsen, Simpson Lamichhane, and Mohammad Al-Assi		8. Performing Organization Report No.	
9. Performing Organization Name and Address  University of Idaho 875 Perimeter Drive MS 1022, Moscow, ID 83844-1022		10. Work Unit No. (TRAIS)	11. Contract or Grant No. UI-17-03
12. Sponsoring Agency Name and Address  Idaho Transportation Department (SPR) Division of Highways, Resource Center, Research Program PO Box 7129 Boise, ID 83707-7129		13. Type of Report and Period Covered  Final Report	14. Sponsoring Agency Code RP 266
15. Supplementary Notes  Project performed in cooperation with the Idaho Transportation and the U.S. Department of Transportation, Federal Highway Administration.			
16. Abstract  Adequate skid resistance is essential component of road safety. Various transportation agencies measure the skid number using a locked-wheel skid trailer at a reference speed (e.g., 40 mph). In many cases the skid number is measured at lower speeds due to state speed limits, geometry of roads and size of skid truck. It is well established that the skid number decreases with speed. In addition, several interstates in Idaho have a speed limit up to 80 mph while the skid number is still measured at 40 mph; potentially unsafe for the operators and motoring public. This study aimed to develop a method that can be used to convert the skid number collected at any speed between 20 mph and 60 mph to the corresponding skid number at a reference speed.  The researchers measured the frictional characteristics of various pavement sections including hot mix asphalt, seal coat, and concrete. The skid number was measured at five different speeds (e.g., 20, 30, 40, 50, and 60 mph) using a locked wheel skid trailer with smooth tire. The macrotexture of test sections was measured using a laser profiler and sand patch test while a dynamic friction tester was used to measure the microtexture. The researchers developed a statistical-based model to describe the change in skid number with speed. The model utilizes the mean profile depth data and skid number measurements at a given speed and calculates the skid number at a reference speed specified by the user. The predicted skid number values correlated well with the measured ones. The model was further validated with skid data from additional eight test sites that were not used in the model development. In addition, the researchers developed an Excel-based utility software to facilitate the process of analyzing the friction and texture data collected using the ITD pavement friction tester and calculating the skid number at a reference speed.			
17. Key Words Skid resistance, skid number, pavements, microtexture, macrotexture, skid truck, mean profile depth		18. Distribution Statement Copies available online at: <a href="#">ITD Research Program Website</a>	
19. Security Classification (of this report) Unclassified	20. Security Classification (of this page) Unclassified	21. No. of Pages 142	22. Price None

**FHWA Form F 1700.7**

## METRIC (SI\*) CONVERSION FACTORS

APPROXIMATE CONVERSIONS TO SI UNITS					APPROXIMATE CONVERSIONS FROM SI UNITS				
Symbol	When You Know	Multiply By	To Find	Symbol	Symbol	When You Know	Multiply By	To Find	Symbol
<u>LENGTH</u>					<u>LENGTH</u>				
in	inches	25.4	millimeters	mm	mm	millimeters	0.039	inches	in
ft	feet	0.3048	meters	m	m	meters	3.28	feet	ft
yd	yards	0.914	meters	m	m	meters	1.09	yards	yd
mi	Miles (statute)	1.61	kilometers	km	km	kilometers	0.621	Miles (statute)	mi
<u>AREA</u>					<u>AREA</u>				
in <sup>2</sup>	square inches	645.2	millimeters squared	cm <sup>2</sup>	mm <sup>2</sup>	millimeters squared	0.0016	square inches	in <sup>2</sup>
ft <sup>2</sup>	square feet	0.0929	meters squared	m <sup>2</sup>	m <sup>2</sup>	meters squared	10.764	square feet	ft <sup>2</sup>
yd <sup>2</sup>	square yards	0.836	meters squared	m <sup>2</sup>	km <sup>2</sup>	kilometers squared	0.39	square miles	mi <sup>2</sup>
mi <sup>2</sup>	square miles	2.59	kilometers squared	km <sup>2</sup>	ha	hectares (10,000 m <sup>2</sup> )	2.471	acres	ac
ac	acres	0.4046	hectares	ha	<u>MASS (weight)</u>				
oz	Ounces (avdp)	28.35	grams	g	g	grams	0.0353	Ounces (avdp)	oz
lb	Pounds (avdp)	0.454	kilograms	kg	kg	kilograms	2.205	Pounds (avdp)	lb
T	Short tons (2000 lb)	0.907	megagrams	mg	mg	megagrams (1000 kg)	1.103	short tons	T
<u>VOLUME</u>					<u>VOLUME</u>				
fl oz	fluid ounces (US)	29.57	milliliters	mL	mL	milliliters	0.034	fluid ounces (US)	fl oz
gal	Gallons (liq)	3.785	liters	liters	liters	liters	0.264	Gallons (liq)	gal
ft <sup>3</sup>	cubic feet	0.0283	meters cubed	m <sup>3</sup>	m <sup>3</sup>	meters cubed	35.315	cubic feet	ft <sup>3</sup>
yd <sup>3</sup>	cubic yards	0.765	meters cubed	m <sup>3</sup>	m <sup>3</sup>	meters cubed	1.308	cubic yards	yd <sup>3</sup>
Note: Volumes greater than 1000 L shall be shown in m <sup>3</sup>									
<u>TEMPERATURE (exact)</u>					<u>TEMPERATURE (exact)</u>				
°F	Fahrenheit temperature	5/9 (°F-32)	Celsius temperature	°C	°C	Celsius temperature	9/5 °C+32	Fahrenheit temperature	°F
<u>ILLUMINATION</u>									
fc	Foot-candles	10.76	lux	lx	lx	lux	0.0929	foot-candles	fc
fl	foot-lamberts	3.426	candela/m <sup>2</sup>	cd/cm <sup>2</sup>	cd/cm <sup>2</sup>	candela/m <sup>2</sup>	0.2919	foot-lamberts	fl
<u>FORCE and PRESSURE or STRESS</u>					<u>FORCE and PRESSURE or STRESS</u>				
lbf	pound-force	4.45	newtons	N	N	newtons	0.225	pound-force	lbf
psi	pound-force per square inch	6.89	kilopascals	kPa	kPa	kilopascals	0.145	pound-force per square inch	psi

---

## Acknowledgements

This project is funded by Idaho Transportation Department (ITD) from SPR funds. It is performed in cooperation with ITD. The authors would like to acknowledge all members of the research project Technical Advisory Committee (TAC) for their valuable feedback and cooperation all over the project tasks. The authors would like also to acknowledge support from the National Institute for Advanced Transportation Technology (NIATT) and the Department of Civil and Environmental Engineering at the University of Idaho.

## Technical Advisory Committee

Each research project is overseen by a technical advisory committee (TAC), which is led by an ITD project sponsor and project manager. The Technical Advisory Committee (TAC) is responsible for monitoring project progress, reviewing deliverables, ensuring that study objective are met, and facilitating implementation of research recommendations, as appropriate. ITD's Research Program Manager appreciates the work of the following TAC members in guiding this research study.

**Project Sponsor** – Mark Snyder, P.E.

**Project Manager** – James Poorbaugh, P.E.

**TAC Members:**

Trek Pallister, Jack Long, Chad Clawson, Jeff Drager, Kevin K. McGhee, Brian L. Schleppi, and Shuo Li

**FHWA-Idaho Advisor** – Kyle Holman, P.E.



---

# Table of Contents

Acknowledgements.....	iii
Table of Contents.....	v
List of Tables .....	ix
List of Figures .....	xi
Executive Summary.....	xiii
Chapter 1 Introduction.....	1
Background .....	1
Problem Statement.....	2
Research Objectives.....	2
Research Tasks .....	2
Task 1: Literature Review.....	2
Task 2: Identify and Select Pavement Sites for Evaluation .....	3
Task 3: Measure Skid Number at Different Speeds .....	3
Task 4: Measure the Surface Friction Characteristics .....	3
Task 5: Analyze Collected Data .....	3
Task 6: Establish Correlations at Different Speeds .....	4
Report Organization.....	4
Chapter 2 Literature Review .....	5
Introduction .....	5
Skid Resistance.....	5
Factors Affecting Skid Resistance of Pavements .....	6
Pavement Texture.....	7
Traffic .....	9
Slip Speed or Slip Ratio .....	10
Tire Properties.....	11
Temperature .....	11
Presence of Water .....	12
Speed .....	13
Characterization of Surface Frictional Characteristics.....	13
Locked-Wheel Devices .....	13
Side Force Devices .....	13
Fixed Slip Devices .....	14
Variable Slip Devices .....	14
British Pendulum Tester (BPT) .....	14
Dynamic Friction Tester (DFT).....	15
Circular Texture Meter.....	15
Laser Profiler .....	16
Volumetric Method.....	16
Current Practice in Measuring Skid Number .....	17
Relation between Skid Resistance and Speed .....	18
Corsello (1993).....	18
Rizenbergs et al. (1973) .....	18

---

Penn State Model.....	19
Kulakowski (1991) .....	19
Jackson (2008).....	21
Flintsch et al. (2010).....	23
Chapter 3 Selection of Test Sections and Field Testing .....	25
Introduction .....	25
Skid Number Measurements .....	29
Measurement of Surface Texture Characteristics .....	30
Measurement Using Dynamic Friction Tester (DFT).....	31
Surface Macrotexture Measurements Using Sand Patch Test .....	32
Surface Macrotexture Measurements Using Laser Profiler.....	33
Chapter 4 Results and Discussion .....	35
Introduction .....	35
Distribution of Skid Number and MPD of The Test Sites .....	35
Effect of Pavement Surface on Friction Characteristics.....	38
Variation of Skid Number Measurements .....	40
Correlation Between Friction, Speed and Texture .....	42
Development of Prediction Model .....	48
Model Validation.....	53
Individual Prediction Models .....	54
Model for Seal Coat Surface .....	55
Model for HMA Pavements .....	56
Model for Concrete Pavements.....	57
Comparison between Models.....	58
Sensitivity Analysis of the Model .....	58
Development of Alternative Approach.....	61
Chapter 5 Development of Skid Prediction Software .....	67
Overview .....	67
Single Test Site .....	68
Command Buttons .....	69
Software Outputs.....	69
Multiple Test Site .....	70
Chapter 6 Conclusions and Recommendations .....	73
Summary.....	73
Findings .....	74
Skid and Texture Data Analysis .....	74
Development of Skid Prediction Model .....	75
Development of a Skid Prediction Software .....	75
Recommendations for Future Research .....	76
References .....	77
Appendix A Test Data.....	81
Appendix B Data for Model Development and Validation .....	87

---

Appendix C Relation between SN And MPD .....	95
HMA Sections.....	95
Seal Coat Sections.....	98
Appendix D Relation Between Skid Number (SN) And DFT <sub>20</sub> .....	101
Appendix E Skid Software Examples .....	105



---

## List of Tables

<b>Table 1. Factors Affecting Skid Resistance of Pavements<sup>6</sup> .....</b>	6
<b>Table 2. Skid Number Adjustment Factors Constants at Various Test Speeds<sup>48</sup> .....</b>	17
Table 3. Statistical Data Related to Ribbed Tire Locked Wheel Speed Gradient <sup>55</sup> .....	21
<b>Table 4. List of Test Sections .....</b>	26
Table 5. Model Statistical Parameters .....	49
Table 6. VIF Values for the Independent Variables in the Model .....	51
Table 7. Statistical Parameters for Individual and General Model .....	58
<b>Table 8. Command Buttons and Their Function .....</b>	69
<b>Table 9. Single Test Site Mode Outputs.....</b>	70

---

---

## List of Figures

<b>Figure 1. Diagrammatic Representation of Friction Force on a Moving Body<sup>2</sup></b> .....	5
<b>Figure 2. Friction Values on a Dense Graded Plant-Mix Asphaltic Surface<sup>15</sup></b> .....	6
<b>Figure 3. Classification of Pavement Surface Texture<sup>11</sup></b> .....	7
Figure 4. Components of Tire Pavement Friction <sup>3</sup> .....	8
<b>Figure 5. Variation of Adhesion and Hysteresis Friction with the Speed<sup>15</sup></b> .....	8
<b>Figure 6. Loss of Skid Resistance Due to Traffic (Reproduced After Shahin 1994)<sup>15</sup></b> .....	9
<b>Figure 7. IFI Versus Polishing Cycles for Limestone Asphalt Mixtures (After Kassem et al. 2013)<sup>12</sup></b> .....	10
<b>Figure 8. Variation of Pavement Friction with Tire Slip<sup>19</sup></b> .....	11
<b>Figure 9. Effect of Water Film on Pavement Friction<sup>19</sup></b> .....	12
<b>Figure 10. (a) DFT device; (b) Bottom of the DFT with three rubber sliders</b> .....	15
Figure 11. Relationship between CTMeter and Sand Patch From NCAT Test Track <sup>44</sup> .....	16
Figure 12. Leu and Henry Model for Skid Number Calculation .....	19
Figure 13. Pennsylvania State University Model for Skid Resistance .....	19
Figure 14. Leu and Henry Alternative Model.....	19
Figure 15. Kulakowski Modification of Pennsylvania State University Model.....	20
Figure 16. Equation for Speed Constant as Defined by Kulakowski (1991) .....	20
Figure 17. Equation for $V_0$ Calculation in Direct Method.....	20
Figure 18. Equation for $SN_0$ Calculation in Direct Method .....	20
Figure 19. Equation for $SN_0$ Calculation in Indirect Method.....	20
Figure 20. Equation for PNG Calculation in Indirect Method .....	20
Figure 21. Plot of Speed Gradient Vs. MPD for Smooth Tire <sup>55</sup> .....	22
Figure 22. Plot of Speed Gradient Vs. MPD for Ribbed Tire <sup>55</sup> .....	22
Figure 23. Sample Skid Testing Results for Two Sections of the Virginia Smart Road <sup>56</sup> .....	23
Figure 24. Speed Adjustment Factor Equation .....	24
Figure 25. Equation to Calculate Skid Number Based on Skid Adjustment Factor .....	24
Figure 26. Locations of the Selected Test Sections in the State of Idaho .....	27
Figure 27. Test Section Distribution by Pavement Surface Type .....	28
Figure 28. Test Section Distribution by District .....	28
Figure 29. Test Section Distribution by Highway .....	29
<b>Figure 30. ITD Locked Wheel Skid Trailer</b> .....	30
<b>Figure 31. Schematic for Locations of DFT and Sand Patch Measurements</b> .....	31
<b>Figure 32. Measurement of Microtexture Using DFT Device</b> .....	31
<b>Figure 33. Coefficient of Friction Measurements by DFT Software</b> .....	32
<b>Figure 34. Sand Patch Test Measurements</b> .....	33
<b>Figure 35. Measurement of MPD Using Laser Profiler</b> .....	33
<b>Figure 36. Examples of Field Testing</b> .....	34
Figure 37. Skid Number Values at 40 mph for All Test Sections .....	36
Figure 38. Distribution of Skid Number Measurements .....	36
Figure 39. MPD Values for All Test Sections .....	37
Figure 40. Distribution of MPD Measurements .....	37

---

Figure 41. Average Skid Number at 40 Mph for Various Pavement Surfaces .....	38
Figure 42. Average MPD for Various Pavement Surfaces .....	39
Figure 43. Average DFT <sub>20</sub> Values for Various Pavement Surfaces .....	39
Figure 44. Distribution of Standard Deviation of Skid Number at 40 mph.....	40
Figure 45. Standard Deviation of Measured Skid Number at 40 mph vs. Speed and MPD .....	41
Figure 46. Skid Number vs. Speed for HMA Test Sections.....	43
Figure 47. Skid Number vs. Speed for Seal Coat Test Sections.....	44
Figure 48. Skid Number vs. Speed for Concrete Test Sections .....	45
Figure 49. Relation of Skid Number Speed Gradient ( $G_V$ ) with Macrotexture .....	46
Figure 50. Relationship between Mean Texture Depth and Mean Profile Depth .....	46
Figure 51. Skid Number at 60 mph Expressed as a Logarithm of Mean Profile Depth (HMA Sections)....	47
Figure 52. Skid Number at 20 Mph vs. DFT <sub>20</sub> .....	47
Figure 53. General Prediction Model Equation .....	48
Figure 54. Predicted vs. Measured Skid Number (SN) .....	49
<b>Figure 55. Plot of Residuals vs. Fitted Data .....</b>	50
<b>Figure 56. Normal Probability Plot for the Prediction Model.....</b>	51
<b>Figure 57. Standardized Residual Plot for the Prediction Model .....</b>	52
<b>Figure 58. Plot of Residual vs. Leverage for the Prediction Model .....</b>	52
Figure 59. Distribution of SN for Test Sections Selected for Validation .....	53
Figure 60. Predicted vs. Measured SN (Model Validation) .....	54
Figure 61. Prediction Model Equation for Seal Coat Surfaces .....	55
Figure 62. Seal Coat Skid Model.....	55
Figure 63. Prediction Model Equation for HMA Surfaces .....	56
Figure 64. HMA Skid Model .....	56
Figure 65. Prediction Model Equation for Concrete Surfaces .....	57
Figure 66. Concrete Skid Model.....	57
Figure 67. Change in Predicted Skid Number with Velocity Ratio and Mean Profile Depth .....	59
Figure 68. Change in Predicted Skid Number with Velocity Ratio and Measured Skid Number .....	60
Figure 69. Change in Predicted Skid Number with Measured Skid Number and Mean Profile Depth (Note: The Velocity Ratio is Maintained Constant at 1.5).....	61
Figure 70. Change of SN with Speed for Sections with Low and High Macrotexture.....	62
Figure 71. Typical Change of Measured SN with Speed for Test Sections with Lower and Higher Microtexture. ....	63
Figure 72. Model for Alternative Approach of Skid Number Prediction .....	63
Figure 73. Relationship between Measured and Calculated Skid Number at Different Speeds .....	64
Figure 74. Diagnostic Check of the Normality of the Developed Model .....	65
<b>Figure 75. Skid Prediction Software Interface.....</b>	67
<b>Figure 76. Interface of the Single Test Site Mode .....</b>	68
<b>Figure 77. Interface of the Multiple Test Sites Mode .....</b>	71
<b>Figure 78. Typical Input File (SN) for the Software Obtained from Skid Truck .....</b>	72
Figure 79. Output of the Multiple Test Site Mode.....	72

## Executive Summary

The Idaho Transportation Department (ITD) measures skid number at 40 mph to ensure adequate friction level for pavements in Idaho. Since the skid number changes with the testing speed, it is important to collect the skid number measurements at a reference speed (e.g., 40 mph). However, field conditions may not permit the collection of skid resistance at the reference speed. This study aimed to develop a method that can be used to convert the skid number collected at any speed between 20 mph and 60 mph to the corresponding skid number at a reference speed.

The researchers measured the frictional characteristics of 34 various pavement sections in all six districts of Idaho. Of the total 34 sections, 11 were hot mix asphalt, 18 were seal coat, and 5 of them were concrete. The skid number was measured at five different speeds (e.g., 20, 30, 40, 50, and 60 mph) using the ITD 1295 Locked Wheel Friction Testing Trailer manufactured by Dynatest. The test was conducted in accordance with ASTM E274 using a smooth tire. The researchers measured the surface macrotexture in terms of mean profile depth (MPD) and mean texture depth (MTD) of the pavement surface. The MPD was measured using a laser profiler attached to the Locked Wheel Friction Testing Trailer, while the MTD was measured using the sand patch test. The microtexture was quantified indirectly by measuring the coefficient of friction at 20 km/hr ( $DFT_{20}$ ) using a portable dynamic friction tester (DFT). The results demonstrated that there is a logarithmic relationship between measured skid number and testing speed. The skid number decreased with the testing speed and the rate was found to be a function of pavement surface macrotexture. A very good correlation was obtained between the MPD measured using laser profiler and MTD obtained from the sand patch test. The MPD was selected as a representation of surface macrotexture as it can be measured simultaneously with the skid number and does not require traffic control.

Based on the collected data in this study, the researchers performed a regression analysis and developed a statistical based model to describe the change in skid number with speed. The model utilizes the MPD data and skid number measurements at a given speed to calculate the skid number at a reference speed specified by the user. Pavement microtexture ( $DFT_{20}$ ) was found to be insignificant in predicting skid number. The microtexture mostly governs the magnitude of pavement friction which is incorporated in the measured skid number used in the model. Furthermore, previous research studies demonstrate that change in skid with speed is influenced by the macrotexture or MPD and not microtexture.

The results demonstrated that the predicted skid number values from the model correlated well with the measured ones. The researchers performed several statistical checks to ensure that the developed model is unbiased and satisfies the assumptions of regression analysis. The model was further validated with skid data from additional eight test sites that were not used in the model development. Good correlation was also found between the measured and predicted skid numbers for the validation sites.

---

The researchers developed an Excel-based utility that can be used to import the skid measurements and texture data collected by the ITD pavement friction tester and use the statistical model to calculate the skid number at a reference speed. The outcome of this study shall assist ITD pavement engineers to collect skid measurements at a safe speed (i.e., lower than 40 mph) when field conditions do not allow data collection at the standard test speed (i.e., 40 mph). In addition, some interstate highways have posted speed limit up to 80 mph and the skid measurements are still collected at 40 mph which impose hazard to motorists. The skid number can be collected at higher speed (e.g., 60 mph) and converted to the corresponding values at a reference speed (e.g., 40 mph). Such practice would improve the safety of the ITD skid crew and motorists. In addition, it can expedite the data collection since the skid can be collected at higher speeds especially on interstate highways.

# Chapter 1

## Introduction

### Background

Skid resistance is a major component of road safety.<sup>1</sup> Skid resistance is defined as the traction force generated between pavement surface and tires as they slide or roll on pavement surface.<sup>2</sup> The presence of water or other contaminants on pavement surface reduces skid resistance significantly since water acts as a lubricant.<sup>3</sup> Skid resistance of pavement is often used interchangeably with pavement friction and is expressed in terms of coefficient of friction, skid number, or friction number. The coefficient of friction is the ratio of tangential force developed between the tire and pavement surface and the normal force acting on the tire.<sup>4</sup> The skid number is a dimensionless value obtained by multiplying the coefficient of friction by 100.<sup>5</sup>

Various factors influence skid resistance of pavements including pavement texture, vehicle speed, slip ratio, tire properties, and environmental (e.g., temperature and presence of water).<sup>6</sup> Among all of these parameters, speed, texture and presence of water are found to be the most dominant factors controlling the friction between tire and pavement surface.<sup>1, 4, 7</sup> Friction decreases with speed due to the reduction in the true contact area between two surfaces and the time duration over which the two surfaces remain in contact.<sup>8</sup> Reduced contact area and duration of contact decrease the molecular bonding between the asperities and rubber tires leading to reduced adhesion and consequently lower friction.<sup>9, 10</sup> Therefore, satisfactory skid resistance at one speed may not be adequate at a higher speed.

Pavement friction is affected by surface microtexture and macrotexture.<sup>11</sup> Microtexture is a function of the roughness of aggregate particles, and it changes during the life of the pavement due to polishing and abrasion under traffic loading. Changes in microtexture depend highly on aggregate quality and its resistance to polishing and abrasion.<sup>12</sup> The macrotexture is a function of the overall irregularities of pavement surface and depends on aggregate gradation. Skid resistance at lower speed and dry conditions is affected mostly by the microtexture whereas the macrotexture is the governing factor at higher speed and wet conditions.

There are two main components of friction; adhesion and hysteresis.<sup>3</sup> The adhesion friction is a result of formation molecular bond between pavement surface and rubber. The hysteresis friction is developed due to energy dissipation caused by the deformation of tire rubber around bulges and depressions in the pavement surface. The tire is in compression when approaching the irregularities of the pavement surface and decompresses when leaving it. The hysteresis component of pavement friction is dominant at higher traveling speeds and wet pavement conditions, while the adhesion component is dominant at lower speeds and dry contact conditions.<sup>2</sup>

## **Problem Statement**

Pavement engineers use the measured skid number to determine if a treatment should be applied to improve surface friction. The current practice in Idaho and several other transportation agencies is to measure the skid number using a locked wheel friction testing trailer. The left wheel of the friction testing trailer is locked and dragged on the surface to measure the skid number at a reference speed (e.g., 40, 50 mph) depending on state specifications. In many cases the skid number is measured at lower speeds due to state speed limits, geometry of roads and size of skid truck. Although the data collection at lower speeds is necessary for safe operation, the data cannot be used in confidence for roadways with higher speed limits. In addition, several interstates in Idaho have speed limits up to 80 mph while the skid number is still measured at 40 mph, which is potentially unsafe for the operators and for motorists. Therefore, there is a need to investigate and develop correlations between skid numbers at lower speeds and higher speeds. Such correlations can be used to predict skid number at a reference speed.

## **Research Objectives**

This study had the following objectives:

- Examine the correlation between skid number and speed (e.g., 20, 30, 40, 50, and 60 mph) for various pavement surfaces in Idaho including flexible pavements, rigid pavements, and seal coat or chip seal surfaces.
- Investigate the effect of pavement characteristics (e.g., microtexture and macrotexture) on the measured skid number and its change with speed.
- Develop a statistical model to describe the change in skid number with speed and predict skid number at a reference speed using measured skid number at other testing speeds and pavement texture information.
- Develop a software utility that can be used by operators to easily convert skid number measurements at different speeds.

## **Research Tasks**

Several tasks were performed to achieve the above-mentioned research objectives. All the tasks performed in the study are listed and described in the following section.

### **Task 1: Literature Review**

The objective of this task was to conduct a comprehensive literature review on various aspects of skid resistance measurements and prediction. The main subjects of the literature review were as follows:

- Factors that affect the skid number of flexible and rigid pavements.
- Test methods used to measure the surface frictional characteristics of pavements including macrotexture and microtexture.

- Relationships between skid number and speed of skid trailer.
- Correlations of skid number at different speeds (e.g., 20 mph to 60 mph) to a reference speed (e.g., 40mph).
- Current practice followed by transportation agencies in measuring skid number at different speeds (e.g., 50 mph).

### **Task 2: Identify and Select Pavement Sites for Evaluation**

Under this task, several test sections were identified and selected across Idaho. The objective of this task was to select sections with different characteristics to represent various pavement types and conditions in Idaho. The test sections were distributed across the six districts in Idaho and included different pavement surfaces (e.g., seal coat, HMA, and concrete). The pavement sections had different mix design, aggregate type, skid number, traffic level, and age.

### **Task 3: Measure Skid Number at Different Speeds**

Under this task, the ITD crew, in coordination with UI research team, measured the skid number of the selected test sections at different speeds (e.g., 20, 30, 40, 50, and 60 mph). The ITD crew used the Dynatest 1295 Locked Wheel Friction Testing Trailer with a smooth tire. During this test, the left wheel of the friction testing trailer is locked to measure the skid number at the wheel path of the outside lane. The test was conducted according to ASTM E274 “Standard Test Method for Skid Resistance of Paved Surfaces Using a Full-Scale Tire”. The common practice in Idaho is to measure the skid number at a reference speed of 40 mph.

### **Task 4: Measure the Surface Friction Characteristics**

The researchers used the Dynamic Friction Tester (DFT) to measure the coefficient of friction of pavement surface. The coefficient of friction measured using DFT at 20 km/hr ( $DFT_{20}$ ).  $DFT_{20}$  is often used as an indirect measure of surface microtexture. The sand patch test was performed to measure of the surface macrotexture in terms of mean texture depth. In addition, the skid trailer is equipped with a laser sensor that measures the mean profile depth. High mean profile indicates coarse surfaces while low mean profile depth indicates fine surfaces.

### **Task 5: Analyze Collected Data**

The collected data under Task 4 including skid number at different speeds, microtexture (measured using the DFT), and macrotexture (measured using the sand patch test and laser profiler) of pavement surface were analyzed.

The main objective of this task was to investigate and establish correlation between skid number and speed. In addition, statistical analysis was conducted to examine the effect of macrotexture and microtexture on the change of skid number with speed.

### **Task 6: Establish Correlations at Different Speeds**

In this task, statistical data analyses were performed to develop a statistical-based model to estimate the skid number at a reference speed (e.g., 40 mph) using skid number measurements at other speeds and pavement texture information. In addition, the researchers developed an Excel-based application that can import the friction and texture data collected by the ITD pavement friction tester and calculate the skid number at a reference speed specified by the user. This utility summarizes the mathematical correlations developed in this study and makes the calculations easier for the users.

## **Report Organization**

This report consists of six chapters and six appendices.

Chapter 1 includes an introduction, problem statement, objectives, research tasks, and report organization. Chapter 2 provides the main findings of the literature review on factors that affect skid resistance, devices used to measure skid resistance in the field and laboratory, relationship between skid resistance and speed, and previous models used to predict skid number at different speeds. Chapter 3 provides information about the test sections examined in this study and data collected at the test sections. It also discusses the parameters considered when selecting the test sites, the distribution and type of the test sections. It presents the data collected in this study including skid number at various speeds using ITD locked wheel skid trailer, coefficient of friction using DFT, mean texture depth using sand patch test, and mean profile depth using the laser profiler.

Chapter 4 discusses the results of various tests and the correlation between skid number and speed. It presents the development of a statistical model to estimate the skid number at a reference speed using skid number measurements at other speeds and pavement texture. It also includes sensitivity analyses of the model parameters. Chapter 5 discusses the development of an Excel-based application that can be used to easily convert skid number measurements at different speeds as a function of pavement texture. Finally, Chapter 6 summarizes the main findings and conclusions of this study and provides recommendations for future research. The appendices provide additional information and figures that were cited and discussed in the report. It provides a summary of data collected during field testing including skid number and texture data.

## Chapter 2

# Literature Review

### Introduction

This chapter summarizes the main findings of previous studies on various aspects of skid resistance measurements and prediction. It provides introduction to skid resistance, discusses factors affecting skid resistance and practices followed by various transportation agencies in the United States for measuring skid resistance. It also discusses the relationship between skid resistance and speed and various statistical models used to describe the change in skid number with speed.

### Skid Resistance

Skid resistance is defined as the traction force generated between pavement surface and tires as they slide or roll on pavement surface (Figure 1).<sup>2</sup> Presence of water or other contaminants on pavement surface reduces skid resistance as water acts as lubricant reducing the friction significantly.<sup>3,13</sup> Water not only reduces the skid resistance but it also affects the change of skid resistance with speed. Moyer (1959) demonstrated that the change in skid with speed is significant in wet conditions compared to dry conditions as shown in Figure 2.<sup>14</sup>

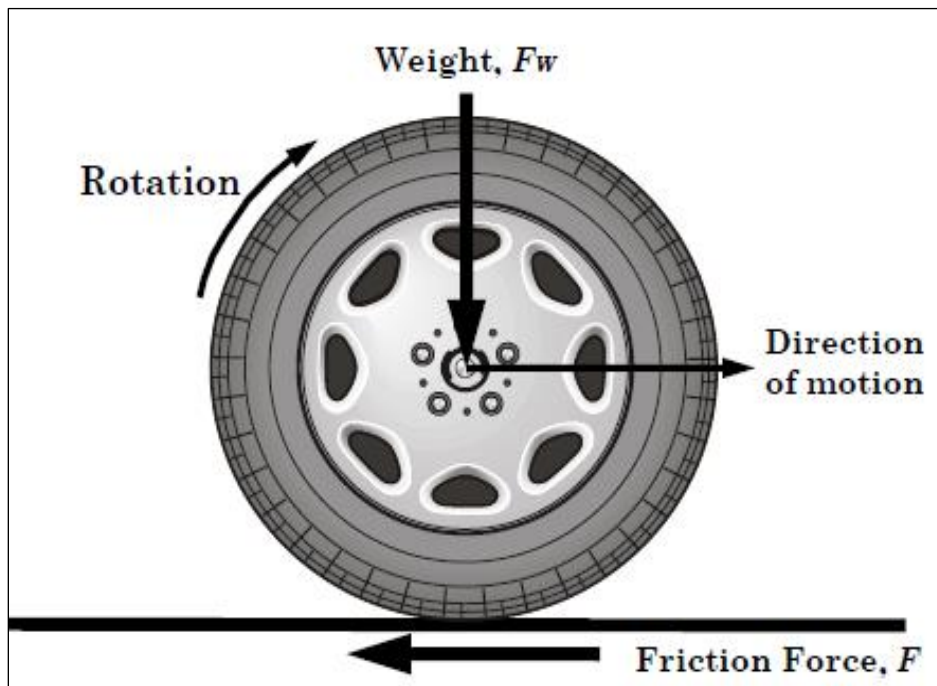
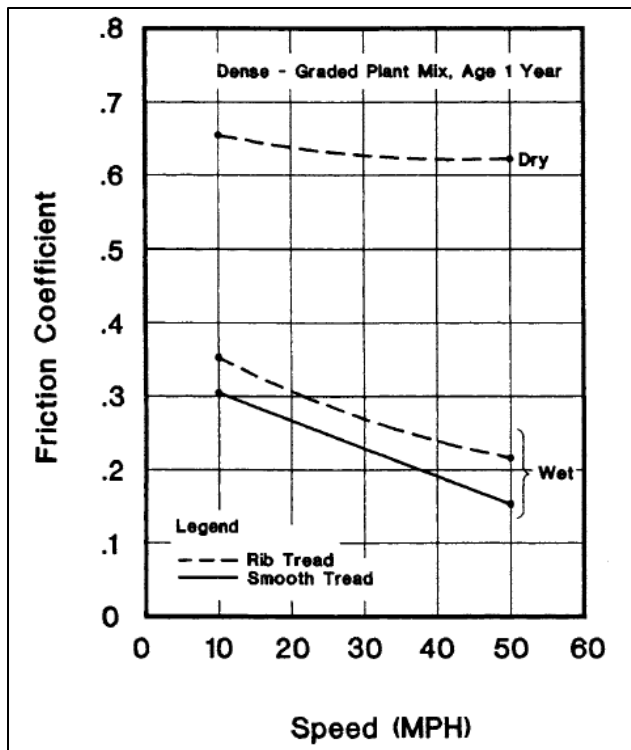


Figure 1. Diagrammatic Representation of Friction Force on a Moving Body<sup>2</sup>



**Figure 2. Friction Values on a Dense Graded Plant-Mix Asphaltic Surface<sup>15</sup>**

This section discusses various factors that play an important role in determining the magnitude of skid resistance of pavements. The major factors affecting the skid resistance include pavement texture, traffic, slip speed, tire properties, temperature, water and speed.

## Factors Affecting Skid Resistance of Pavements

There are several factors that affect the skid level of pavements. These factors include pavement texture, traffic level, slip speed, tire properties, temperature, presence of water and speed. Several studies were conducted to investigate these factors. Fuentes (2009) categorized these factors into four groups as presented in Table 1. Factors that have significant effect on skid resistance are briefly described in this section.<sup>6</sup>

**Table 1. Factors Affecting Skid Resistance of Pavements<sup>6</sup>**

Pavement Factors (Texture)	Vehicle Factors	Tire Factors	Environmental Factors
Microtexture	Vehicle slip ratio	Tire tread (pattern/depth)	Temperature
Macrotexture	Vehicle Speed	Tire pressure	Rainfall /Moisture

## Pavement Texture

The properties of pavement texture are directly related to its frictional properties.<sup>16</sup> Pavement texture is expressed as surface deviations from a true planar surface. It is classified by the World Road Association (PIARC 1987) based on the wavelength of the surface irregularities (Figure 3). Pavement texture is categorized into microtexture with wavelengths < 0.5 mm, macrotexture with wavelengths between 0.5 mm to 50 mm, and megatexture with wavelengths ranging from 50 mm to 500 mm. Pavement friction is affected mainly by the microtexture and macrotexture.<sup>11</sup> Microtexture refers to the roughness of individual particles forming the pavement, and it is dependent upon the characteristics of the aggregates or stones in the mixture. Pavement microtexture decreases over time due to polishing and abrasion caused by traffic. The rate of change in pavement microtexture depends on resistance of aggregates to abrasion and polishing.<sup>12</sup> Macrotexture is the overall irregularities in the pavement surface due to size, spacing or voids between aggregate particles. Macrotexture of the pavement surface is dependent on the aggregate gradation. Skid resistance at lower speed and dry conditions is affected mostly by the microtexture whereas the macrotexture is the governing factor at higher speed and wet conditions.<sup>13</sup>

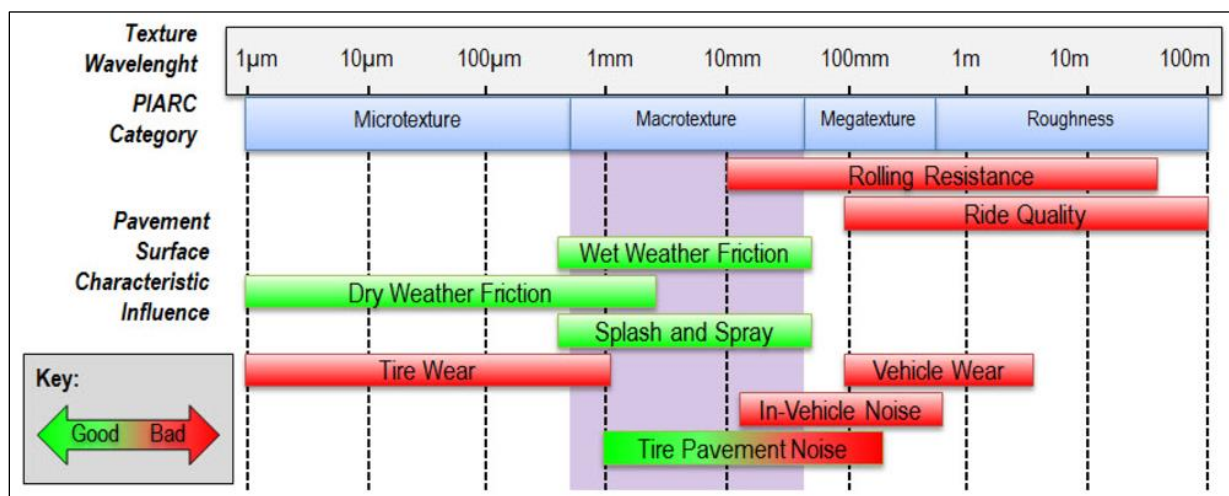


**Figure 3. Classification of Pavement Surface Texture<sup>11</sup>**

Adhesion and hysteresis friction are two main components of pavement surface friction (Figure 4).<sup>3</sup> Adhesion friction is a result of formation molecular bond between the pavement surface and tire, while hysteresis friction is the result of energy dissipation caused by the deformation of the tire rubber around bulges and depressions in the pavement surface.<sup>13</sup> Figure 5 demonstrates that the hysteresis friction is dominant at higher speed and wet pavement conditions, while the adhesion friction is dominant at lower speeds and dry contact conditions.<sup>2</sup>

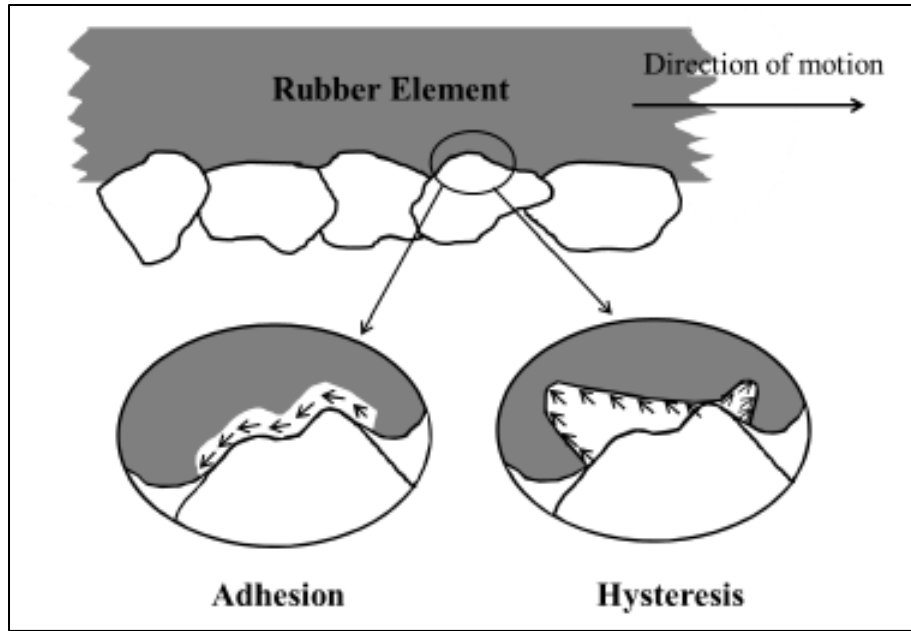


Figure 4. Components of Tire Pavement Friction<sup>3</sup>

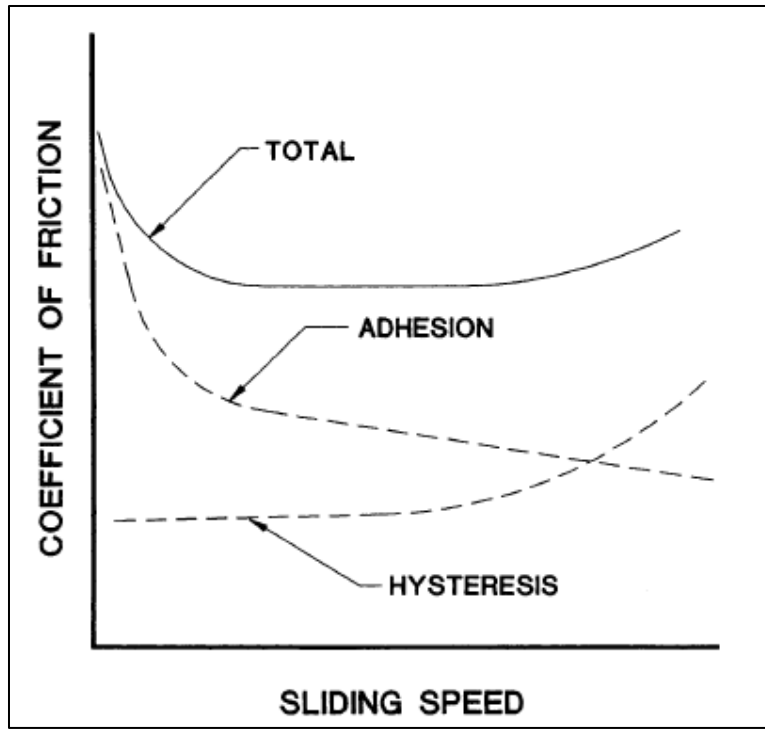


Figure 5. Variation of Adhesion and Hysteresis Friction with the Speed<sup>15</sup>

## Traffic

Skid resistance is greatly affected by traffic volume over time. Previous studies showed that pavement surface is polished under traffic which reduces the microtexture leading to decreased friction.<sup>12, 17</sup> Ragland *et al.* (2010) conducted a study which involved examining the effects of traffic and environment on skid resistance.<sup>18</sup> They used the data set containing more than 50,000 observations along five routes of freeway in seven districts in California and used the skid number at 40 mph (SN40) as a reference measure of skid resistance. The results showed that seasonal conditions and temperature to have significant influence on skid resistance. They found that the skid number decreases considerably with the increase in average daily traffic (ADT). The National Cooperative Highway Research Program (NCHRP) synthesis of practices documented the effect of traffic volume on skid resistance. The volume of truck and passenger car daily volume was found to affect the side friction factor. Trucks were found to have significant effect on skid resistance compared to passenger cars.<sup>15</sup> Skid resistance decreases with traffic until it reaches a terminal value as shown in Figure 6. This terminal or minimum value depends on the aggregate properties and gradation.<sup>12</sup> The terminal value is higher for coarse graded mix such as Pavement Friction Course (PFC) and Stone Matrix Asphalt (SMA) compared to fine graded mix such as Type F and Type C (Figure 7). Asphalt mixtures prepared with aggregates that have rough texture and higher resistance to abrasion and polishing (e.g., sandstone) have better skid resistance compared to aggregates with smooth texture and less resistance to abrasion and polishing (e.g., limestone)<sup>12</sup>.

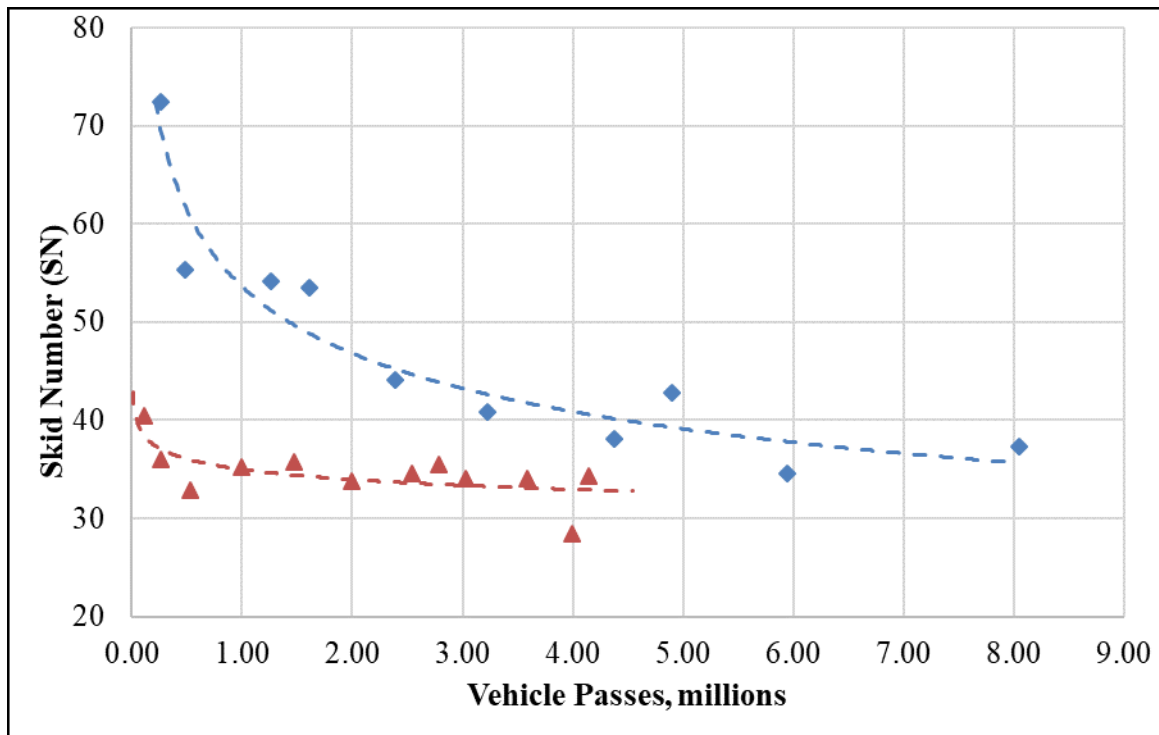
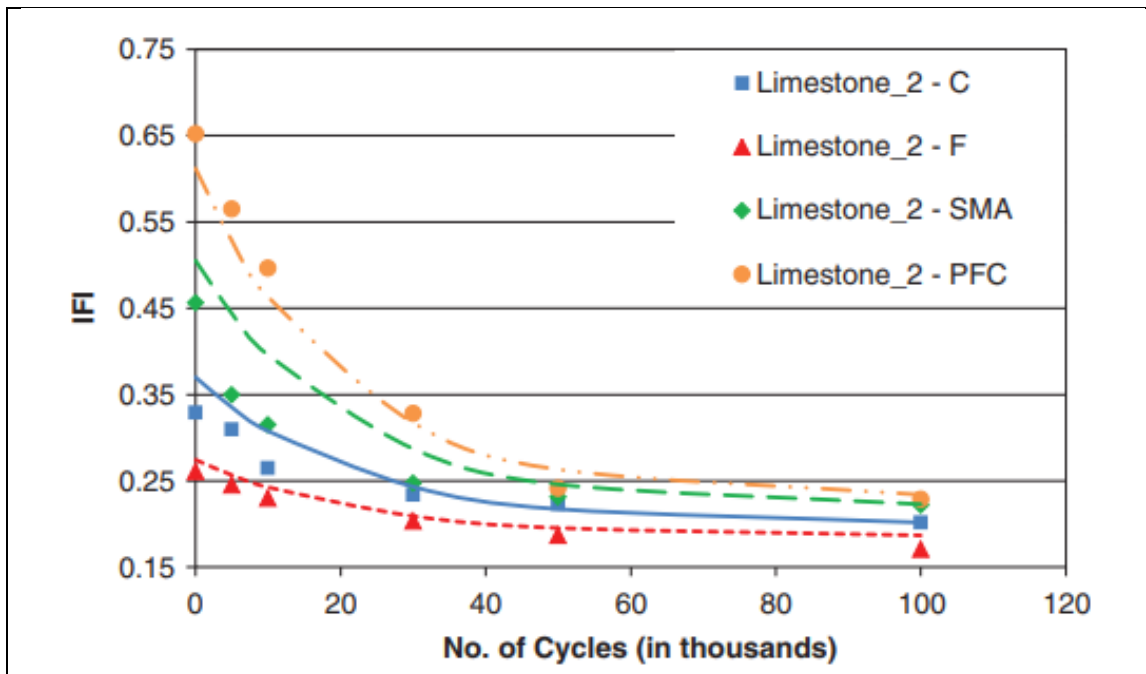


Figure 6. Loss of Skid Resistance Due to Traffic (Reproduced After Shahin 1994)<sup>15</sup>



**Figure 7. IFI Versus Polishing Cycles for Limestone Asphalt Mixtures (After Kassem *et al.* 2013)<sup>12</sup>**

#### Slip Speed or Slip Ratio

Slip speed or slip ratio is defined as the difference between the vehicle speed and actual tire rotational speed. Slip speed is equal to the vehicle speed and the slip ratio is 100 percent at fully locked conditions. The slip speed and ratio equal zero at free rolling conditions. The tire pavement friction varies with the variation in slip speed or slip ratio. There is a critical slip ratio at which the coefficient of friction is maximum. The friction increases with the increase in slip ratio until the critical slip ratio, then it decreases to an approximately constant value at 100 percent of slip as shown in Figure 8. The constant value of the friction is called coefficient of sliding friction. In general, the friction is highest at the slip ratio between 10 and 20 percent.<sup>2,19</sup> The reduction in coefficient of friction at critical slip condition to fully locked condition is about 50 percent and can increase if the pavement surface is wet.<sup>19</sup> This decrease in friction is mostly affected by pavement texture characteristics such as microtexture and macrotexture along with the amount of water presents on the surface. It is also important to note that the friction before the critical slip condition is affected mostly by tire properties whereas pavement texture affects friction after the critical slip.<sup>3</sup>

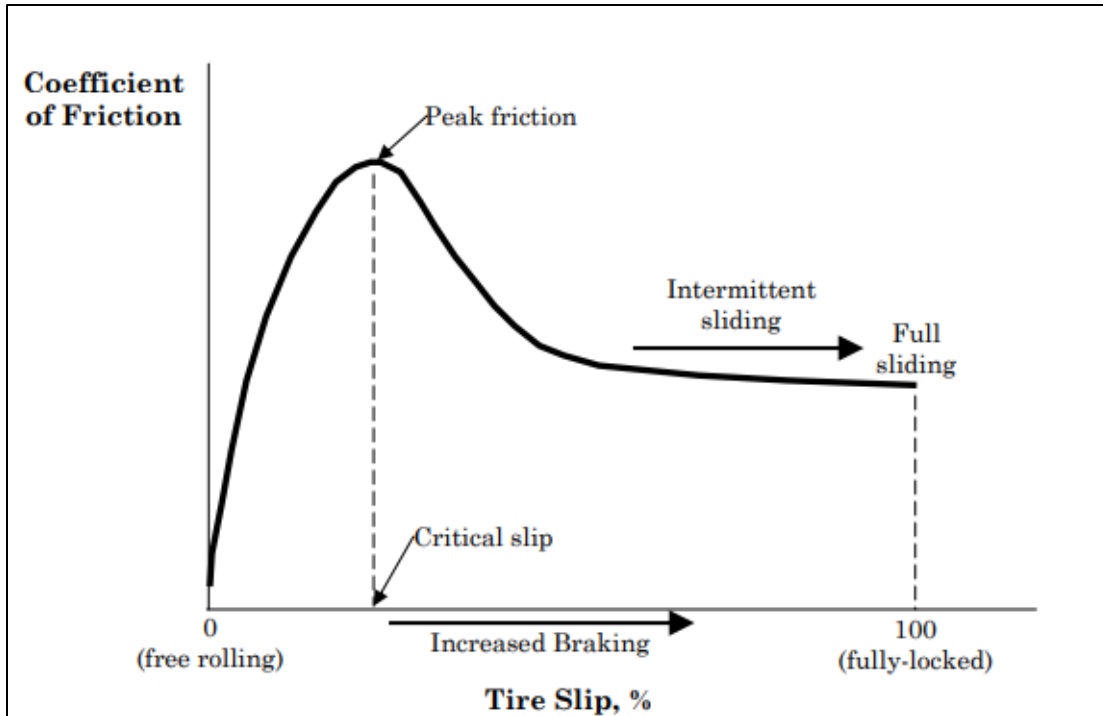


**Figure 8. Variation of Pavement Friction with Tire Slip<sup>19</sup>**

### Tire Properties

Properties of tire such as tread depth and pattern, inflation pressure and wheel load also affect the skid resistance of the pavements. The tire tread provides a path for trapped water between pavement surface and tire to escape leading to higher friction.<sup>6</sup> Tire inflation pressure is another factor that affects skid resistance. The contact area between the tire and pavement surface decreases with the increase in inflation pressure. The heat generated during skidding is dissipated over a large area which reduces the tire temperature and increases the friction.<sup>15</sup> Lower contact area also reduces the adhesion friction.<sup>20</sup> Al-Assi and Kassem (2017) found a fair correlation between the adhesion between tire rubber and aggregate and pavement friction.<sup>21</sup> They also obtained a strong correlation between rubber properties (i.e., elastic properties) and friction. Softer rubber provided higher friction.<sup>21</sup>

### Temperature

Rubber is a viscoelastic material and its properties are affected by temperature. Previous studies demonstrated that the tire pavement friction reduces with the increase in temperature which explains the seasonal fluctuations of the skid resistance.<sup>21,15</sup> A study by Jayawickrama and Thomas (1998) documented that the skid resistance measured at 40 mph (SN40) decreased with the increase of air temperature.<sup>22</sup> Another study by Ragland *et al.* (2010) demonstrated temperature to have a major effect on skid resistance.<sup>18</sup> The skid resistance values were higher in fall and winter compared to summer and spring where temperature is higher. Luo (2003) investigated the effect of pavement temperature on frictional properties.<sup>18</sup> The study concluded that pavement temperature had a considerable effect on

the frictional properties of pavements, and it is influenced by the test speed. There was a slight decrease in friction with the increase in temperature at low speeds compared to the reduction in friction at higher speeds.

### Presence of Water

Water acts as a lubricant between tires and pavement surface leading to reduction in skid resistance.<sup>24</sup> There may be little to no contact between tires and pavement surface based on water film thickness.<sup>20</sup> In addition, water fills up the asperities present on pavement surface which prevents the molecular bonding to form between pavement surface and tires leading to reduced adhesion friction. Beaufru *et al.* demonstrated that there is a considerable decrease in skid resistance with little amount of moisture on pavement surface.<sup>25</sup> Hall *et al.* demonstrated the effect of water film thickness on skid resistance for different tires (e.g., smooth tire, new ribbed tire, and worn ribbed tire).<sup>19</sup> The reduction in skid resistance was higher for smooth tires compared to ribbed tires (Figure 9). Harwood found that a water film thickness of 0.002 inches on pavement surface reduced pavement friction by 20 to 30 percent of dry friction.<sup>26</sup> Further increase in water film thickness at high speed can lead to hydroplaning. Hydroplaning occurs when there is no contact between tires and pavement surface leading to a complete traction loss.<sup>27</sup>

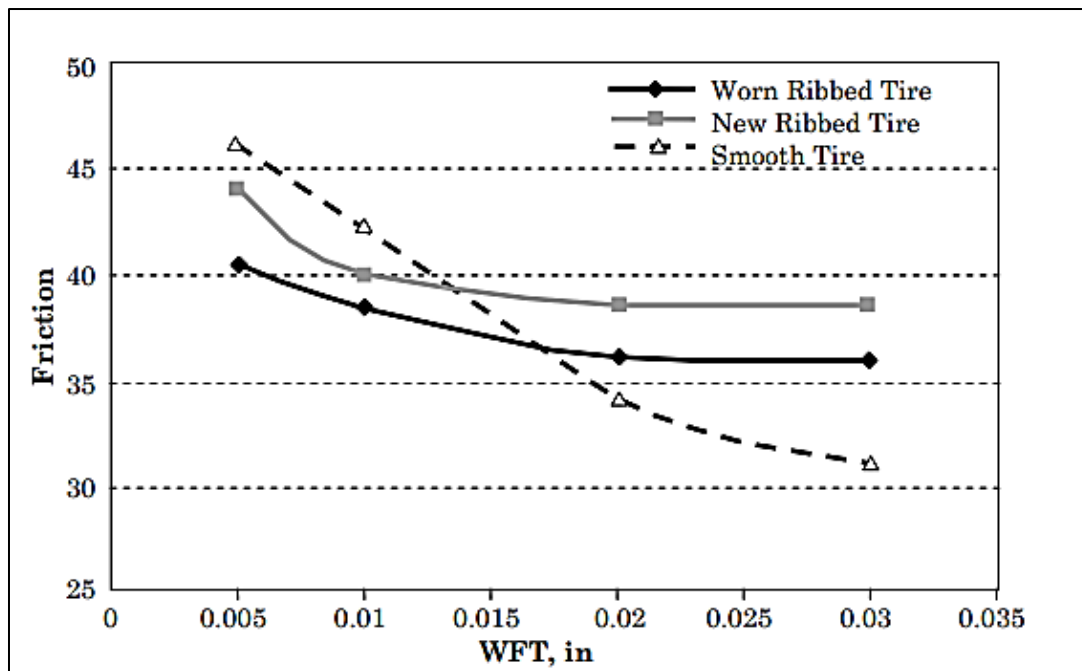


Figure 9. Effect of Water Film on Pavement Friction<sup>19</sup>

### Speed

Pavement friction decreases with the speed. Several studies showed that the decrease is not significant in dry conditions compared to wet conditions.<sup>15</sup> The relationship between skid resistance and speed in wet conditions is discussed in detail later in this chapter.

## Characterization of Surface Frictional Characteristics

There are several devices and methods available to characterize the frictional properties of pavement surface in terms of friction and texture. There are various devices that are used to measure skid resistance based on different principles such as locked wheel devices, side force devices, fixed slip ratio devices, and variable slip devices. Dynamic Friction Tester (DFT) and British Pendulum Tester (BPT) also measure pavement friction but the measurements are more related to the pavement microtexture. The sand patch test or volumetric method is a technique used to measure mean texture depth, while mean profile depth is often measured using a laser-based technique.

### Locked-Wheel Devices

The locked-wheel devices typically operate at a slip ratio of 100 percent.<sup>28</sup> ASTM E274 devices are a specialized trailer pulled by a truck which operates at a standard reference speed. The testing wheel is equipped with either smooth or ribbed tires. The test standards for smooth and ribbed tires are provided in ASTM E524 and ASTM E501, respectively. A water delivery nozzle is positioned on the trailer just in front of the test tire and applies water on pavement surface in front of the locked wheel. About 0.5 mm thick layer of water is sprayed to achieve wet conditions.<sup>2, 19, 28</sup> When the skid truck reaches the desired speed and location, the test is initiated by the operator pressing a trigger button. The water delivery is started, the brake is applied to the test wheel and fully locked for just over 1 second. Upon the completion of the test, the brake is released, and the water delivery is stopped. Data is collected from a 2-axis transducer located on the trailer axle at the wheel. The horizontal channel measures the force required to drag the wheel on the pavement surface, and the vertical channel measures the normal force or wheel load. The Skid Number (SN) is calculated by dividing the drag (traction) force by wheel load and multiplying by 100. It takes approximately 2.5 seconds to complete one friction test. The process is repeated for additional measurements. An E274 locked wheel tester can also be used to measure the maximum friction level (also known as peak value) when used according to ASTM E1337. The operation is similar to the slide method described above except the peak traction value is used along with the corresponding load value to calculate the Peak Brake Coefficient (PBC).

### Side Force Devices

The side force devices measure the sideways friction coefficient (SFC). The testing wheel has an angle to the direction of travel which is called yaw angle, or skew angle. The test is conducted in accordance with ASTM E670. The British Mu-Meter and British Sideway Force Coefficient Routine Investigation Machine (SCRIM) are two common side force friction devices. The Mu-Meter device measures the friction at a

yaw angle of 7.5 degrees while the SCRIM measures the friction at a yaw angle of 20 degrees. These devices can be used to measure the friction on straight portion of roadways as well as at corners and curves. Meanwhile, the friction measurements of these side force devices are influenced by pavement distresses such as potholes and cracks. These devices operate at low slip speed since they are sensitive to pavement microtexture. Separate devices are used to measure pavement macrotexture during friction testing.<sup>2, 19, 28</sup>

### **Fixed Slip Devices**

These devices operate at a fixed slip ratio which is usually between 10 to 20 percent. To maintain a fixed slip ratio, the angular velocity of the wheel is reduced by means of gear reduction, chains, belts or hydraulic braking systems. Similar to other friction testing equipment, water is sprayed in front of the testing tire. The trailer is towed by a truck that moves at 40 mph.<sup>2, 28</sup> Both the drag force and wheel load are measured to calculate the coefficient of friction. Some of the typical fixed slip devices are Grip Tester, Slab Friction Tester, Road Analyzer and Recorder, Airport Surface Friction Tester (ASFT), and Highway and Runway Friction Tester (HFT & RFT). The standards for the tires that are used in fixed slip devices are provided in ASTM E1551.<sup>19</sup>

### **Variable Slip Devices**

The variable slip devices measure friction at various slip ratios in accordance with ASTM E1859 standard. The slip ratio varies between zero (free rolling conditions) to 100 percent (fully-locked conditions). Similar to the other devices, 0.5 mm of water film is sprayed on the surface in front of the test tire to achieve wet conditions. Test speed, wheel load, drag force on the wheel, and rotational speed of the tire are measured during the test and used to calculate the coefficient of friction at various slip ratios. From the relationship between slip skid number and slip speed, other parameters including peak slip friction, critical slip ratio, longitudinal slip friction, and Rado shape factor can be calculated. French IMAG, Norwegian Norsemeter RUNAR, ROAR and SALTER systems are some examples of variable slip devices.<sup>19, 28</sup>

### **British Pendulum Tester (BPT)**

The British Pendulum Tester (BPT) is a portable device that is used to measure the friction in the field as well as in the laboratory in accordance with ASTM E303. It consists of a rubber slider attached to a pendulum which is released from a certain height for the rubber slider to just touch the pavement surface. The amount of energy lost when the rubber slider passes over the pavement surface is proportional to the amount of travel of the pendulum arm after contact with the surface. The results from the BPT are reported in terms of British Pendulum Number (BPN).<sup>36, 37</sup> The speed at which the rubber slider strikes the surface is about 10 km/h. Since the BPT measurements are performed at low speeds, it correlates well with pavement microtexture. The BPT is used to measure the skid at selected locations since it cannot be used for continuous measurements. Also, the results of BPT can be affected by the wind and operator performance.<sup>37, 19</sup>

### Dynamic Friction Tester (DFT)

The Dynamic Friction Tester (DFT) consists of three rubber sliders attached to a rotating circular disk as shown in Figure 10. The circular disk rotates at a desired test speed (up to 100 km/h) then the disk is dropped so that the rubber sliders are in contact with the pavement surface. The coefficient of friction is measured as the speed of the rotating disk gradually decreases.<sup>25, 38, 39</sup> The coefficient of friction at 20 km/h ( $DFT_{20}$ ) was found to correlate well with the pavement microtexture, and it is often used as an indirect method to measure pavement microtexture.<sup>25</sup> The DFT is a portable device which can be used both in the field and the laboratory. The friction test can be measured in dry as well as wet conditions and it is conducted in accordance with ASTM E1911.

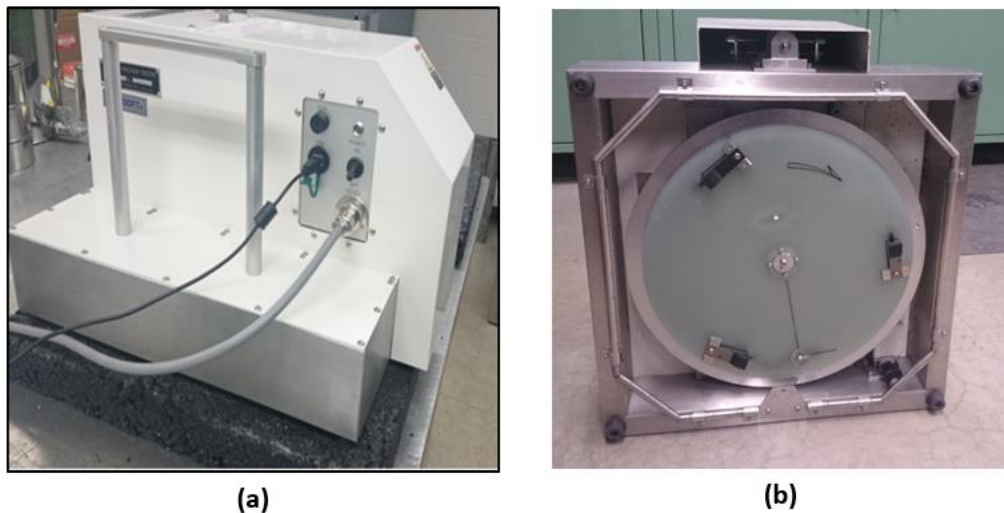


**Figure 10. (a) DFT device; (b) Bottom of the DFT with three rubber sliders**

### Circular Texture Meter

The Circular Texture Meter (CTMeter) device is a portable device used to measure the pavement macrotexture. It can be used in the field as well as in the laboratory. The test is conducted in accordance with ASTM E2157. The CTMeter has a charge-coupled device (CCD) laser displacement sensor attached to an arm mounted to the device. The arm rotates in a circular path with a diameter of 28.4 cm. The laser sensor can collect about 1024 data points per revolution. The average MPD is calculated and reported according to ASTM E2157. Masad *et al.* and Abe *et al.* found good correlation between the MPD measured using the CTMeter and the MTD measured using the sand patch test which was confirmed by Hanson and Prowell (2004).<sup>42,43,44</sup> Figure 11 shows the sand patch measurements against the CTMeter values based on data collected at the National Center for Asphalt Technology (NCAT) test tracks. There was a strong correlation ( $R^2 = 0.95$ ) between MPD measured using CTMeter and MTD measured using sand patch test. The use of CTMeter in the field requires traffic control which limits its use in the field testing.

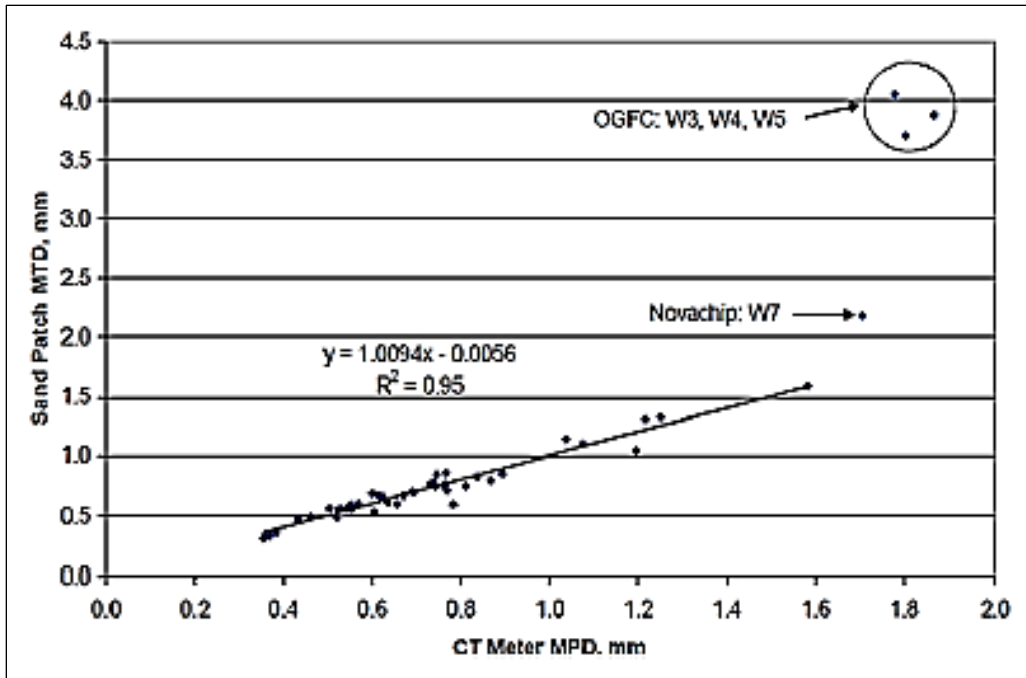


Figure 11. Relationship between CTMeter and Sand Patch From NCAT Test Track<sup>44</sup>

### Laser Profiler

With the advancement in laser-based technology, more accurate methods are available to measure the pavement texture such as the laser profiler.<sup>45</sup> These devices use triangulation technique for measuring distance. They project a laser spot or line on the pavement surface and the reflection is recorded in an optical detector.<sup>20</sup> Several parameters can be determined to represent the texture. The most common and widely used is MPD defined by ASTM E1845 Standard. The MPD represents the average value of the profile depth over a certain segment of surface profile.<sup>3</sup> The MPD measured by the laser profile is correlated with the MTD calculated by sand patch method.

### Volumetric Method

The volumetric method or sand patch test is a simple method to measure the macrotexture of pavement surface.<sup>2</sup> The sand patch test is conducted in accordance with ASTM E965. In this test, a known volume of glass spheres is spread over a pavement surface and levelled using a spreader similar to a hockey puck. Prior to the use, the glass spheres are sorted by passing them through sieve No. 50 and retained on sieve No. 100. The glass beads are recommended over sand since they are more uniform and can be manufactured commercially.<sup>1,37</sup> The pavement surface should be cleaned using a brush to remove any loose materials. Also, the surface should be free of any cracks or other irregularities before applying and spreading the glass spheres. The spheres are applied and levelled in a circular pattern. The average diameter of the circular patch is then calculated. The volume of the sand and the area of the patch are used to calculate the average depth of the circular patch which is referred to the MTD of pavements.<sup>36</sup>

## Current Practice in Measuring Skid Number

Several highway agencies measure the skid resistance periodically (often every two years) to ensure adequate level of friction. Minnesota Department of Transportation (MnDOT) utilizes the Dynatest 1295 skid truck-trailer in accordance with ASTM E274 to measure skid resistance. MnDOT uses both ribbed as well as smooth standard test tires to measure skid resistance at a standard test speed of 40 mph in wet condition. A skid number above 25 measured using a smooth tire is considered adequate while skid number below 15 indicates that the pavement requires surface treatment.<sup>47</sup>

Pennsylvania Department of Transportation (PennDOT) uses a skid friction tester (SFT) to measure skid number in accordance with ASTM E274. The test is conducted using standard smooth or ribbed test tires according to ASTM E524 and ASTM E501, respectively. Using both smooth as well as ribbed tires gives more data but it is suggested to use smooth tires if the testing to be performed using only one type.<sup>48</sup> At least five skid number measurements are collected for each test segment to ensure accuracy. PennDOT performs the friction testing at speeds between 25 to 50 mph, and the measured skid numbers are adjusted to an equivalent speed of 40 mph. The adjustments are made solely based on previous practice and experience. Table 2 summarizes the adjustment factors at various speeds. If the speed is greater than 45 mph, constant values are added to the measured skid number while constant values are subtracted from the skid number if the speed is lower than 40 mph. PennDOT policy is to take remedial actions and apply surface treatments if the skid number is less than 35 for the ribbed test tire or 20 for the smooth test tire.

**Table 2. Skid Number Adjustment Factors Constants at Various Test Speeds<sup>48</sup>**

Test speed (mph)	Skid number adjustment constants
25	Subtract 7
30	Subtract 5
35	Subtract 2
40	No adjustment.
45	Add 2
50	Add 5

Texas Department of Transportation (TxDOT) performs annual skid resistance measurements using the locked-wheel skid trailer. The test is performed at only 50 mph using a smooth tire in accordance with ASTM E274 test standard. No standard practice has been established yet to conduct friction testing at various speeds.<sup>39, 49</sup>

Idaho Transportation Department (ITD) manages about 12,000 lane miles of roadways. ITD pavement engineers use the measured skid numbers to determine the need for surface treatments to improve the skid resistance. The current practice at ITD is to measure the skid number using a Dynatest 1295 Locked Wheel Friction Testing Trailer according to ASTM E274 using a smooth tire. The standard practice by ITD is to measure the skid number at 40 mph every tenth of a mile.<sup>50</sup> ITD recommends surface treatments if the skid number measured at 40 mph is less than 40.

## **Relation between Skid Resistance and Speed**

Speed is one of the most important factors affecting the friction between two surfaces. If an object is moving with a higher speed over another surface, there will be an increase in its momentum in the normal direction resulting in upward force on the upper surface. This upward force creates a separation between the two surfaces which decreases the true area of the contact between them. Further, when the speed is higher, the time duration over which the two surfaces remain in contact decreases.<sup>8</sup> Reduced area and duration of contact decrease the molecular bonding between the asperities and rubber tires leading to reduced adhesion and consequently lower friction.<sup>9, 10</sup> Therefore, skid resistance found to be satisfactory at one speed may not be adequate at a higher speed. A number of studies examined the relationship between skid resistance and speed. The findings of some of these efforts are summarized in this section.

### **Corsello (1993)**

Moyer (1943) demonstrated that the coefficient of friction of rubber tires on a slippery surface is higher at low speeds and it decreases rapidly with speed which is consistent with the findings of Byrd.<sup>51, 52</sup> In addition, the driver demand for friction increases as the speed of the vehicle increases.<sup>52</sup> The dependency of frictional force on speed in wet conditions is influenced by the net contact area between the tire and pavement surface. This contact area is affected by how fast the water is removed from the pavement surface through the tire treads. Water presence on the pavement surface causes a degradation in the ability of tires to form a bond with the pavement surface at higher speed preventing them to maintain dry and adequate contact area.<sup>5</sup>

### **Rizenbergs et al. (1973)**

Rizenbergs et al (1973) examined the correlation between the skid resistance measured using a skid trailer on various pavement surfaces including flexible and rigid pavements.<sup>53</sup> As expected, the skid number of pavements decreased with the increase in speed. The speed gradient (i.e., the change in skid number with speed) had an average value of about 0.4 between the speed of 40 mph and 60 mph (i.e., if the speed increases from 40 mph to 60 mph, the skid decreases by 8 points). It was also found that the relationship between skid number and speed is not always linear.<sup>53</sup> They found a strong linear relationship between skid number at 70 mph (SN70) and skid number at 40 mph (SN40) for asphalt pavements and Portland cement concrete (PCC) pavements. The R<sup>2</sup> values were 0.934 and 0.954 for asphalt and PCC pavements, respectively.

### Penn State Model

Leu and Henry (1978) proposed a model for skid resistance prediction as a function of speed and pavement texture measurements as represented Figure 12.<sup>54</sup>

$$SN = C_0 * \exp(C_1 V)$$

where:

SN = skid number

C<sub>0</sub> = zero speed intercept

C<sub>1</sub> = change in slope gradient

V = speed (km/h)

**Figure 12. Leu and Henry Model for Skid Number Calculation**

Leu and Henry (1978) modified the equation in Figure 12 to obtain a modified model (i.e., Pennsylvania State University model) for skid resistance speed behavior as presented in Figure 13.<sup>54</sup>

$$SN = (-31 + 1.38 * BPN) * \exp[-0.041 * V * (MTD) - 0.47]$$

where:

BPN = British pendulum number

MTD = Mean texture depth

**Figure 13. Pennsylvania State University Model for Skid Resistance**

The equation in Figure 13 can be used to predict the skid number at any speed (V) based on BPN and MTD values. The results showed good correlation between predicted skid numbers obtained from the equation and measured skid numbers. Also, they proposed alternative model (Figure 14) that can be used to predict the skid number based on skid number at 40 mph and MTD of the surface.

$$SN = SN_{40} * \exp[-0.041 * (V-40) * MTD^{-0.47}]$$

**Figure 14. Leu and Henry Alternative Model**

The equation in

Figure 14 was used to predict skid number at 60 mph using the measured skid number at 40 mph and MTD and the results showed a good correlation between the predicted skid numbers with R<sup>2</sup> value as high as 0.98.

### Kulakowski (1991)

Kulakowski modified of the Pennsylvania State University model and proposed a new model as presented in Figure 15. The Pennsylvania state model was modified by replacing percent normalized

gradient (PNG) with speed constant ( $V_0$ ) as shown in Figure 16. PNG is a normalized gradient of skid number and speed in percentage.<sup>7</sup>

$$SN_V = SN_0 * \exp [-(V/V_0)]$$

**Figure 15. Kulakowski Modification of Pennsylvania State University Model**

$$V_0 = 100 / \text{PNG}$$

**Figure 16. Equation for Speed Constant as Defined by Kulakowski (1991)**

The speed constant ( $V_0$ ) is a measure of the rate of change of the skid number with speed which was found to be related to the pavement macrotexture. The model requires two parameters ( $SN_0$  and  $V_0$ ) for the prediction of skid number. Kulakowski proposed two methods for the calculation of the model parameters; direct method and indirect method. In the direct method, the skid number is measured in accordance with ASTM E274 at two speeds ( $V_1$  and  $V_2$ ). Thus, two values for skid number ( $SN_{v1}$  and  $SN_{v2}$ ) were obtained at two different speeds (i.e.,  $V_1$  and  $V_2$ ). Equations presented in Figure 17 and Figure 18 are proposed to calculate the values of  $V_0$  and  $SN_0$ , respectively.

$$V_0 = (V_2 - V_1) / \ln (SN_{v1} / SN_{v2})$$

**Figure 17. Equation for  $V_0$  Calculation in Direct Method**

$$SN_0 = SN_{v1} * e^{v1/v0}$$

**Figure 18. Equation for  $SN_0$  Calculation in Direct Method**

In the indirect method, the skid number was measured using ribbed and smooth tires at 40 mph. The equation shown in Figure 19 was developed to determine  $SN_0$  while the equation presented in Figure 20 was proposed to determine PNG.

$$SN_0 = 35.4 - 0.682 SN^B + 2.894 SN^R - 12.75 (SN^R)^{1/2} + 24.7 / (SN^B)^{1/2}$$

**Figure 19. Equation for  $SN_0$  Calculation in Indirect Method**

$$PNG = -0.49 - 0.01996 SN^B + 0.0106 SN^R + 0.113 (SN^R)^{1/2} + 3.48 / (SN^B)^{1/2}$$

where:

$SN^R$  = Skid resistance measurement obtained using ribbed tire

$SN^B$  = Skid resistance measurement obtained using smooth (blank) tire

**Figure 20. Equation for PNG Calculation in Indirect Method**

### Jackson (2008)

Jackson conducted a study to harmonize the skid resistance measurements with speed using the concept of International Friction Index (IFI) as described in ASTM E1960.<sup>55</sup> The objective of the study was to implement IFI in Florida so that the friction test can be performed at variable speeds. Ten different sections were selected and DFT and CTMeter tests were performed at the same locations. Full scale friction tests were conducted using locked wheel friction test unit of Florida DOT using ribbed and smooth tires as per ASTM E274. The researchers found that the CTMeter data to be highly correlated with a high-speed laser texture measuring device used by Florida DOT.

The study found a good correlation between DFT data and full-scale locked wheel friction data. However, the correlation between the speed gradient from the DFT data and the MPD from the CTMeter was significant only for smooth tire and not for ribbed tire as shown in Figure 21 and Figure 22. As such, IFI index could not be used for harmonization of friction testing performed with ribbed tires.

Jackson proposed another method to relate the pavement friction and test speed for ribbed tire. The study examined the speed gradient of the locked wheel friction unit and found that the slopes were almost similar for ribbed tires.<sup>55</sup> Jackson suggested using the average speed gradient, for the tested pavements, to convert locked wheel ribbed tire friction data at 30 mph and 50 mph to the standard 40 mph value (Table 3). They proposed this method as a practical procedure for transforming friction number at various speeds measured using the Florida DOT locked wheel friction unit with ribbed tire.

**Table 3. Statistical Data Related to Ribbed Tire Locked Wheel Speed Gradient<sup>55</sup>**

Locked-Wheel Friction Number	30 mph	40 mph	50 mph	Mean Difference
Mean	44.4	41.9	39.6	± 5.5 %
Standard Deviation	7.84	7.21	6.52	± 2.4
95 Percent Conf. Interval	± 4.9	± 4.5	± 4.0	± 2.7

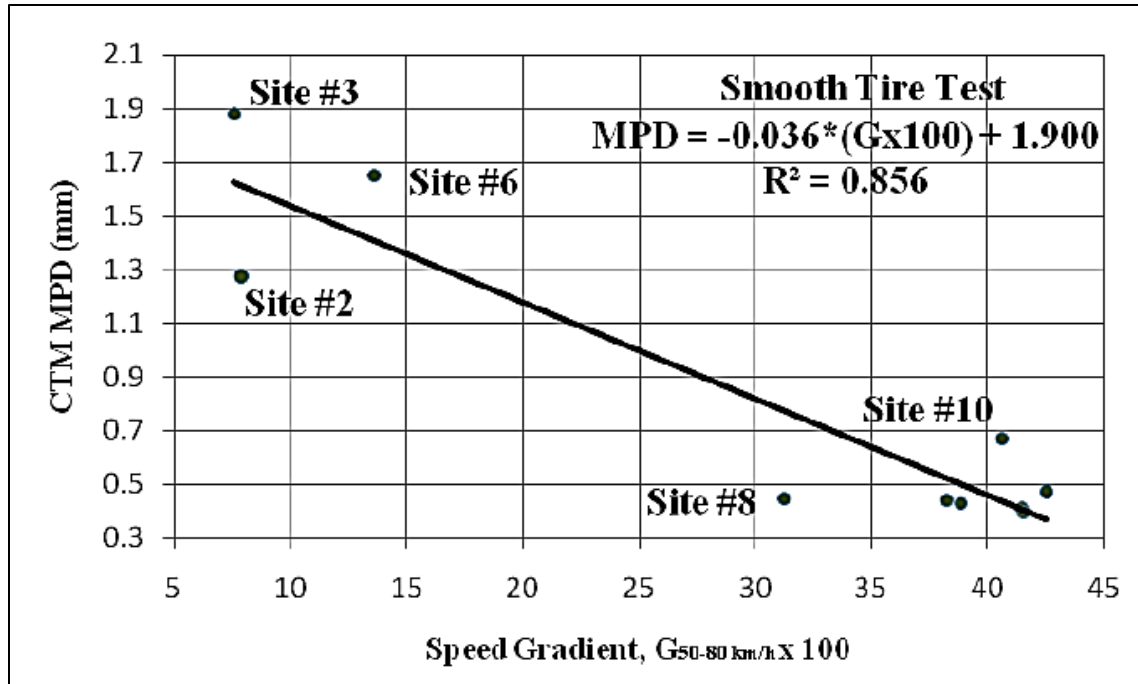


Figure 21. Plot of Speed Gradient Vs. MPD for Smooth Tire<sup>55</sup>

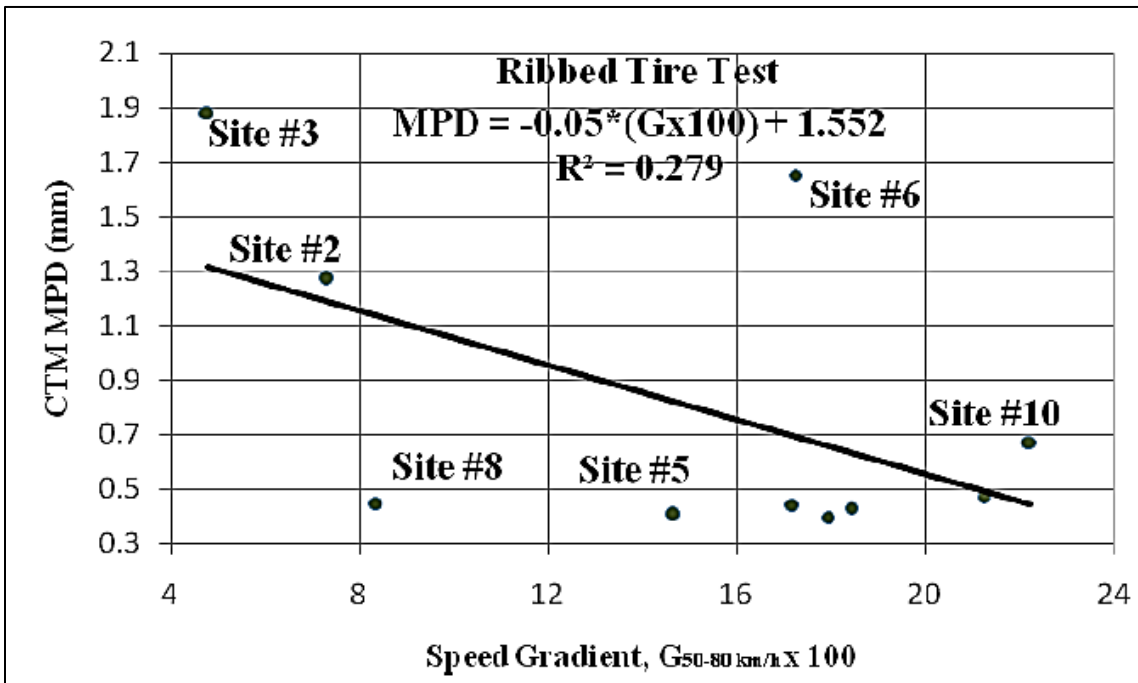
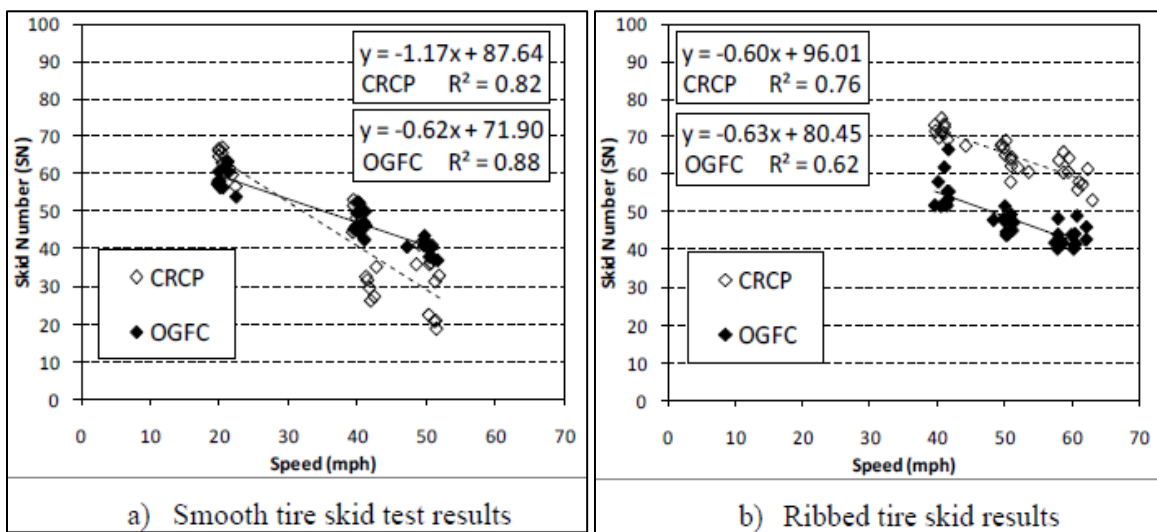


Figure 22. Plot of Speed Gradient Vs. MPD for Ribbed Tire<sup>55</sup>

### Flintsch et al. (2010)

Flintsch et al. (2010) described a methodology to calculate an adjustment factor to convert a skid number measured at one speed to a skid number at different speeds.<sup>56</sup> They used friction data measured on Virginia Smart Roads from 2007 to 2009. A skid trailer was used to measure the skid number and a CTMeter was used to measure the mean profile depth. The test sites included flexible pavements (Superpave mixes, Stone Matrix Asphalt [SMA], and Open Graded Friction Coarse [OGFC]) as well as rigid pavements (Continuously Reinforced Concrete Pavement [CRCP]). They measured the skid number at different speeds using both smooth and ribbed tires. They found an inverse linear relationship between measured skid number and speed for both smooth and ribbed tires. Figure 23 shows such relationship for OGFC and CRCP. Figure 23a shows that the trend lines for OGFC and CRCP have different slopes and they cross each other at about 30 mph for smooth tires, while they are almost parallel to each other for ribbed tires (Figure 23b). They indicated that the smooth tire was sensitive to the macrotexture compared to the ribbed tire.



**Figure 23. Sample Skid Testing Results for Two Sections of the Virginia Smart Road<sup>56</sup>**

Flintsch et al. (2010) developed an adjustment factor for estimating skid resistance at different speeds if measured at a given speed.<sup>56</sup> They grouped the surfaces according to their frictional behavior in three categories; SM and SMA, OGFC, and CRCP using principal component analysis method (PCAM). They established linear regressions between skid number and speed and computed the slope of the regression lines. The variation in skid number for the smooth tires were higher than those with ribbed tires. The researchers indicated that the smooth tires were more sensitive to macrotexture than ribbed tires. The adjustment factors were found to have a good correlation with the mean profile depth for the smooth tires ( $R^2 = 0.76$ ). The correlation between the adjustment factors and the ribbed tire were very poor ( $R^2 = 0.05$ ). Based on the obtained correlations for the smooth tires, a relationship for the speed adjustment factor as a function of MPD was developed as presented in Figure 24.

$$C = 0.85 \text{ MPD} - 1.64$$

where:

C = speed adjustment factor for all smooth tire units

MPD = Mean Profile Depth (mm)

**Figure 24. Speed Adjustment Factor Equation**

The equation presented in Figure 25 is a generalized form to convert skid number at one speed to another speed using the adjustment factor.

$$F_{v_2} = F_{v_1} + \Delta F$$

where:

$F_{V_2}$  = skid number at desired speed ( $V_2$ )

$F_{V_1}$  = skid number at measured speed ( $V_1$ )

$\Delta F = C \Delta V = (0.85 * \text{MPD} - 1.64) * \Delta V$

$\Delta V = V_2 - V_1$

**Figure 25. Equation to Calculate Skid Number Based on Skid Adjustment Factor**

## **Chapter 3**

# **Selection of Test Sections and Field Testing**

### **Introduction**

Several candidate pavement sites were identified and selected across Idaho for field testing and evaluation. These sections were selected to cover different pavement types in the state. A total number of 34 test sites were selected by the research team and ITD skid crew. Several criteria were considered when selecting the test sections including:

- Pavement type: flexible and rigid pavement test sections as well as seal coat surfaces were selected.
- Skid number: test sections with different levels of skid resistance were selected and evaluated.
- Environmental conditions: the test sections were distributed across the state and sites from all six districts were included in this study.
- Traffic level: interstate highways, US highways, and state highways subjected to different traffic levels were considered.
- Service life: pavement sites with different age were included. Old pavements are expected to provide lower skid numbers compared to newer pavement due to abrasion and polishing under traffic.

Out of the total 34 pavement sections that were evaluated in this study, 12 sites were hot mix asphalt (HMA), 17 were seal coat and five sections were concrete pavements. Table 4 provides the list of test sections along with their type and location. Several criteria were considered when selecting the location of the test sections including:

- Each test section should be at least one mile long.
- Test sections should be a straight segment (i.e., no curve or sharp turns).
- Test sections should have a low grade as possible.
- Test sections should have a minimum number of exits/entrances.

The above criteria were considered to ensure that the skid truck can collect the skid numbers safely at various speeds and minimize traffic interruptions and expedite field testing.

Figure 26 shows the location of test sections distributed across the state of Idaho. Figure 27 illustrates the distribution of the test sites by pavement type. About 53 percent of the test sections were flexible pavement surfaced with seal coat, and 32 percent and 15 percent were HMA and concrete, respectively. The relatively low number of concrete sections is due to fact that most (about 95 percent) of pavements in Idaho are flexible pavements. The current practice in Idaho is to seal flexible pavement surface with chip seal early on after the construction. This explains the relatively large number of seal coat sections.

Figure 28 shows that the test sections were distributed across the six districts of Idaho. Twelve test sections were evaluated from District 5 representing about 35 percent of the total test sections followed by 8 sections (32 percent) in District 3, whereas four test sites (12 percent) were selected in both District 2 and District 6. Three sections (9 percent) in both Districts 1 and 4 were examined.

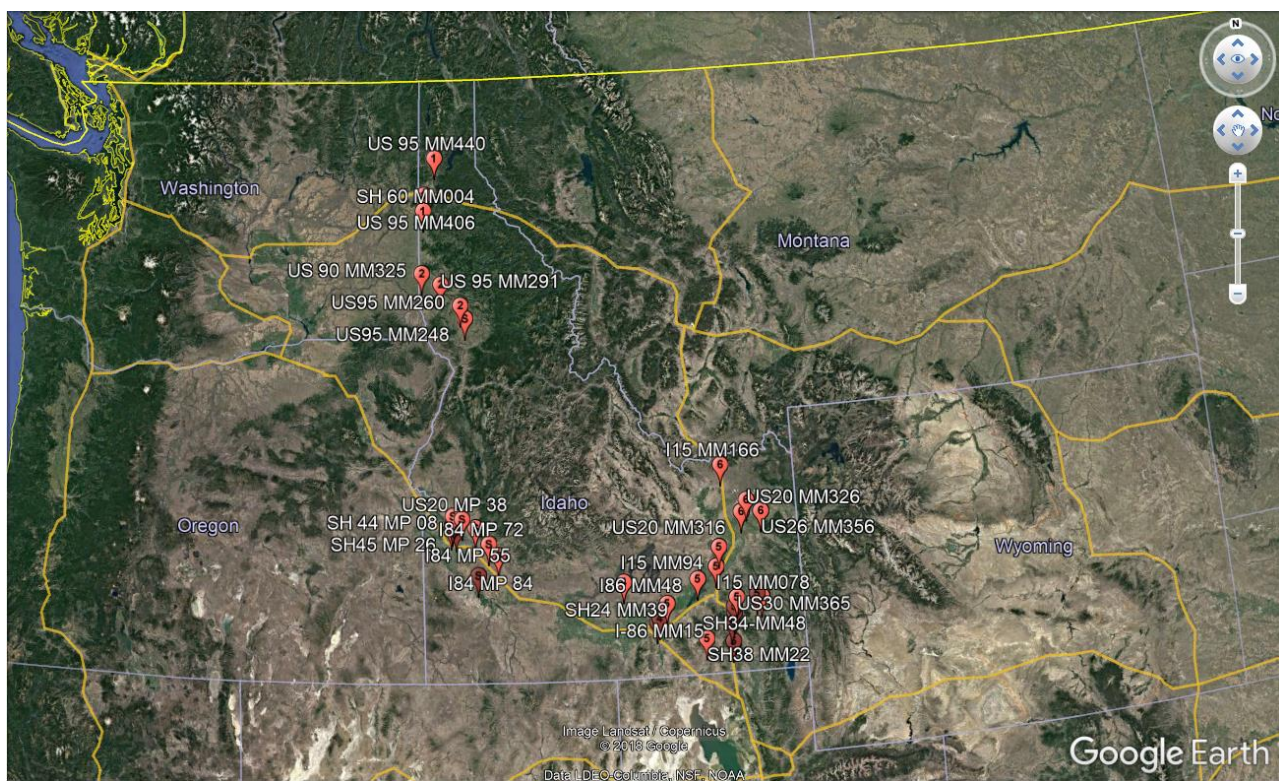
Figure 29 shows that most of test sections (i.e., 76 percent) were US highways and Interstate highways. These highways have relatively high traffic volumes and speed which are two major factors affecting skid resistance of pavements.

**Table 4. List of Test Sections**

District	Highway	Milepost	Surface Type
District 1	SH-60	MP 003	Seal coat
District 1	US-95	MP 440	HMA
District 1	US-95	MP 405	HMA
District 2	US-95	MP 325	Seal coat
District 2	US-95	MP 247	Seal coat
District 2	US-95	MP 259	Concrete
District 2	US-95	MP 289	HMA
District 3	I-84	MP 36	Concrete
District 3	I-84	MP 55	HMA
District 3	I-84	MP 72	Concrete
District 3	I-84	MP 84	HMA
District 3	SH-44	MP 08	Seal coat
District 3	SH-45	MP 26	Seal coat
District 3	SH-78	MP 56	Seal coat
District 3	US-20	MP 38	HMA
District 4	I-84	MP 236	Seal coat
District 4	SH-24	MP 039	Seal coat
District 4	SH-81	MP 006	HMA
District 5	I-15	MP 078	HMA
District 5	I-86	MP 047	HMA
District 5	US-30	MP 365	Seal coat
District 5	US-30	MP 382	Seal coat
District 5	I-15	MP 031	Concrete
District 5	I-15	MP 022	Seal coat

**Table 4. List of Test Sections (Cont'd)**

District	Highway	Milepost	Surface Type
District 5	I-15	MP 007	Seal coat
District 5	I-15	MP 037	Seal coat
District 5	I-15	MP 096	HMA
District 5	I-86	MP 016	Concrete
District 5	SH-34	MP 048	Seal coat
District 5	SH-38	MP 023	Seal coat
District 6	I-15	MP 165	Seal coat
District 6	US-20	MP 326	HMA
District 6	US-20	MP 315	HMA
District 6	US-26	MP 355	Seal coat

**Figure 26. Locations of the Selected Test Sections in the State of Idaho**

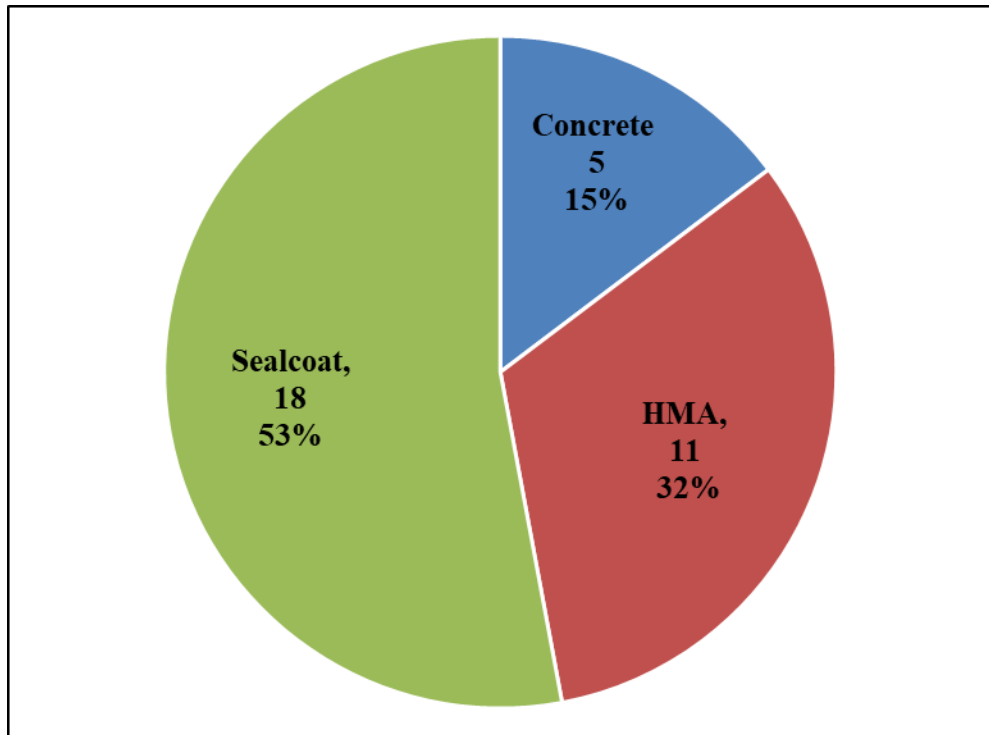


Figure 27. Test Section Distribution by Pavement Surface Type

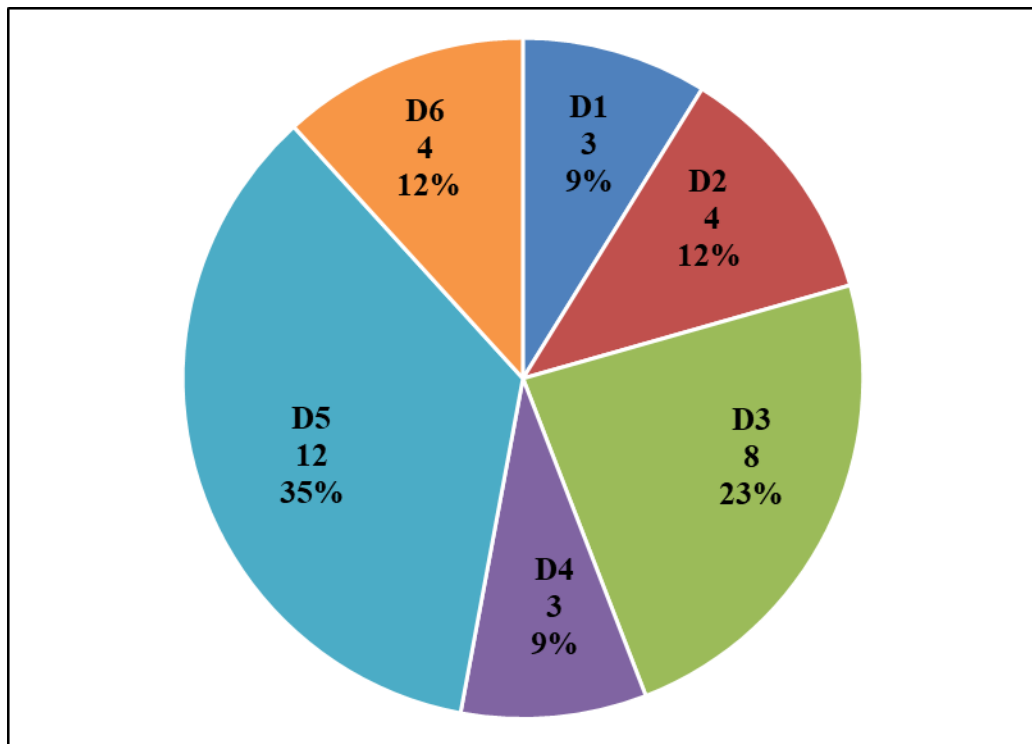


Figure 28. Test Section Distribution by District

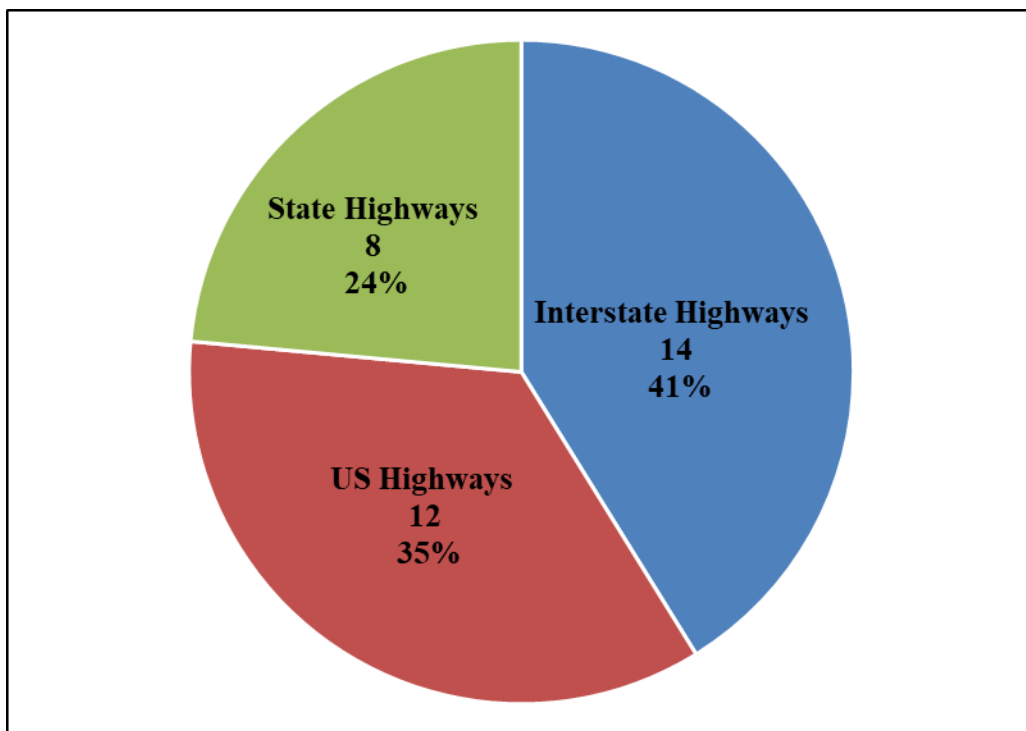


Figure 29. Test Section Distribution by Highway

## Skid Number Measurements

Skid number measurements were collected using the ITD locked-wheel skid trailer (Figure 30). ITD uses the 1295 Locked Wheel Friction Testing Trailer manufactured by Dynatest to measure the skid number at a standard speed of 40 mph in accordance with ASTM E274. The test is performed using a smooth tire, ASTM E524. The locked wheel skid trailer is used by various transportation agencies across the United States. The skid trailer is towed by a truck that travels at the desired testing speed (e.g., 40 mph) to measure the skid number. The truck has a storage for water supply, in addition to a data acquisition system to record, store and analyze the measured data. When the towing truck reaches the desired speed, the left wheel of the skid trailer is fully locked, and the locked wheel is dragged along the pavement surface at a constant speed. The horizontal force required to drag the locked wheel is recorded along with the speed of the vehicle and the vertical load acting on the locked wheel.<sup>48</sup> The skid number is calculated as the ratio of the horizontal drag force to the vertical load on the wheel multiplied by 100. The skid number is a representation of skid resistance of the pavement as per ASTM E274. A stretch of one mile of the outer lane of each test sites was selected for skid measurements at different speeds (i.e., 20, 30, 40, 50, and 60 mph). At least seven skid number measurements were recorded at each speed and the average skid number was calculated.

It should be noted that the skid testing could not be conducted at all five test speeds for all test sections. For example, in District 3 and due to the high posted speed limit and traffic levels, the friction testing was not conducted at lower speeds (i.e., 20 and 30 mph), instead the skid number was measured at three speeds (i.e., 40, 50, and 60 mph). Similarly, it was not possible to measure skid number at 60 mph for two other sections due to speed limit and road geometry restrictions.



**Figure 30. ITD Locked Wheel Skid Trailer**

## **Measurement of Surface Texture Characteristics**

The surface texture characteristics of the test sections were measured using a dynamic friction tester (DFT), sand patch test and laser sensor installed on the ITD skid trailer. The researchers measured the microtexture and macrotexture at the wheel path of the outer lane. Figure 31 shows a schematic for the locations of test spots in a typical test section. For each test section, the DFT and sand patch test were conducted at three locations separated by a distance of 200 ft. At each location, measurements were rerecorded at two spots 20 ft apart from each other. At least two DFT measurements were recorded at each spot to ensure the data accuracy. The selected test spots were free of any cracks, potholes, loose materials and other irregularities to avoid misleading texture results.

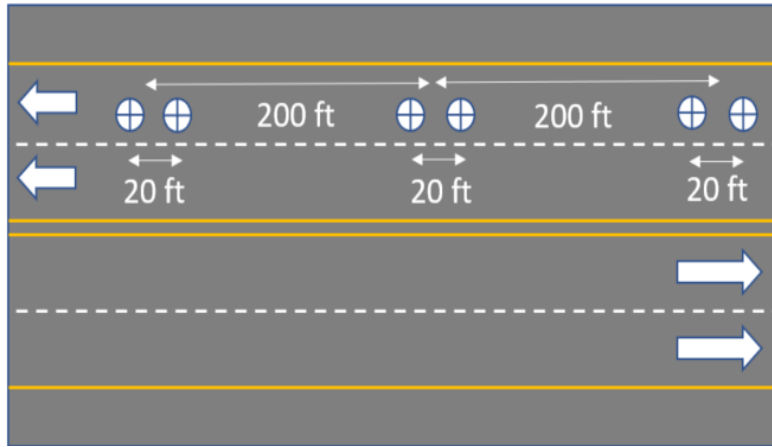


**Figure 31. Schematic for Locations of DFT and Sand Patch Measurements**

#### Measurement Using Dynamic Friction Tester (DFT)

The surface microtexture was measured using the DFT device (Figure 32). The DFT is a portable device so it was taken to the field to measure surface microtexture at each testing spot. Figure 31 shows typical testing operation in the field using the DFT. Traffic control was provided during field testing. The DFT consists of three rubber sliders attached to a rotating circular disk. The circular disk rotates at a desired test speed (up to 100 km/h), then the disk is dropped so that the rubber sliders are in contact with the pavement surface. The coefficient of friction is measured continuously as the speed of the rotating disk gradually decreases to zero<sup>38,57</sup>. The DFT test is conducted in wet conditions where water is sprayed automatically before the rubber touches the surface. The DFT accompanied software was used to operate the device and record the coefficient friction during the test. Figure 33 shows the interface of the DFT software. After a number of friction tests and depending on the level of surface friction, the rubber sliders were replaced with a new set as they worn out. The coefficient of friction at 20 km/h (DFT<sub>20</sub>) was found to correlate with pavement microtexture; thus it is used as an indirect method to measure pavement microtexture.<sup>58</sup>

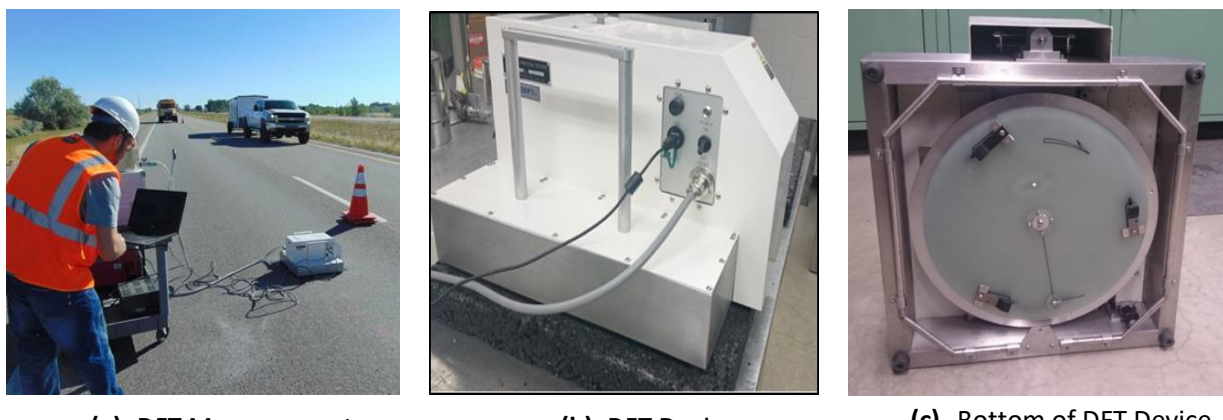


**Figure 32. Measurement of Microtexture Using DFT Device**

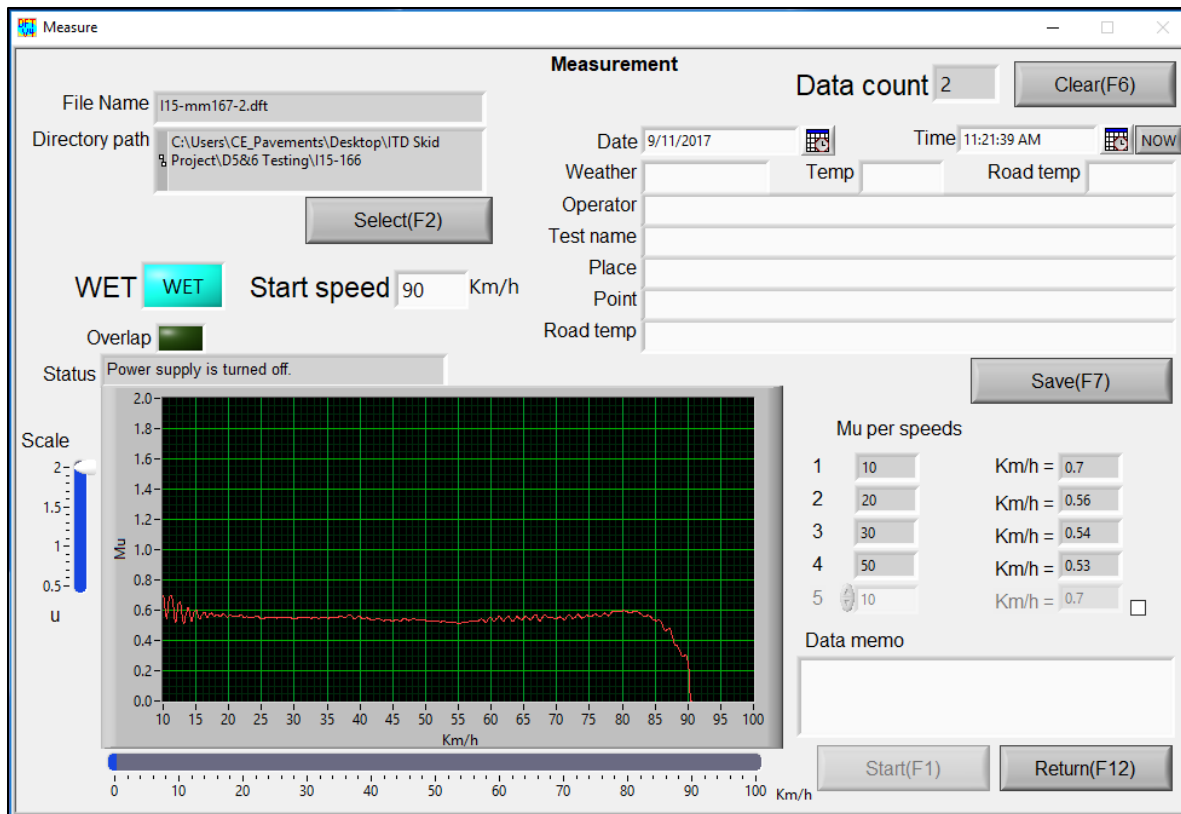


**Figure 33. Coefficient of Friction Measurements by DFT Software**

#### Surface Macrotexture Measurements Using Sand Patch Test

The surface macrotexture was measured at the same locations where the DFT was used to measure the microtexture. The sand patch test was used to measure the mean texture depth (MTD) of pavement surface as shown in Figure 34. The test surface was cleaned with a brush to remove any loose stones or debris. Then, a known volume of glass beads was spread over the section in a circular pattern and leveled throughout with a spreader. The average diameter of the circular patch was measured. The volume of the sand and the area of the patch were used to calculate the average depth of the circular patch which is referred as MTD of pavement surface<sup>36</sup>. At each location, two sand patch tests were conducted just adjacent to the DFT measurements with a total of six tests at each site. The average MTD was calculated and used as a measure of surface macrotexture. Wind, rain and moisture may influence the results of the sand patch test; therefore, the selected test spots were dry, and a box was used to shield the testing spot from wind if there was any. In some cases, a hot air blower was used to dry the pavement surface.

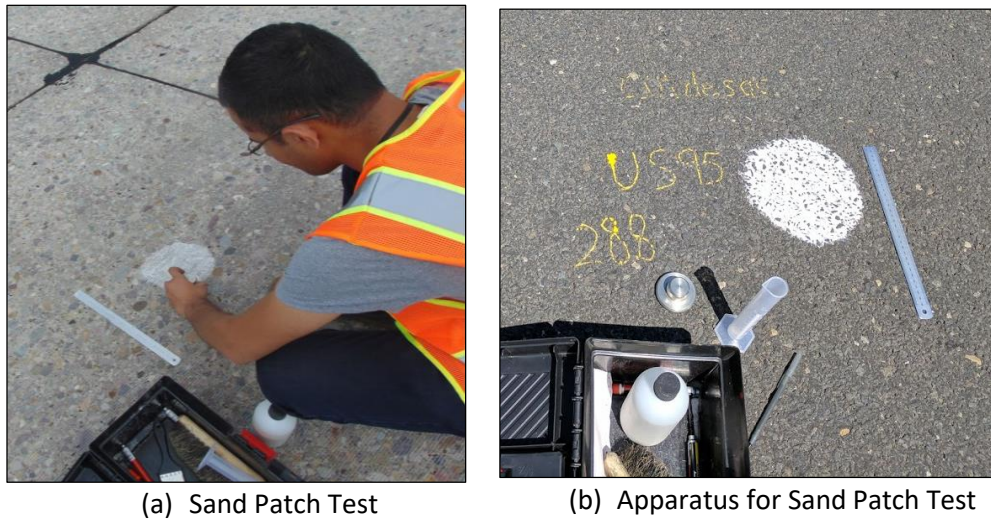


**Figure 34. Sand Patch Test Measurements**

#### Surface Macrotexture Measurements Using Laser Profiler

With the advancement in laser-based technology, more accurate methods are available to measure the pavement texture such as the laser profiler<sup>45</sup>. In this study, pavement macrotexture was also measured using a laser sensor installed on the skid truck as shown in Figure 35a. The pavement macrotexture is measured in terms of mean profile depth (MPD). The texture measurements were recorded simultaneously during skid number measurements using the skid trailer. The laser profiler uses triangulation techniques for measuring distance. The MPD is calculated in accordance with ASTM E1845. The measured profile of road is divided into segments of 100 mm (baseline) and each segment is further divided into two halves as shown in Figure 35b. The mean segment depth and the mean depth for the entire profile are explained in detail in ASTM E1845. Figure 36 shows examples of typical field testing of friction and texture.

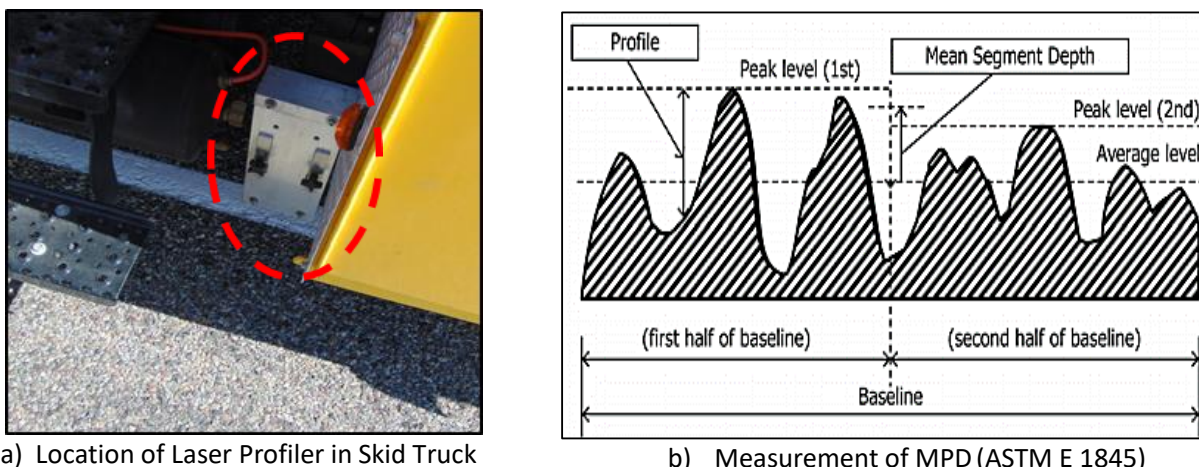


**Figure 35. Measurement of MPD Using Laser Profiler**

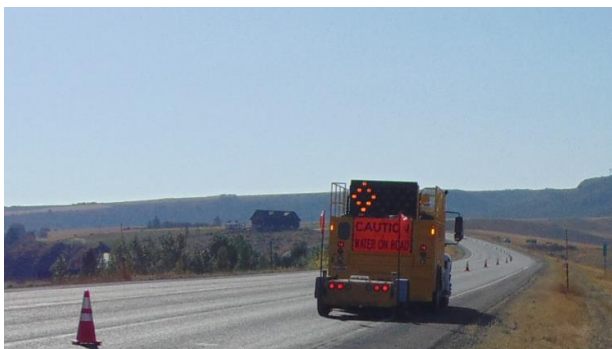


**Figure 36. Examples of Field Testing**

## **Chapter 4**

## **Results and Discussion**

### **Introduction**

Several tests were conducted in the field including measuring skid number using the ITD skid trailer at various speeds (e.g., 20, 30, 40, 50, and 60 mph), measuring microtexture using the DFT device and macrotexture using the sand patch test and laser profiler. In this chapter, the collected data was analyzed, and statistical analysis was performed to develop a statistical-based model that describe the change in skid number with testing speed. In addition, the authors conducted sensitivity analysis of the model parameters to examine their effects on predicted skid number.

### **Distribution of Skid Number and MPD of The Test Sites**

Figure 37 shows the average skid number values measured at 40 mph (standard test speed in Idaho) for all test sections divided into three categories; HMA, seal coat, and concrete sites. It can be seen from Figure 37 that the seal coat sections had the highest skid number values compared to all other sections followed by HMA surfaces. Figure 38 shows the skid number distribution. It shows that the majority of the test sites (81 percent) have skid number of 40 or higher at 40 mph. Higher skid number indicates better resistance to skidding in wet conditions and improved safety.

Figure 39 shows the average MPD values for all test sections. The seal coat sections had the highest MPD which contributed to its higher skid number. MPD data from the laser profiler demonstrated that most sites have MPD between 0.5 mm and 2.0 mm with few sections outside this range as shown in Figure 40. A similar observation was made for the MTD values obtained using the sand patch test. Surfaces with higher MPD had higher MTD, and vice versa. Both MTD and MPD are used to describe the irregularities of pavement surface which is referred to as macrotexture. Two concrete sections had relatively high MPD and this is typical for textured concrete surface (e.g., longitudinal grooving).

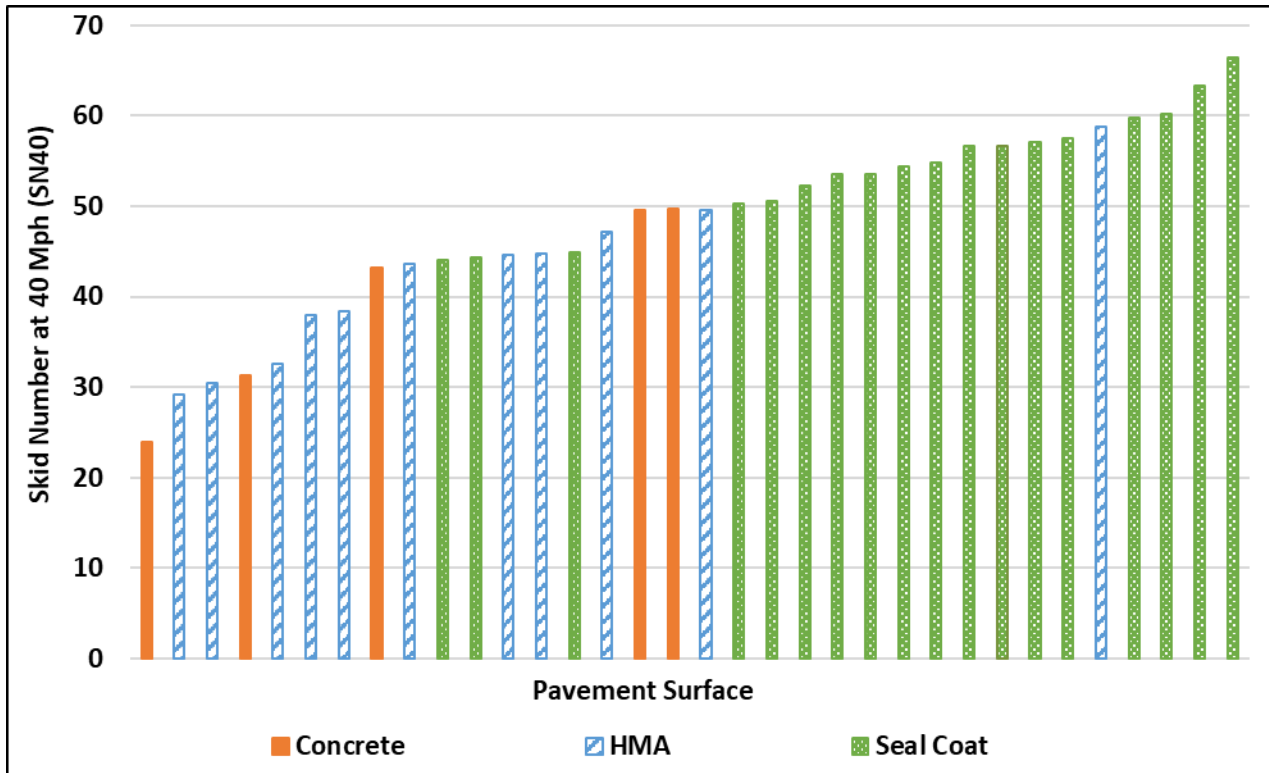


Figure 37. Skid Number Values at 40 mph for All Test Sections

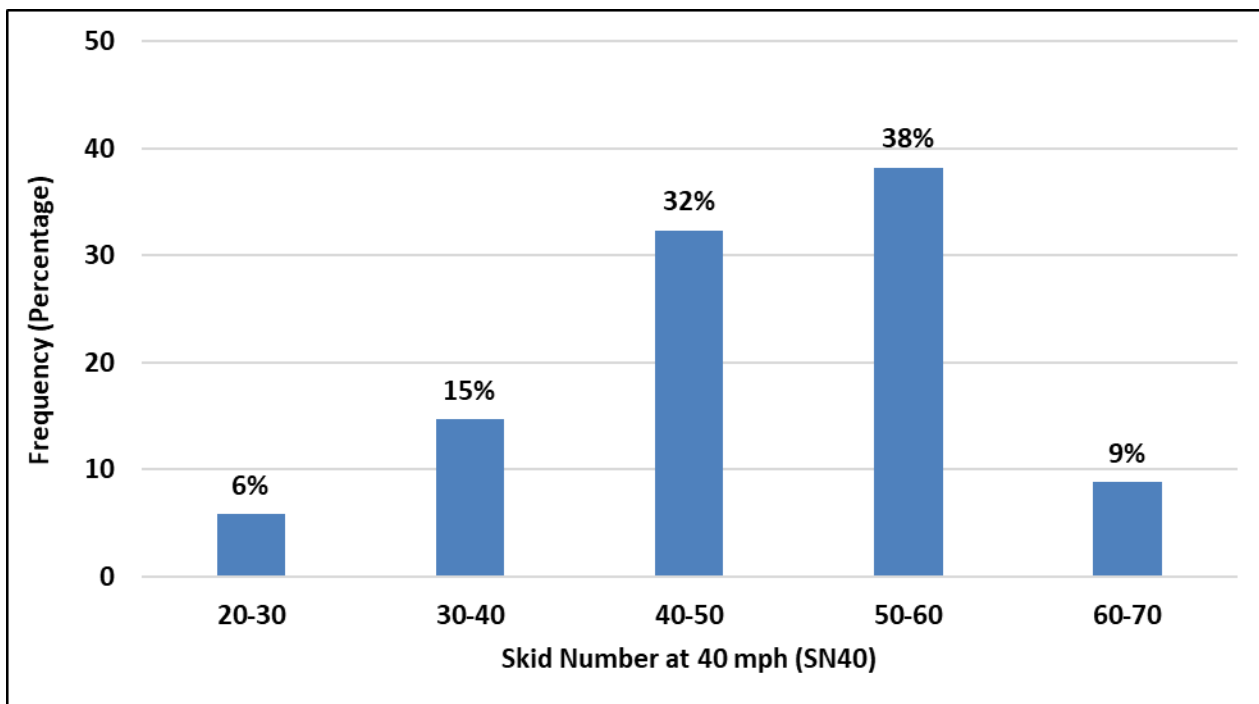


Figure 38. Distribution of Skid Number Measurements

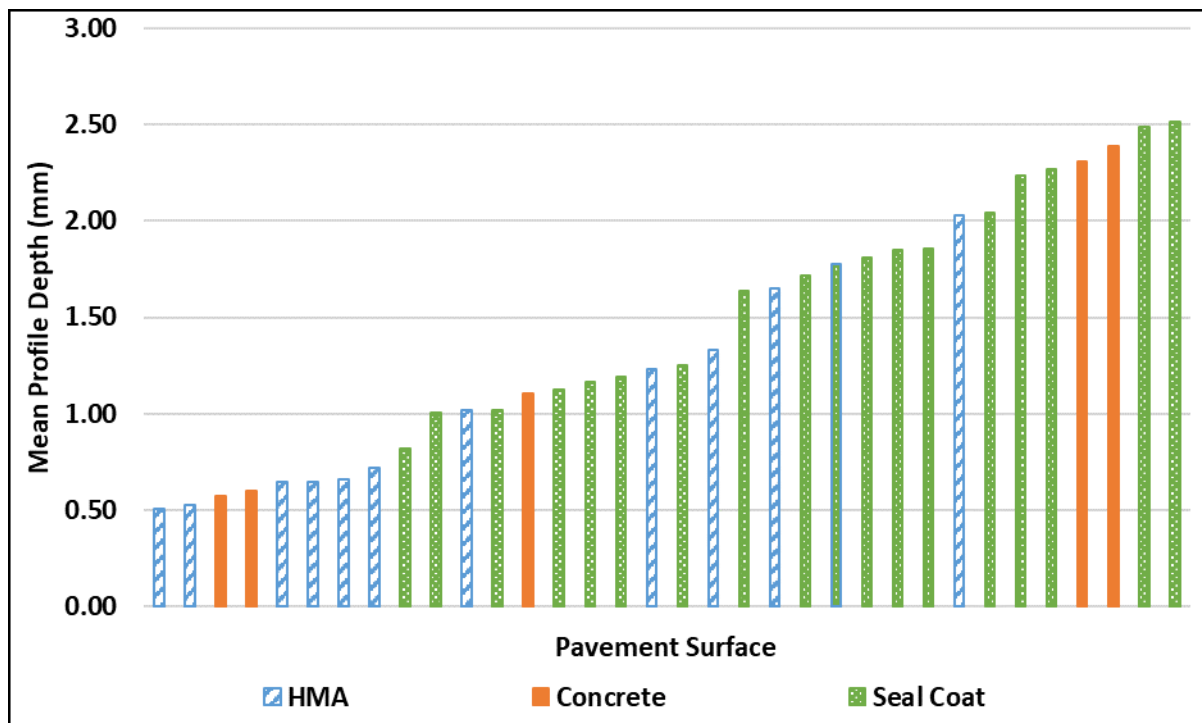


Figure 39. MPD Values for All Test Sections

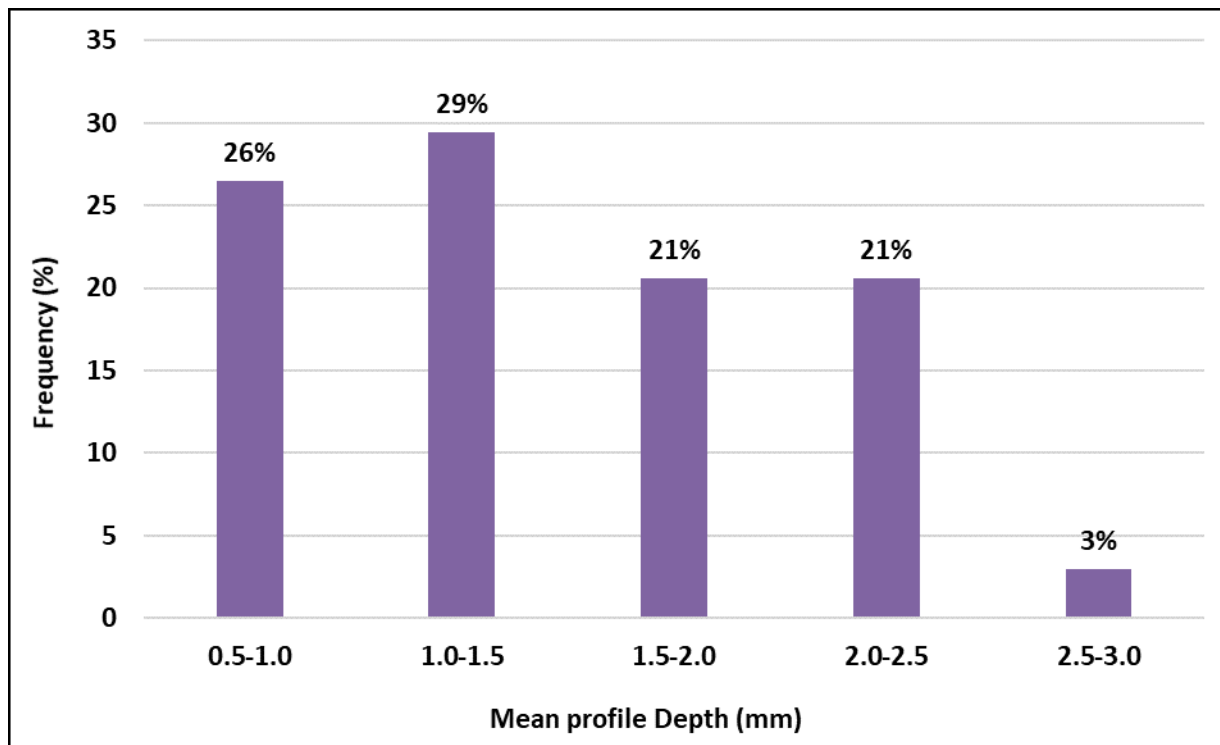


Figure 40. Distribution of MPD Measurements

## Effect of Pavement Surface on Friction Characteristics

The Analysis of Variance (ANOVA) was performed to examine the statistical significant difference ( $P < 0.05$ ) among various surface types (e.g., seal coat, HMA and concrete) in terms of skid number at 40 mph (SN40), pavement macrotexture (MPD) and microtexture (DFT). Tukey's Honestly Significant Differences (Tukey's HSD) results are presented in a form of letters. There is no statistically significant difference in the test results between surface types if they share the same letter (e.g., A, B, and C). Figure 41 demonstrates the results of Tukey's HSD analysis of skid number at 40 mph (SN40) for different pavement surfaces. The results showed that SN40 values for seal coat are statistically different from HMA and concrete at 95 percent confidence interval. Both HMA and concrete share the same letter (i.e., B). Figure 42 shows the MPD results. There is no significant statistical difference between HMA and concrete and between concrete and seal coat; however, the Tukey's HSD results showed that there is a significant difference in MPD between seal coat and HMA. The seal coat had higher MPD compared to HMA surfaces evaluated in this study.

Tukey's HSD results presented in Figure 43 showed that there is no significant difference in the microtexture (i.e., DFT<sub>20</sub>) among different surface types since all of them share the same letter (i.e., A) at 95 percent confidence interval. The DFT<sub>20</sub> values for various test sections had a small range which indicates insignificant difference in microtexture.

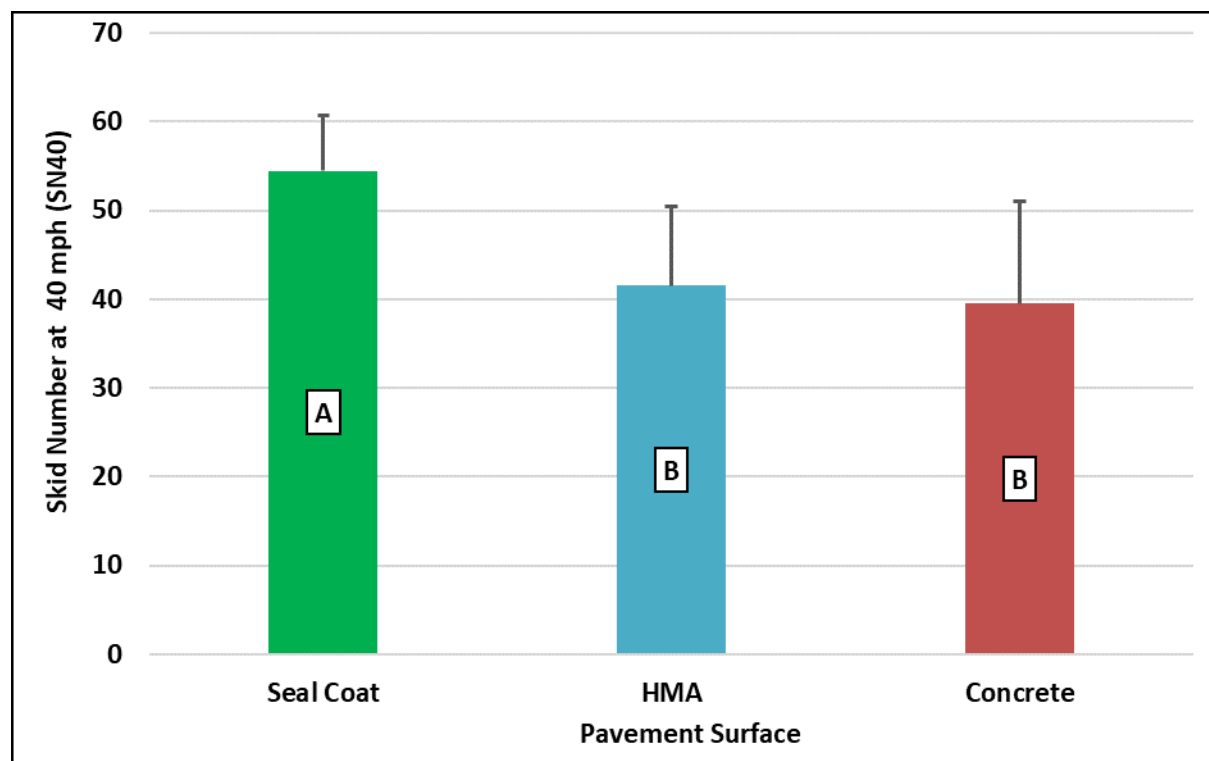


Figure 41. Average Skid Number at 40 Mph for Various Pavement Surfaces

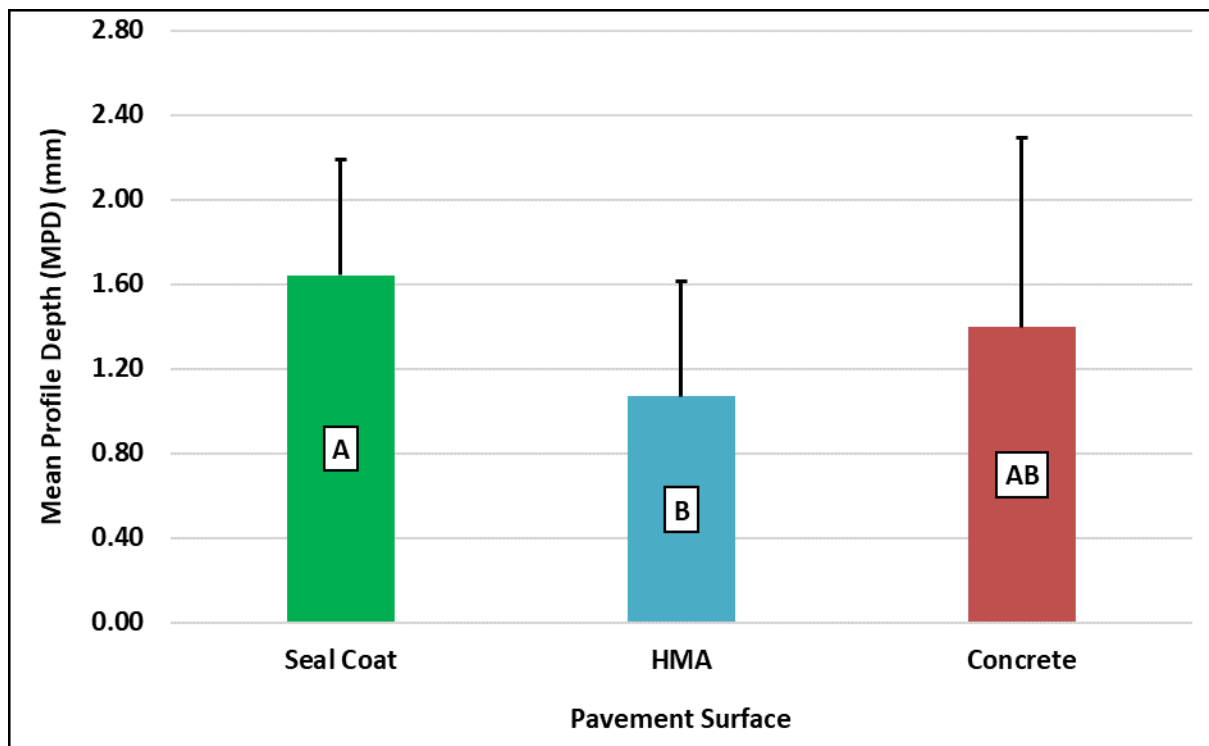


Figure 42. Average MPD for Various Pavement Surfaces

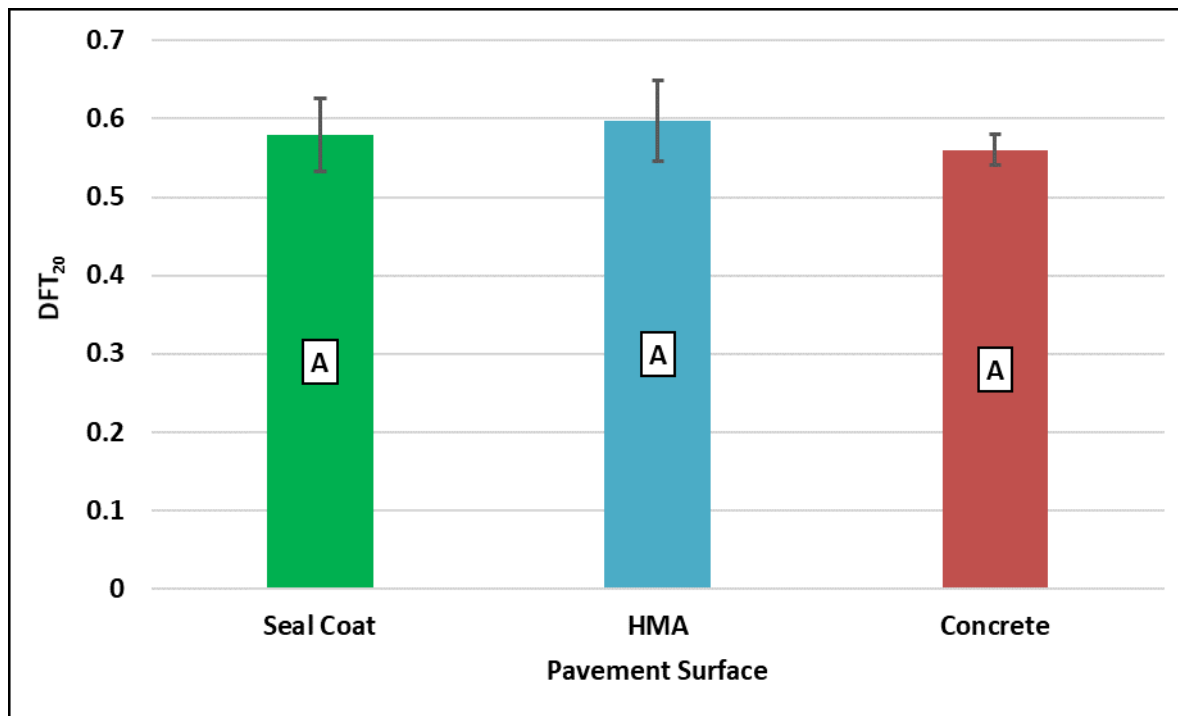
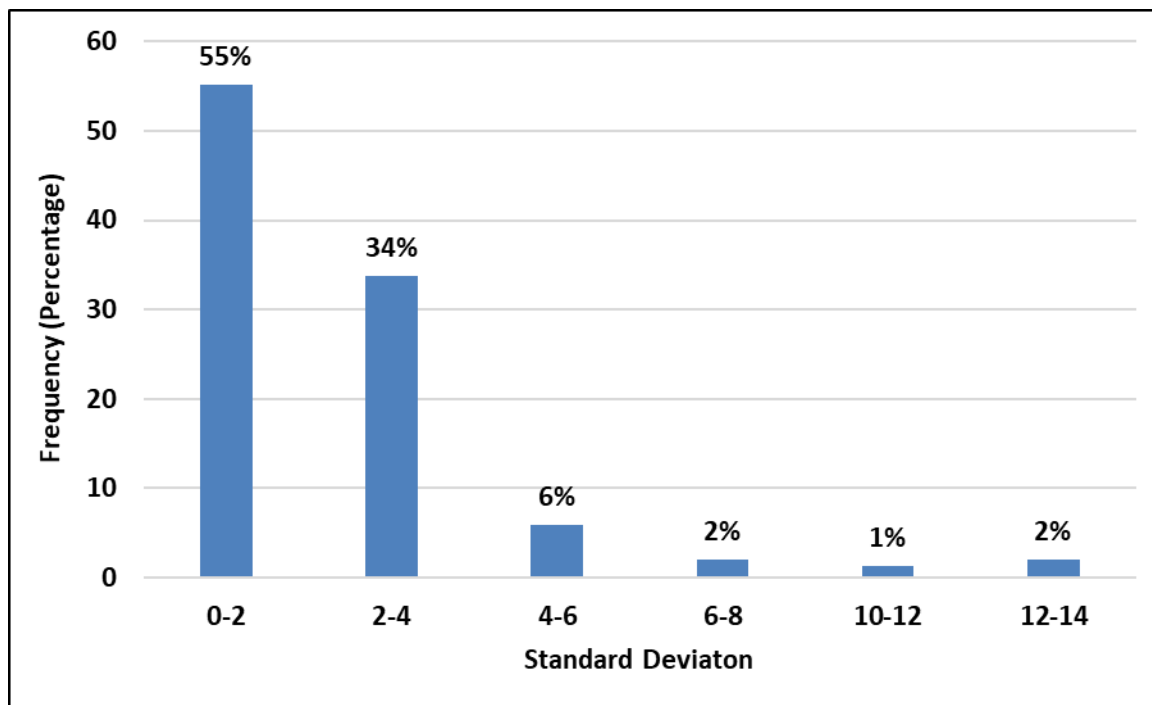


Figure 43. Average DFT<sub>20</sub> Values for Various Pavement Surfaces

## Variation of Skid Number Measurements

The skid trailer was used to collect several skid numbers each run, and the average skid number was calculated and considered to represent the skid resistance or number at a given speed. There is variation in the collected skid numbers since the pavement surface is not uniform and has irregularities. Figure 44 shows the frequency distribution for the standard deviation of skid number collected at 40 mph. The standard deviation ranged from 0.82 to 13.11, meanwhile, most of the test sections (89 percent) had low standard deviation (less than 4). The average standard deviation for test sections was 2.40.

Figure 45 shows the standard deviation with respect to the testing speed and mean profile depth. Overall, the standard deviation for the measured data was found to increase with the testing speed. The average standard deviation for the measured skid number was 2.71 at 20 mph and it increased to 3.21 at 60 mph. No significant difference was found in standard deviation of skid number measurements with MPD of the test sections.



**Figure 44. Distribution of Standard Deviation of Skid Number at 40 mph**

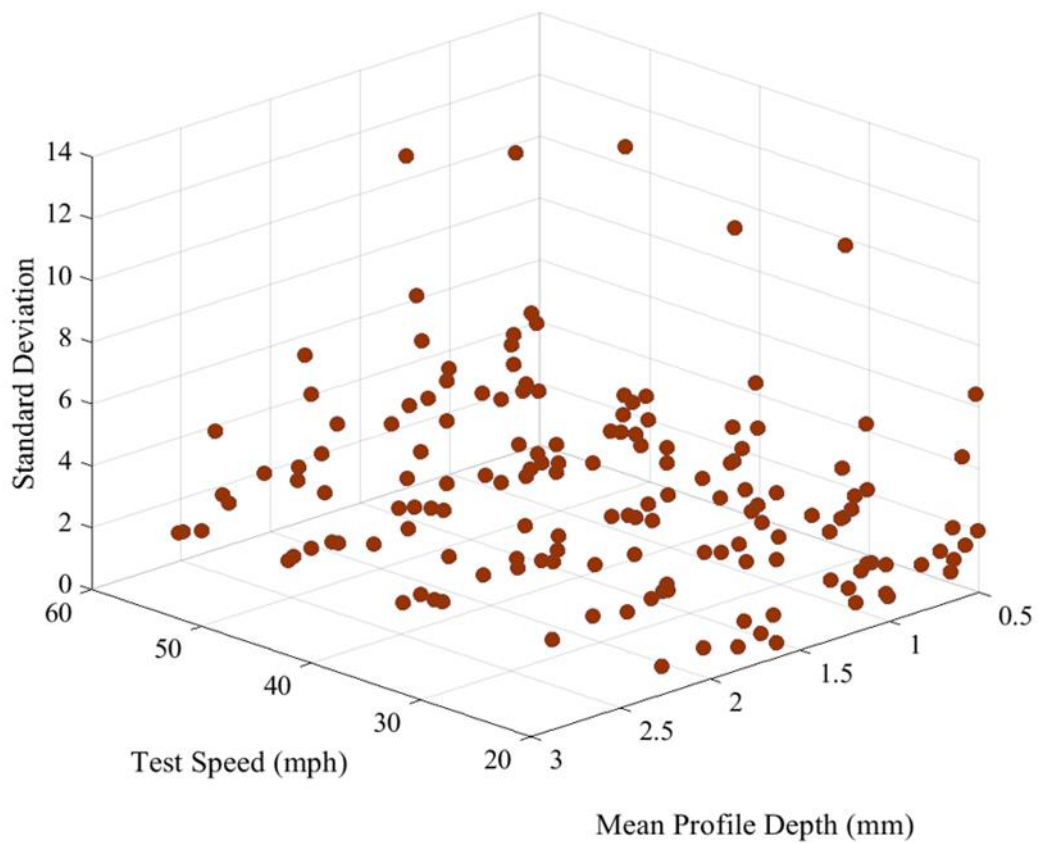


**Figure 45. Standard Deviation of Measured Skid Number at 40 mph vs. Speed and MPD**

## Correlation Between Friction, Speed and Texture

The measured skid number decreased with the increase in speed for all test sites as shown in Figure 46 to Figure 48. Most of the test sections and almost all HMA sections showed a logarithmic decrease in skid number as the speed increases. The  $R^2$  of the correlation was greater than 0.9 for all test sites. Some researchers reported linear relationship between skid number and speed while others found exponential decay with speed.<sup>7, 54, 56</sup> The change in skid number with speed was also found to be affected by the surface macrotexture as discussed in Chapter 2.<sup>19</sup> The skid number speed gradient ( $G_v$ ) was calculated to quantify the decrease in skid number with testing speed. The  $G_v$  is defined in ASTM E867 as the rate of change in skid number per unit change in speed. In this study, the  $G_v$  was calculated between 20 mph and 60 mph since most of friction tests were conducted over this range of testing speed. To maintain consistency in the  $G_v$  calculations and analysis, test sections where the skid testing could not be performed at either 20 mph or 60 mph were not considered in the  $G_v$  calculations.

Figure 49 shows the relationship between the  $G_v$  and MPD. The results demonstrated that the skid number speed gradient had a strong correlation with MPD. The  $G_v$  decreases with the increase in MPD. These results demonstrate that pavement surfaces with high MPD have less change in skid number with speed compared to those with low MPD. This finding is supported by previous research where it was found that the rate of change in skid number with speed is dependent on pavement macrotexture.<sup>19</sup> This information was used later in model development to describe the change in skid number with speed (Figure 53).

Figure 50 shows the relationship between mean texture depth (MTD) measured using the sand patch test and mean profile depth (MPD) measured using the laser profiler. The results demonstrated that there was a strong linear relationship between MTD and MPD. One can predict MPD by measuring MTD if the laser profiler is not available due to its cost. These findings are in good agreement with previous research studies where MTD and MPD were found to have good correlation.<sup>41, 45, 61, 62, 63, 64</sup> It should be noted that this relationship (Figure 50) was used in this study to estimate the MPD as a function of MTD for eight test sections where the researchers experienced some issues with the laser profiler.

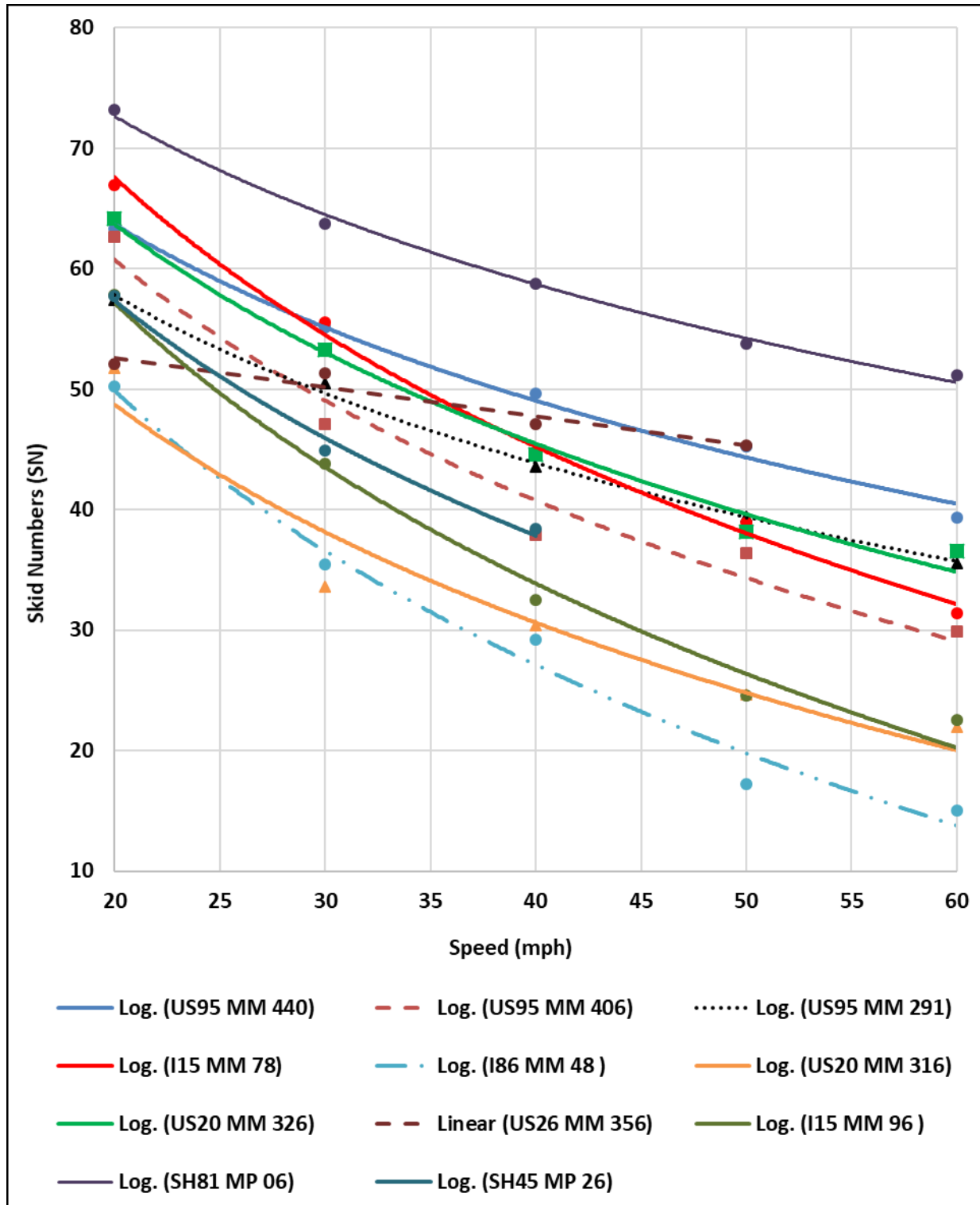


Figure 46. Skid Number vs. Speed for HMA Test Sections

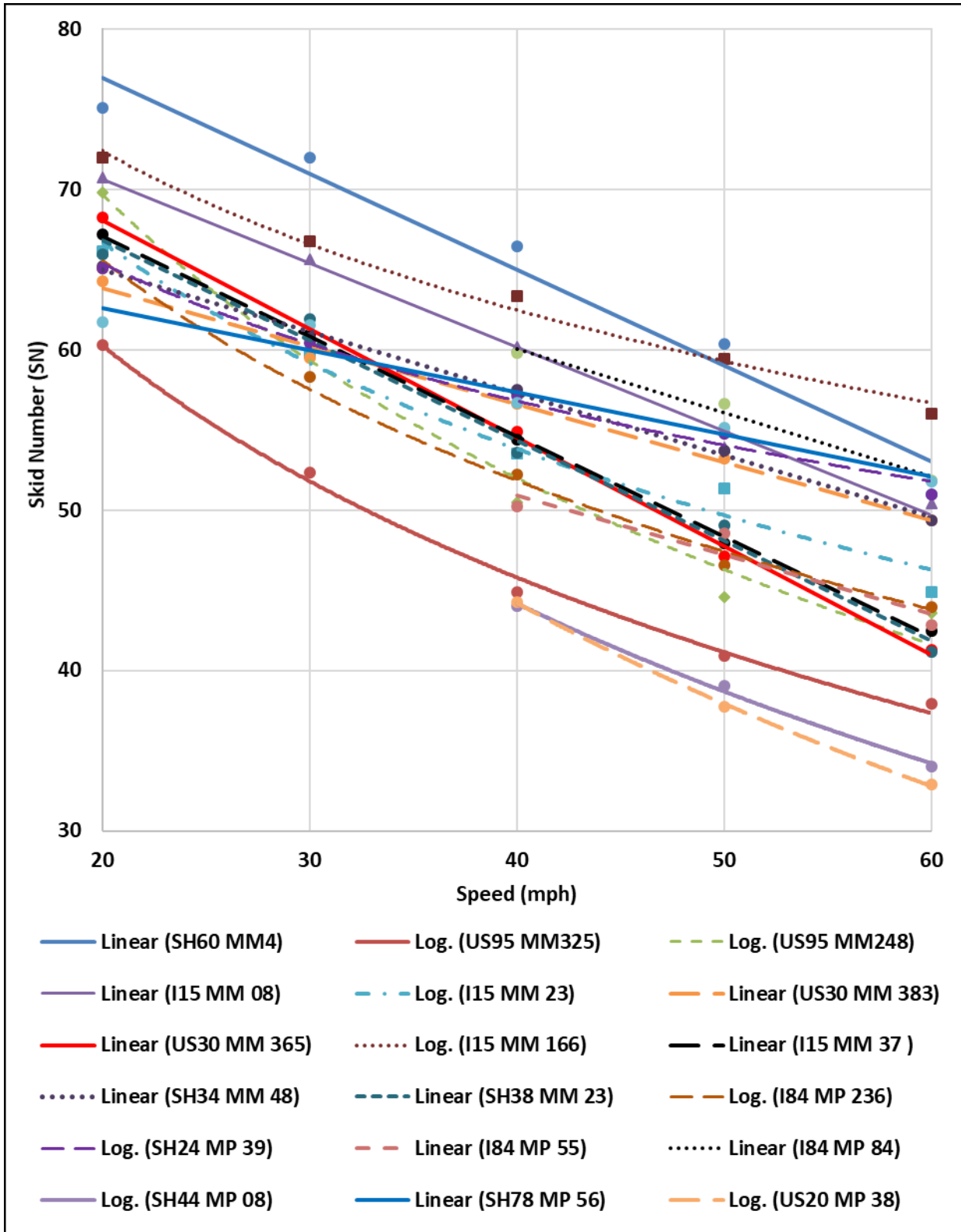
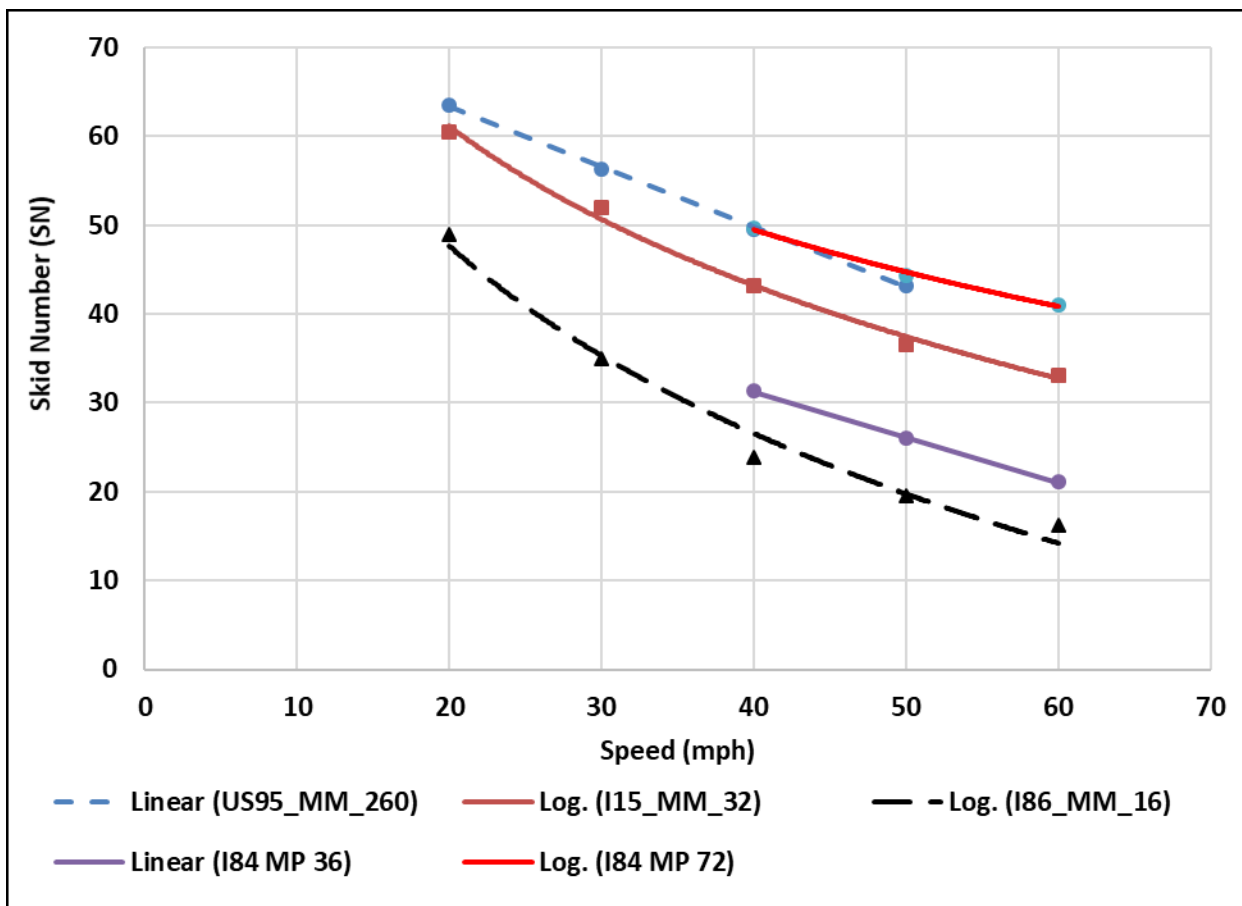


Figure 47. Skid Number vs. Speed for Seal Coat Test Sections



**Figure 48. Skid Number vs. Speed for Concrete Test Sections**

The results also demonstrated that there was a good correlation between the skid number at 60 mph and MPD for HMA and seal coat surfaces. The relatively low number of concrete sections may have affected the relationship between skid number and speed.

Figure 51 shows that there is a logarithmic correlation with  $R^2$  of 0.78 between skid number at 60 mph and MPD for HMA. The  $R^2$  of the correlation between the skid number and MPD increased with speed. The  $R^2$  increased from 0.03 (at 20 mph) to 0.78 (at 60 mph). Also, the  $R^2$  of the correlation between skid number and MPD increased from 0.01 at 20 mph to 0.16 at 60 mph for the seal coat surfaces. These findings are consistent with the literature since the macrotexture is more significant at high speed.<sup>26</sup> Appendix C provides additional figures that show the relationship between skid number and MPD for HMA and seal coat surfaces. On the other hand, the DFT<sub>20</sub> values measured using the DFT did not show any correlation with the measured skid number at various speeds (20, 30, 40, 50 and 60 mph) as demonstrated in Figure 52. It should be noted that most of the DFT<sub>20</sub> measurements were between 0.52 and 0.63. This indicates that most of the test sections had good microtexture. All plots of DFT<sub>20</sub> with skid number at various speeds are included in Appendix D.

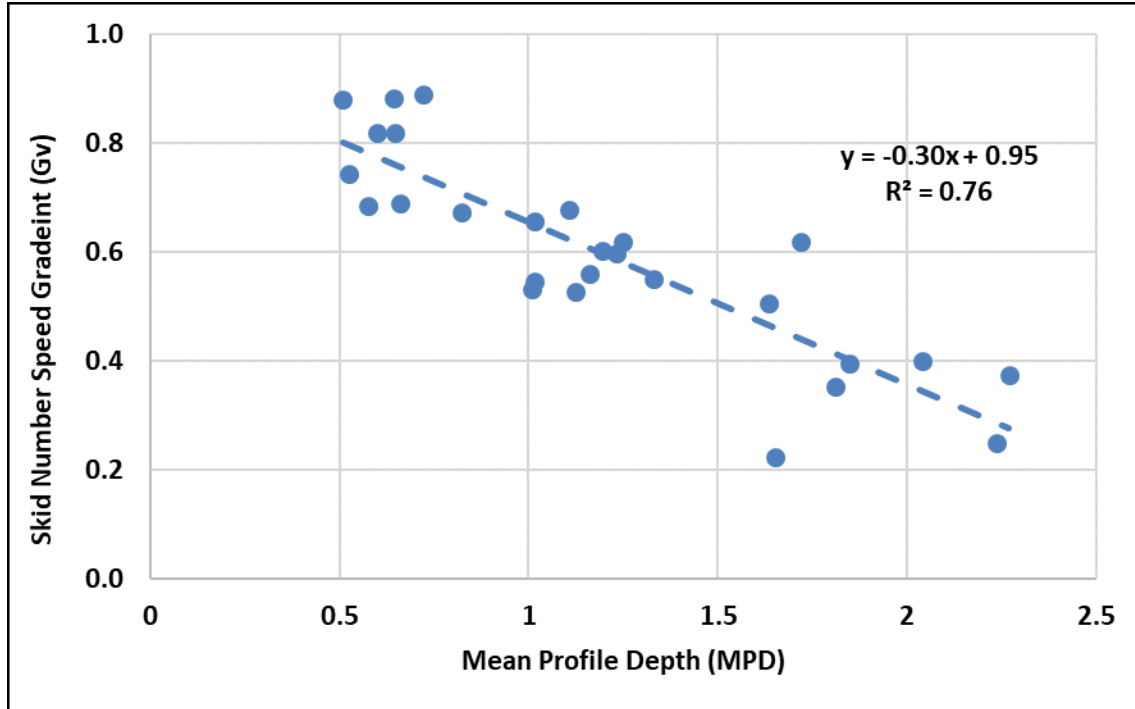


Figure 49. Relation of Skid Number Speed Gradient ( $G_v$ ) with Macrotexture

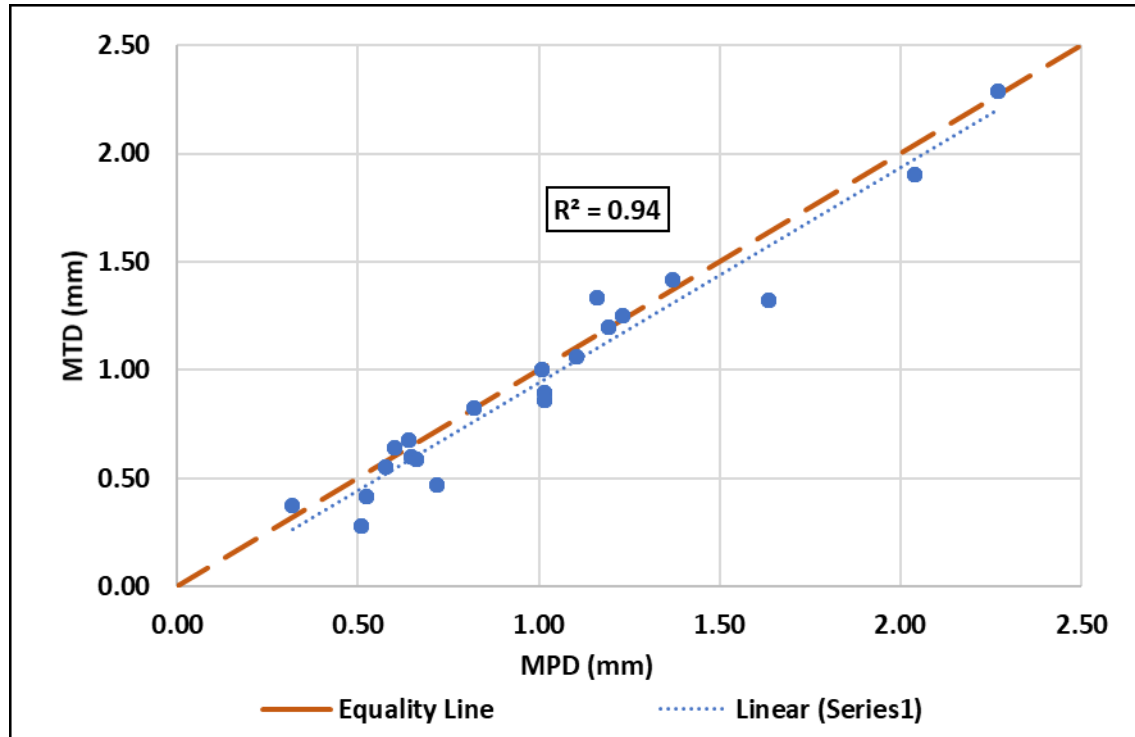


Figure 50. Relationship between Mean Texture Depth and Mean Profile Depth

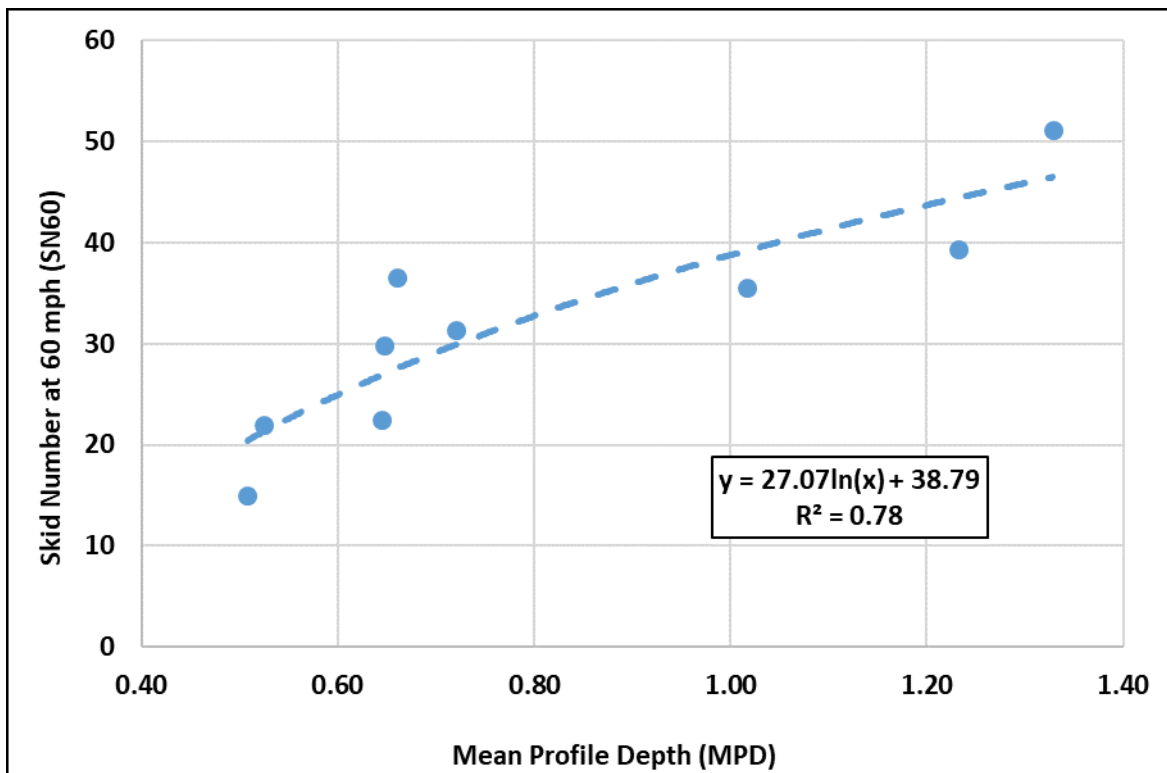


Figure 51. Skid Number at 60 mph Expressed as a Logarithm of Mean Profile Depth (HMA Sections)

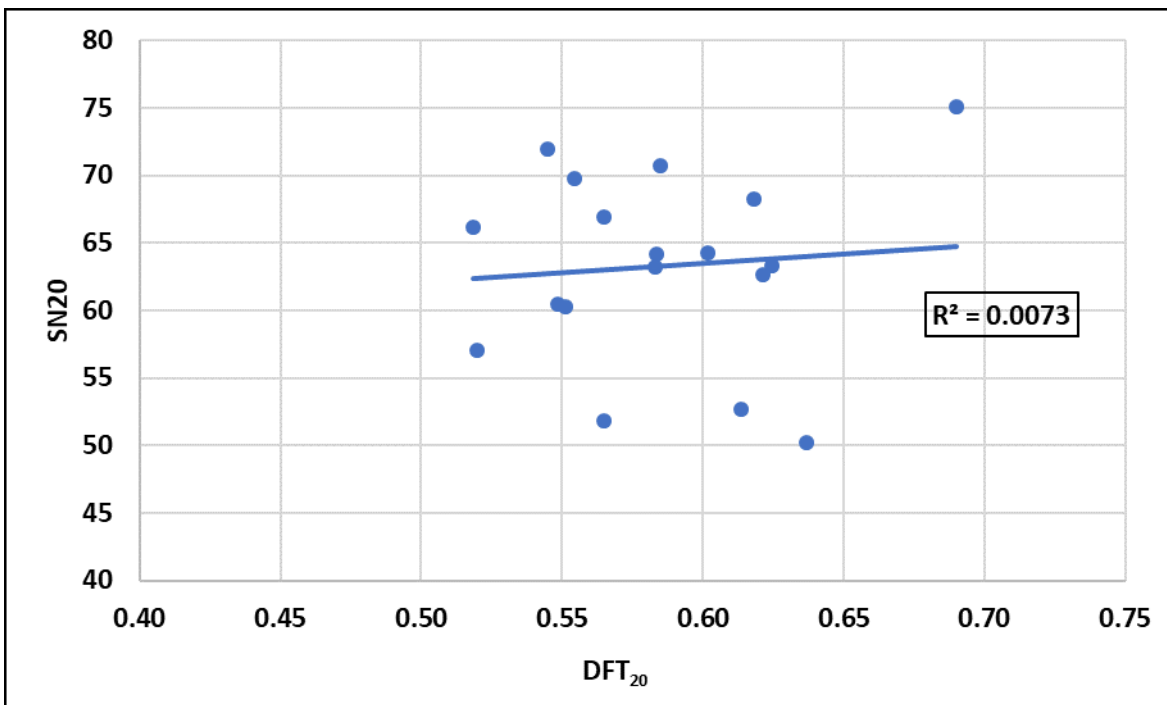


Figure 52. Skid Number at 20 Mph vs. DFT<sub>20</sub>

## Development of Prediction Model

This study investigated the correlation between skid number measurements at different speeds and surface texture measurements. The texture measurement included macrotexture measured using the laser profiler and sand patch test and microtexture measured using the DFT. The MPD can be measured simultaneously with skid testing unlike the MTD which requires traffic control. Since both MPD and MTD showed good correlation as one expects, MPD was used to describe the macrotexture. The statistical RStudio software was used to develop a model to describe the change in skid number as a function of surface texture.<sup>65</sup> The results showed that the change in skid number can be described using Equation presented in Figure 53. It should be noted that DFT<sub>20</sub> values were available for only 23 test sections out of 34 sections evaluated in this study since the use of DFT device in the field requires the use of traffic control. Including the DFT values didn't influence the rate of change of skid number with speed for these subset of test sections. Meanwhile, the microtexture mostly governs the magnitude of pavement friction which is incorporated in the measured skid number used in the model. Furthermore, previous research studies demonstrate that change in skid with speed is influenced by the macrotexture or MPD and not microtexture<sup>19</sup>. The proposed general model is represented in Figure 53.

$$SN_2 = 0.9991 * SN_1 - 22.2351 * \log(V_2/V_1) + 12.8467 * \log(MPD) * \log(V_2/V_1)$$

where,

$SN_2$  = Predicted Skid number at desired speed (V<sub>2</sub> mph)

$SN_1$  = Measured Skid Number at any speed (V<sub>1</sub> mph)

V<sub>2</sub> = Desired reference speed at which the skid number is predicted

V<sub>1</sub> = Speed at which the skid number is measured using skid trailer

MPD = Mean Profile Depth of surface texture (mm)

**Figure 53. General Prediction Model Equation**

The skid number measured at each speed was used along with the MPD to predict the skid number at other speeds. For example, the skid number measured at 30 mph was used to predict skid number measured at 20, 40, 50, and 60 mph. The predicted skid number values were within  $\pm 5.6$  of the measured skid number at 95 percent confidence level. Figure 54 shows the predicted skid number versus the measured skid number. The adjusted R<sup>2</sup> for the developed model is 0.95. The model presented in Figure 53 was developed based on 201 skid number data points. Table 5 summarizes the statistical parameters for the skid prediction model presented in Figure 53.

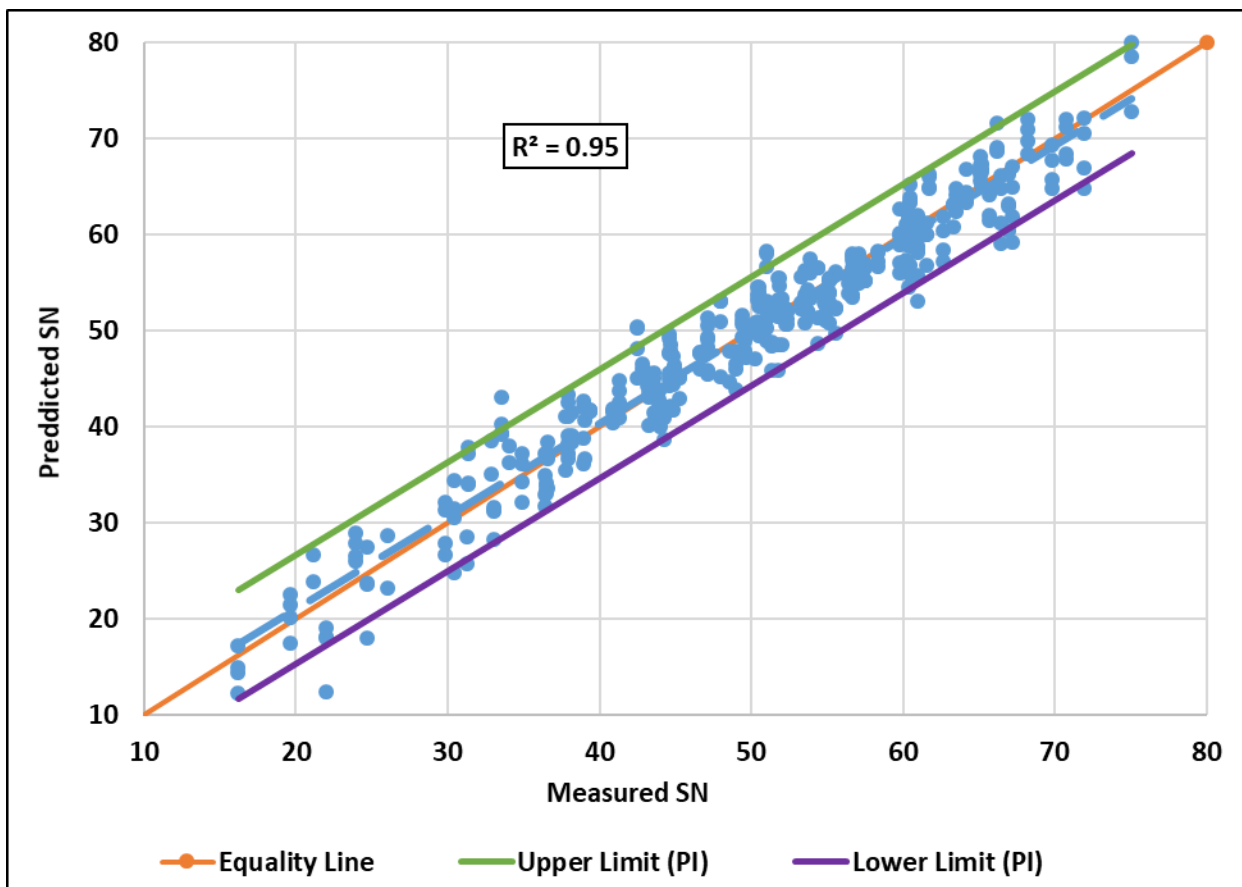


Figure 54. Predicted vs. Measured Skid Number (SN)

Table 5. Model Statistical Parameters

Parameter	Value
Adjusted R -Square	0.95
Residual Standard Error	2.42
Number of Observations	201
Prediction Interval (95 percent confidence)	$\pm 5.7$

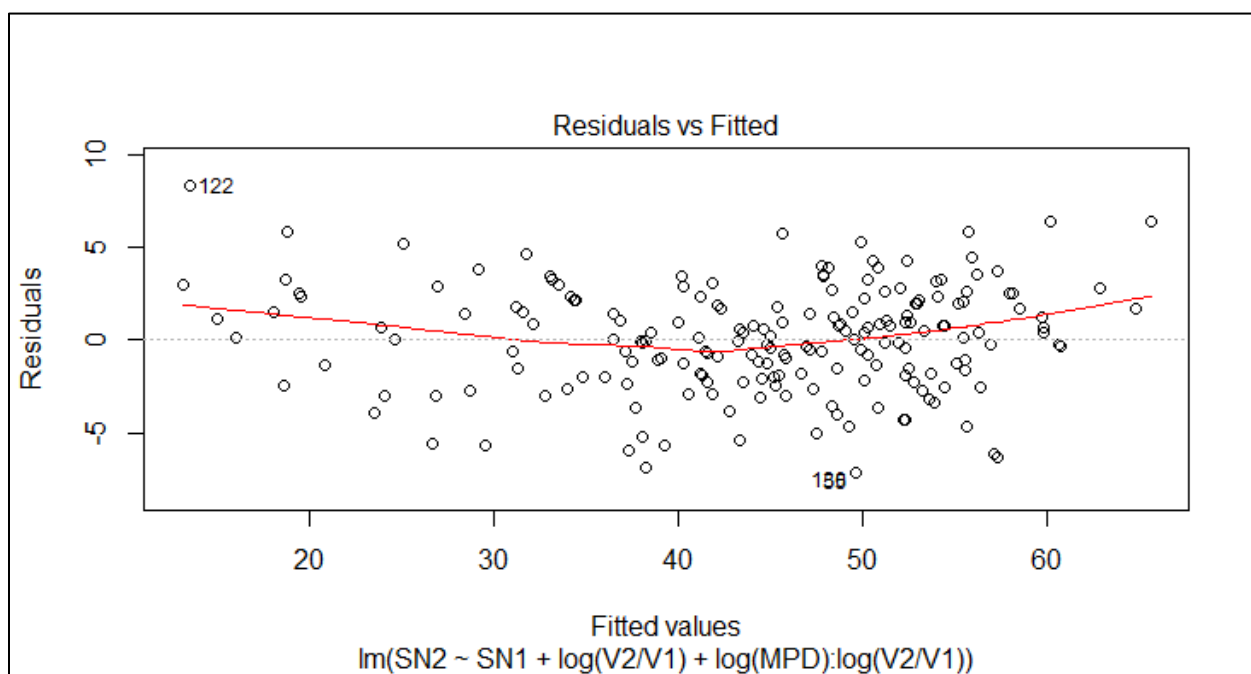
The researchers performed statistical checks for the developed prediction model using Rstudio.<sup>65</sup> The diagnostic checks were performed to statistically validate the prediction model including:

- Linear relationship between the outcome and the independent variable
- Normal distribution of the residuals
- Multi-collinearity between the independent variables
- Homoscedasticity

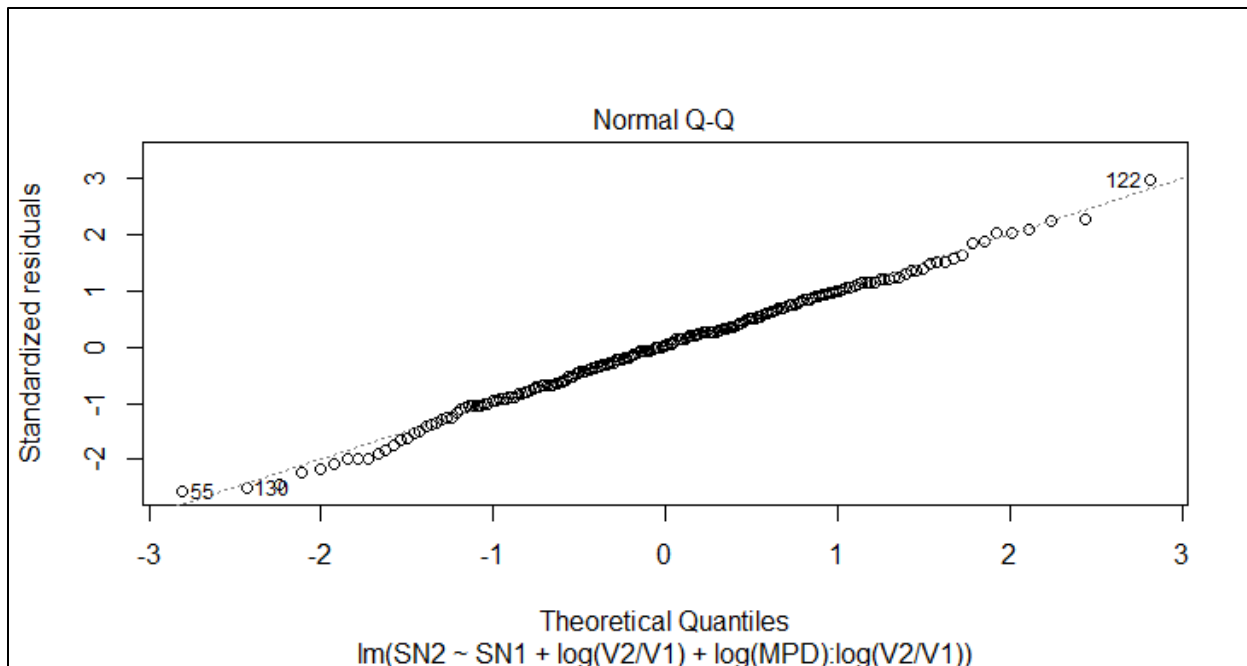
The diagnostic plot from RStudio was used to verify the assumption of the multilinear regression analysis. Figure 55 shows the model residuals versus fitted values (predicted skid number) of the model. The  $R^2$  for the developed model obtained from multilinear regression suggest that there is a strong linear relationship between the dependent and the independent variables. The results of Figure 55 demonstrate that there is no definite pattern between predicted values and residuals of the model, which indicates that there is no nonlinear relationship between the predicted and the predicting parameters of the model.

Figure 56 shows the normal probability plot of the residuals. This plot is used to check whether the residuals follow the standard normal distribution. The results of Figure 56 demonstrate that the residuals formed an approximate straight line and the points are close and equally distributed to the either side of the reference line. The linear regression assumes the residuals of the model are normally distributed which was satisfied for the developed model (Figure 56).

The variation inflation factor (VIF) was used to check for possible correlation between the independent variables of the model. It is assumed that if VIF is less than five, there is no significant correlation between the independent variables.<sup>66,67</sup> Table 6 presents the VIF values for the three independent parameters of the model. All the parameters had VIF values less than five which demonstrate that there is no multi-collinearity.



**Figure 55. Plot of Residuals vs. Fitted Data**



**Figure 56. Normal Probability Plot for the Prediction Model**

**Table 6. VIF Values for the Independent Variables in the Model**

$\text{SN}_1$	$\text{Log}(V_2/V_1)$	$\text{Log}(V_2/V_1) * \text{log}(\text{MPD})$
1.52	1.38	1.14

Figure 57 shows the scale or the spread location plot. This plot is used to check another assumption of multilinear regression which is homoscedasticity. The homoscedasticity is a condition when all residuals of the model are similar across all independent variables.<sup>68</sup> A horizontal line with equally spaced points in scale location plot indicates that the residuals are equally spread around the predictor variables. Figure 57 shows that this assumption of homoscedasticity is satisfied and accepted for the proposed model.

Besides the verification of the model assumption, it is also necessary to ensure that the developed model is free from any data that can significantly change the model fit or the regression. Such data points are called influential points. Figure 58 is the residual versus leverage plot for the obtained prediction model. The data points are influential if they are outside the Cook's Cutoff distance and have high leverage. Excluding or including those data points will change the regression model significantly. For the proposed model in this study, all data points with higher leverage are well inside the Cook's distance as shown in Figure 58 (the Cook's distance boundary is not visible). These results demonstrated that the proposed model is free from influential data points.

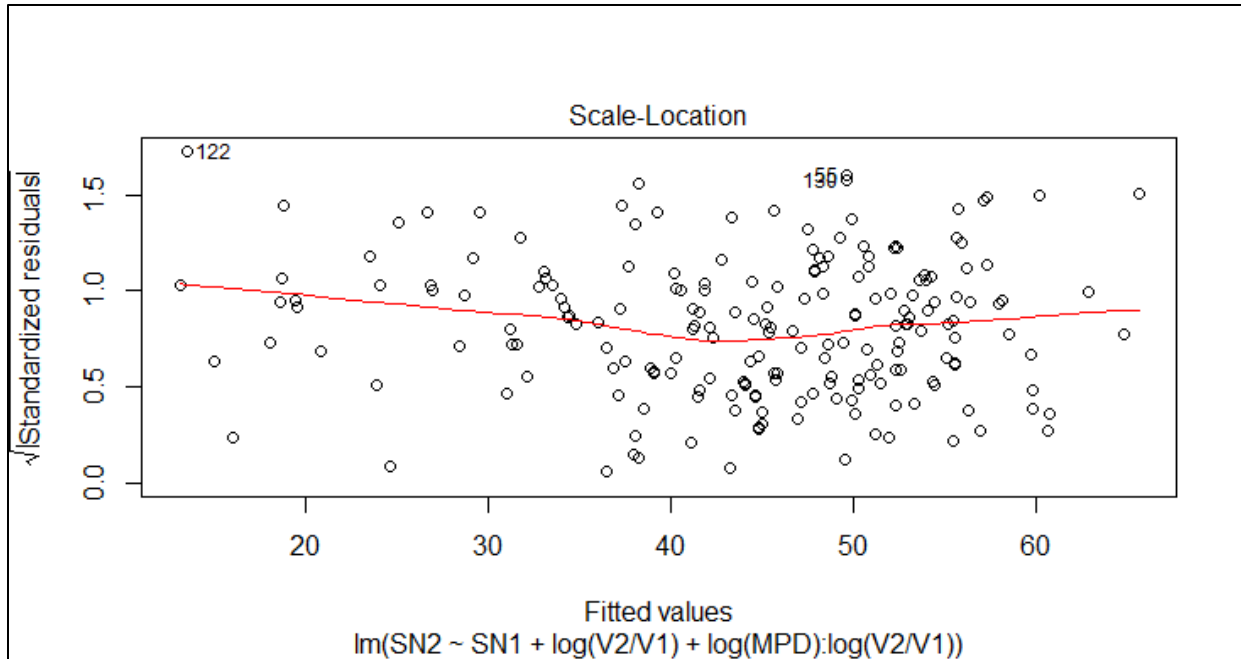


Figure 57. Standardized Residual Plot for the Prediction Model

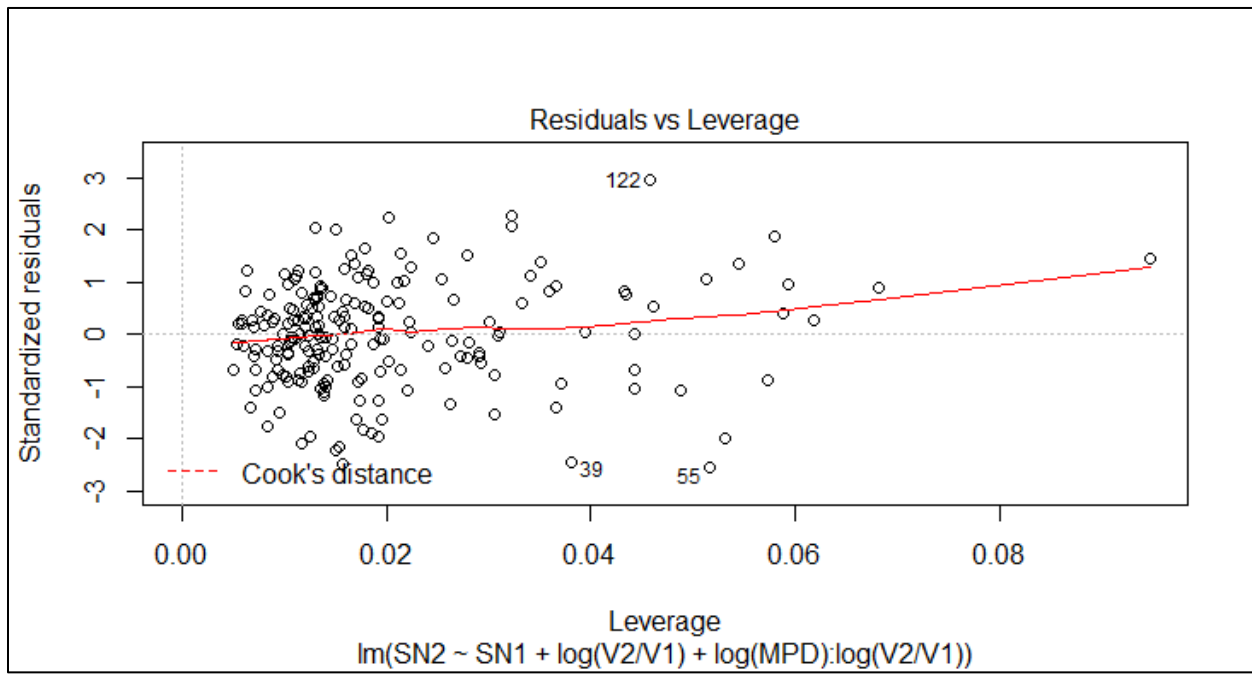
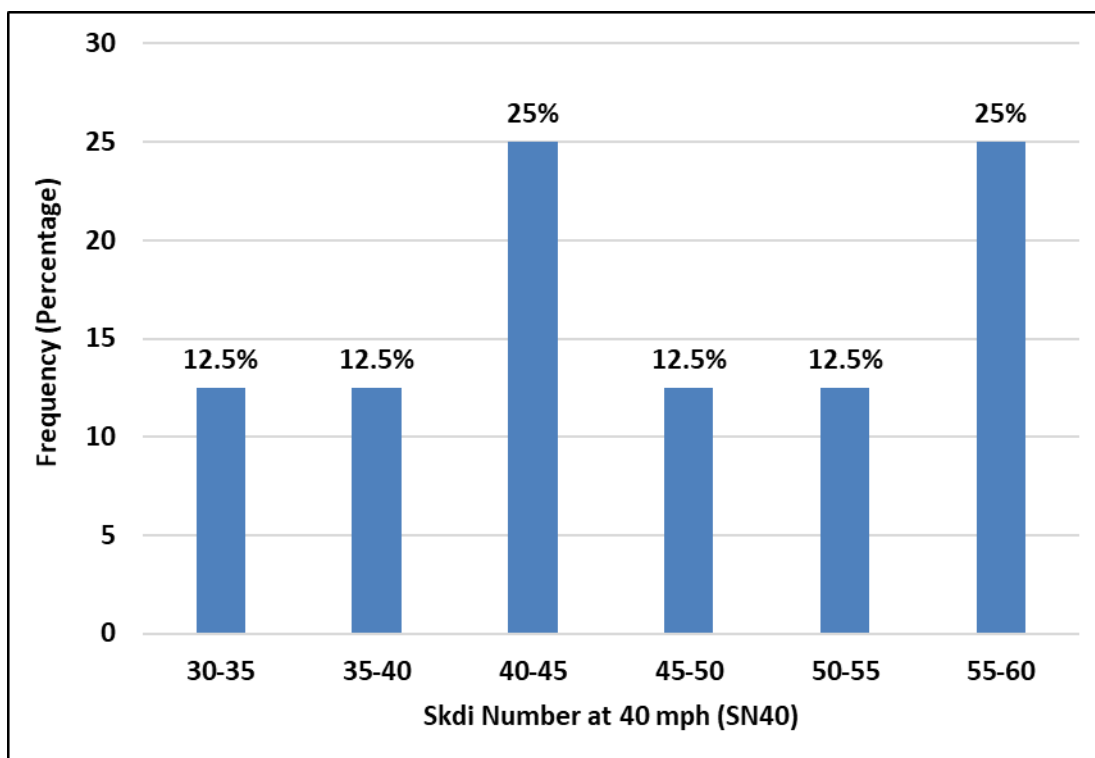


Figure 58. Plot of Residual vs. Leverage for the Prediction Model

## Model Validation

Eight test sections were used to validate the proposed prediction model. The skid measurements were collected at different speeds (i.e., 40, 50, and 60 mph). It was not possible to measure the skid at 20 and 30 mph for two sections due to safety of the crew since these measurements were collected at interstate and state highways where the posted speed limit is 70 mph and above. Figure 59 shows the distribution of the skid number at 40 mph for the test sections selected for validation. The sections cover a wide range of skid numbers similar to the sections used in model development. Figure 60 shows the relationship between predicted skid numbers and the measured ones for both model development and validation points. The results demonstrate that most of the validation points for the model are within the 95 percent prediction interval of the proposed model. In addition, the  $R^2$  for the validation is 0.94 which is similar to the one for model development ( $R^2 = 0.95$ ). These results clearly demonstrate that the model can be used to describe the change in skid number with speed as a function of MPD.



**Figure 59. Distribution of SN for Test Sections Selected for Validation**

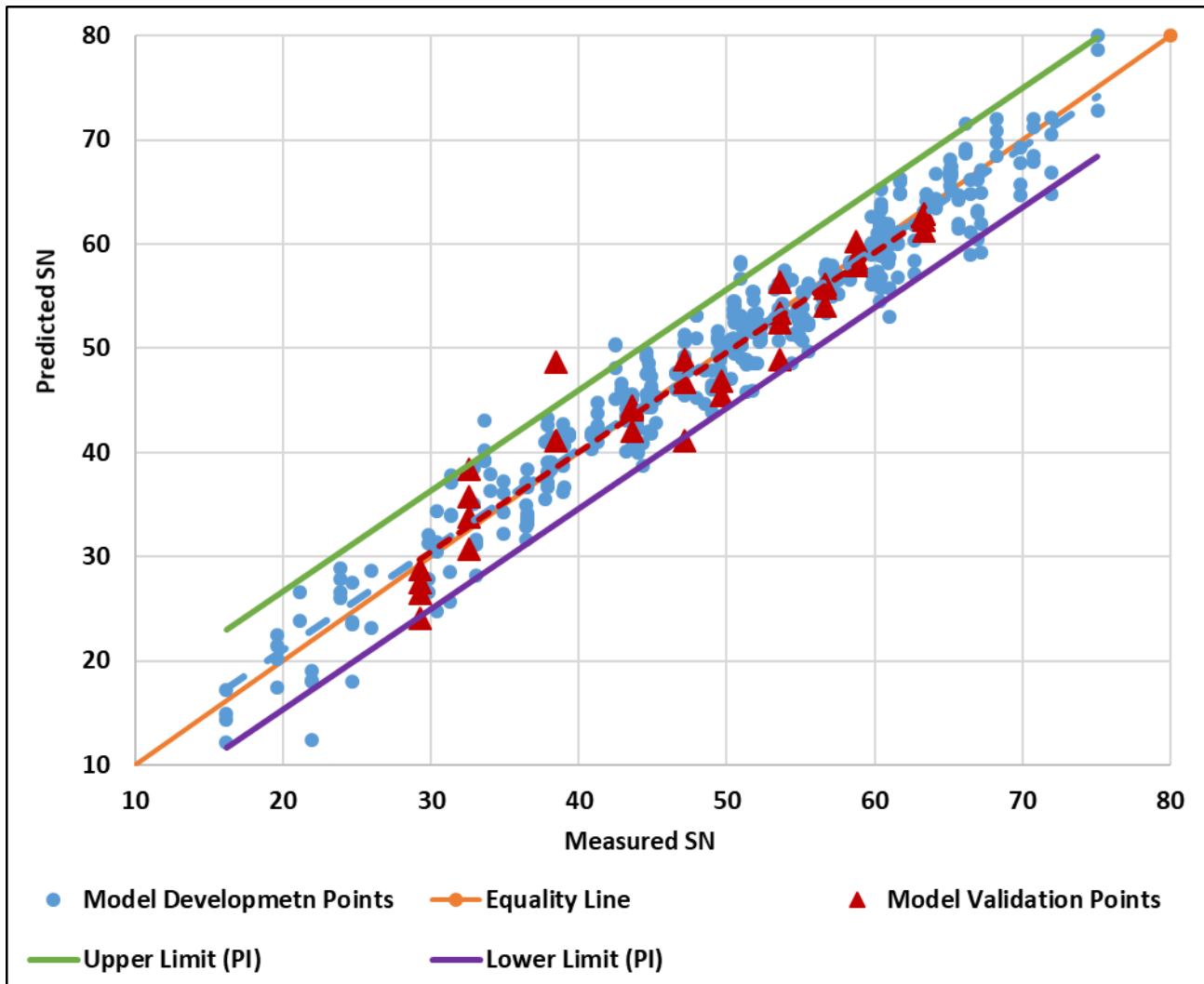


Figure 60. Predicted vs. Measured SN (Model Validation)

## Individual Prediction Models

This study also investigated the development of separate prediction models for each pavement surface (i.e., seal coat, HMA, and concrete). The objective was to assess any advantage of the separate models over the general model (Figure 53) in terms of model accuracy. The researchers utilized the same model parameters used in Figure 53 to describe the change in skid number with speed for each pavement surface. This section discusses the development of separate prediction models and a comparison with the general model.

### Model for Seal Coat Surface

Figure 61 presents the final proposed model for seal coat surfaces. Similar to the general model, the skid number at a reference speed is a function of measured skid number ( $SN_1$ ), pavement macrotexture (MPD) and the ratio of reference speed ( $V_2$ ) to test speed ( $V_1$ ). A total number of 113 data points were used for model development and 18 for model validation. Figure 62 shows the predicted and measured skid numbers for seal coat surfaces. Similar to the general models, most of the data points used for model development and validation were within the 95 percent prediction interval of the proposed model.

$$SN_2 = 1.09 * SN_1 - 24.69 * \log(V_2/V_1) + 16.10 * MPD * \log(V_2/V_1) - 5.55$$

**Figure 61. Prediction Model Equation for Seal Coat Surfaces**

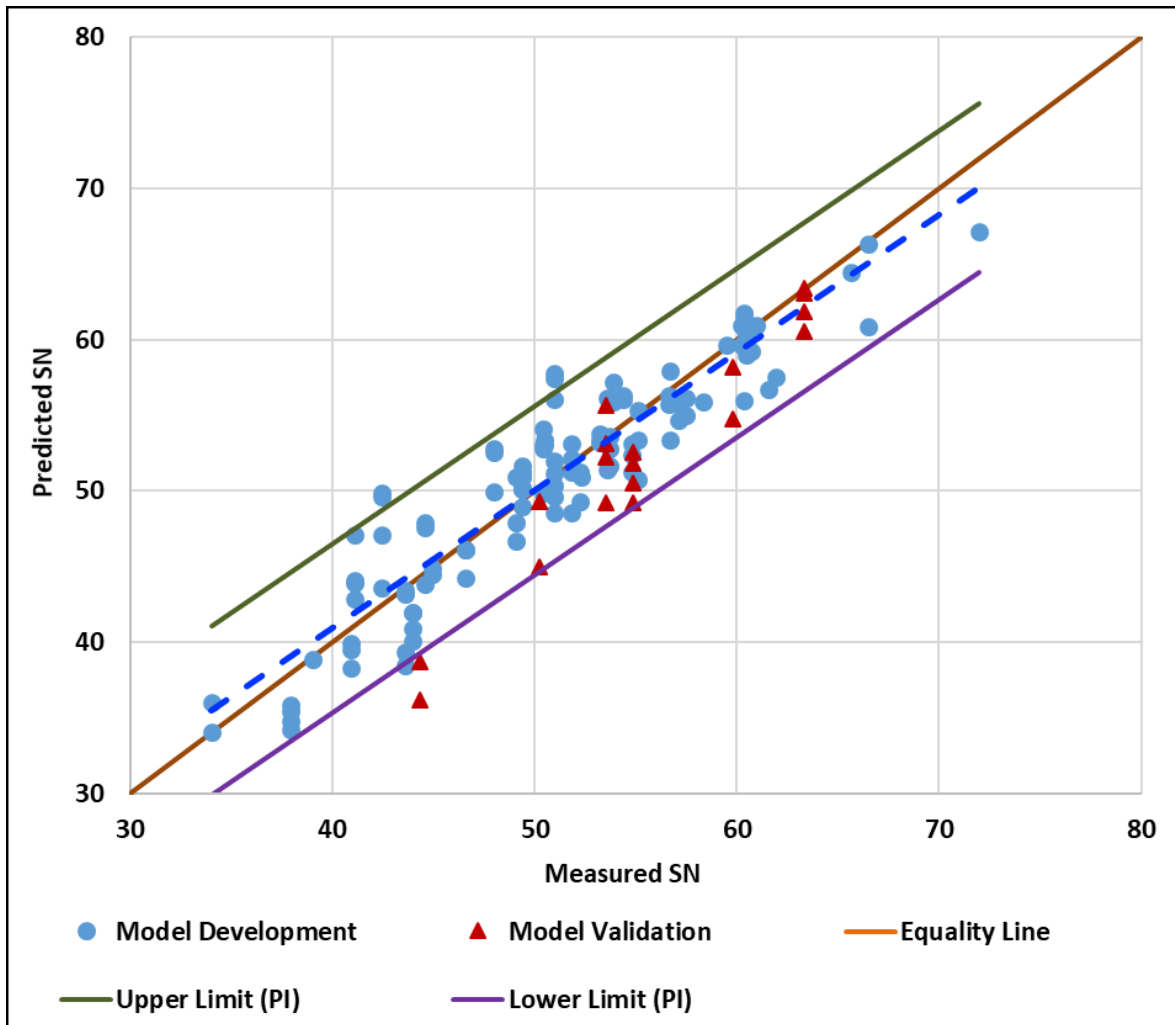


**Figure 62. Seal Coat Skid Model**

### Model for HMA Pavements

Figure 63 represents the prediction model for HMA pavements. The prediction model is similar to that of seal coat with slightly different values for the model parameters. A total number of 69 data points were used for model development and 12 for model validation. Figure 64 shows the model development and validation for HMA pavements. Although the HMA model used a smaller number of data points for model development and validation compared to seal coat model, the  $R^2$  (0.92) for the HMA was higher than the one of seal coat model ( $R^2 = 0.69$ ). However, the seal coat model has lower prediction interval ( $\pm 5.6$ ) as compared to that of HMA ( $\pm 6.98$ ) suggesting lower variation in predicted skid number by seal coat model. The model slightly overestimates the skid number before 40 mph and slightly underestimates the skid number after 40 mph. With few validation data points, all of them are within the range of model development.

$$SN_2 = 0.79 * SN_1 - 18.84 * \log(V_2/V_1) + 11.92 * \log(MPD) * \log(V_2/V_1) + 8.62$$

**Figure 63. Prediction Model Equation for HMA Surfaces**

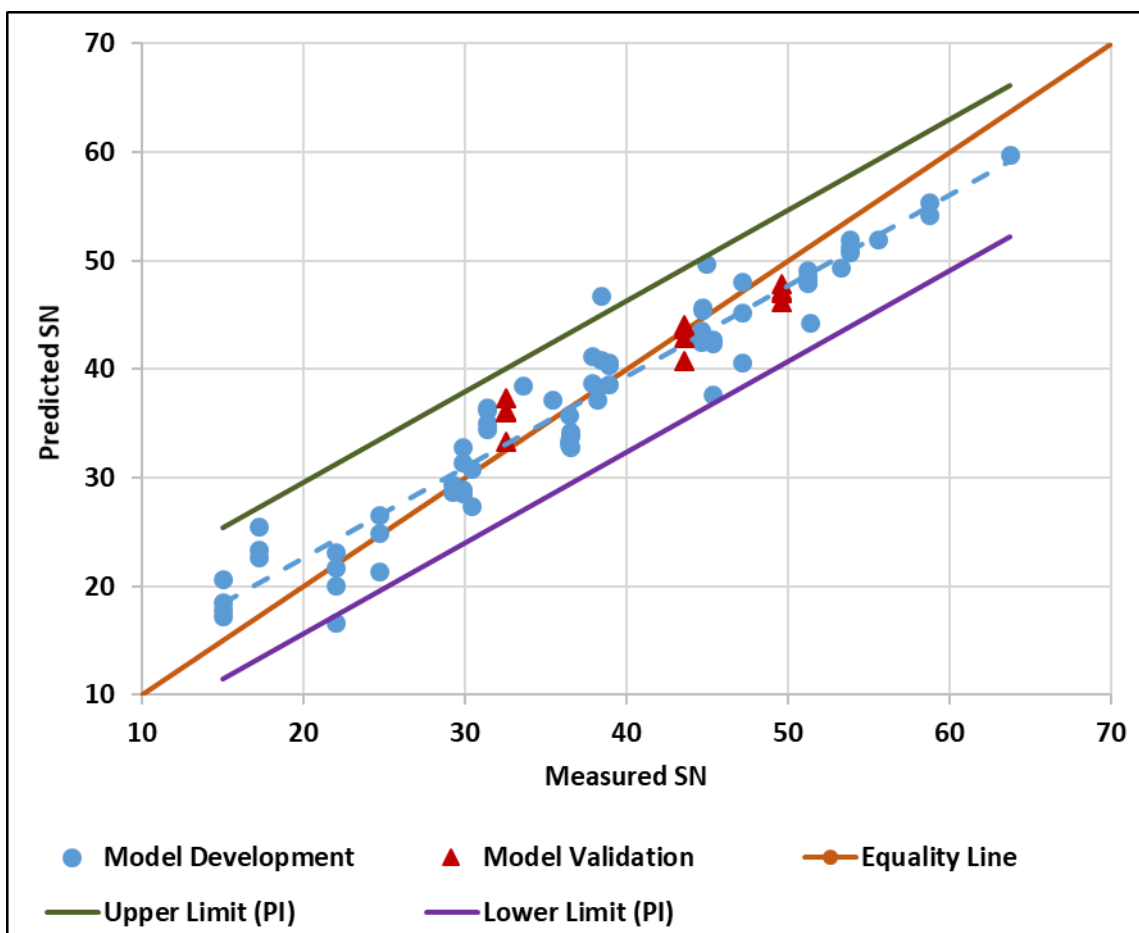


**Figure 64. HMA Skid Model**

### Model for Concrete Pavements

The model for the concrete pavement used the same parameters as seal coat and HMA except for the intercept (constant) value as shown in equation presented in Figure 65. The model intercept was found to be insignificant for concrete surfaces, therefore it was not included. The model development is similar to HMA with predictions slightly higher for speed below 35 mph and slightly lower for speed above 35 mph. The model validation data; however, were all in the lower range of model development as shown in Figure 66. A total number of 26 data points were used for model development and 4 for model validation. Due to the limited number of concrete sections included in this study, it is recommended to validate the model with additional test sections.

$$SN_2 = 0.88 * SN_1 - 19.70 * \log(V_2/V_1) + 11.74 * \log(MPD) * \log(V_2/V_1)$$

**Figure 65. Prediction Model Equation for Concrete Surfaces**

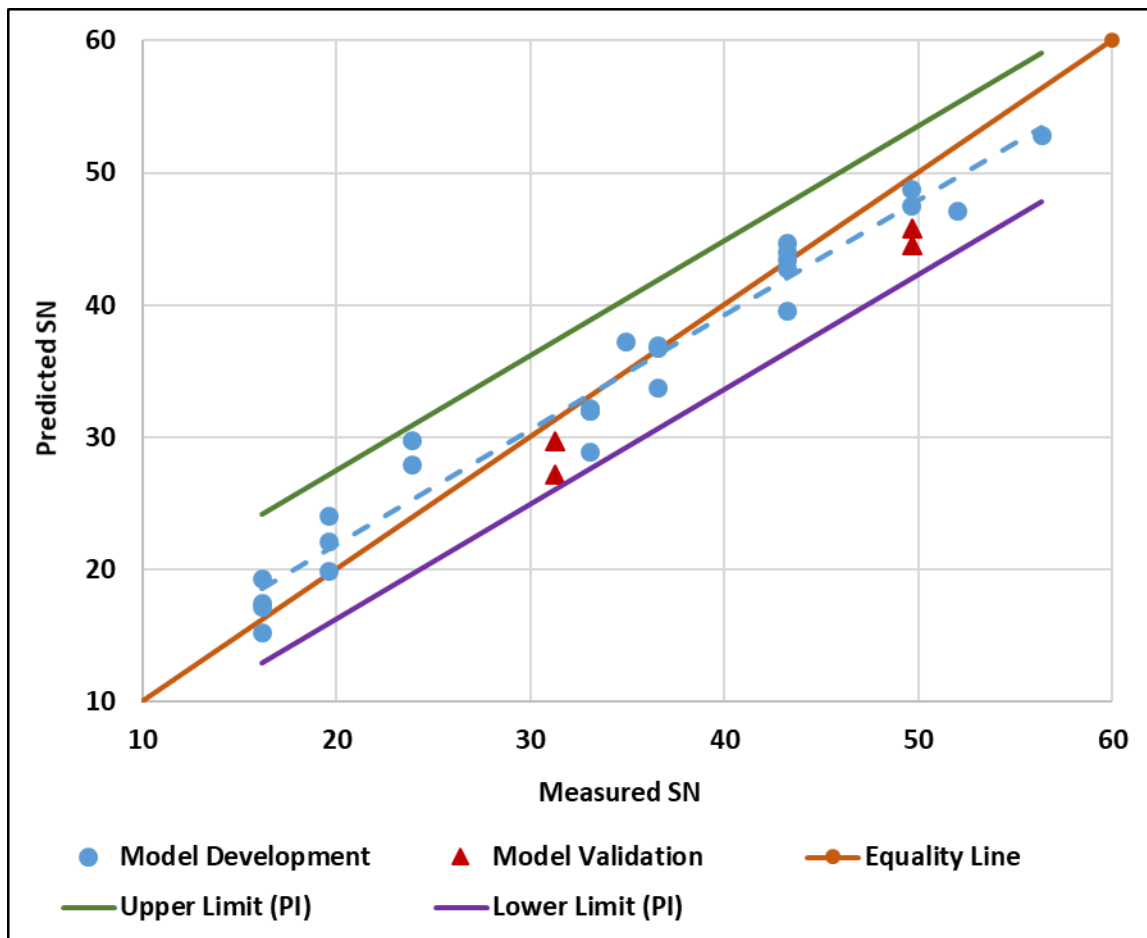


**Figure 66. Concrete Skid Model**

## Comparison between Models

Table 7 summarizes the main statistical parameters of the individual and general models. The coefficient of determination ( $R^2$ ) is approximately same for all the models except for seal coat model ( $R^2 = 0.69$ ) which is considerably lower compared to HMA ( $R^2 = 0.92$ ) and concrete surfaces ( $R^2 = 0.96$ ). The quality of seal coat construction and proper application rate may affect the skid resistance of seal coat surfaces. The residual standard error was the lowest for the general model. The HMA and concrete models had higher residual standard errors compared to seal coat and the general model. The number of data points used for model development is 201 for the general model while, only 26 data points were used for the model development of skid model for concrete. The prediction interval of skid number for all models was similar (about  $\pm 5.6$ ) except for HMA which was higher ( $\pm 6.98$ ). Comparing all the parameters for the developed prediction models, it was found that the general model can be used to describe the change in skid with speed regardless the surface type with an accepted accuracy. The general model was developed based on a large of data set with good  $R^2$  of 0.94 and low residual standard error.

**Table 7. Statistical Parameters for Individual and General Model**

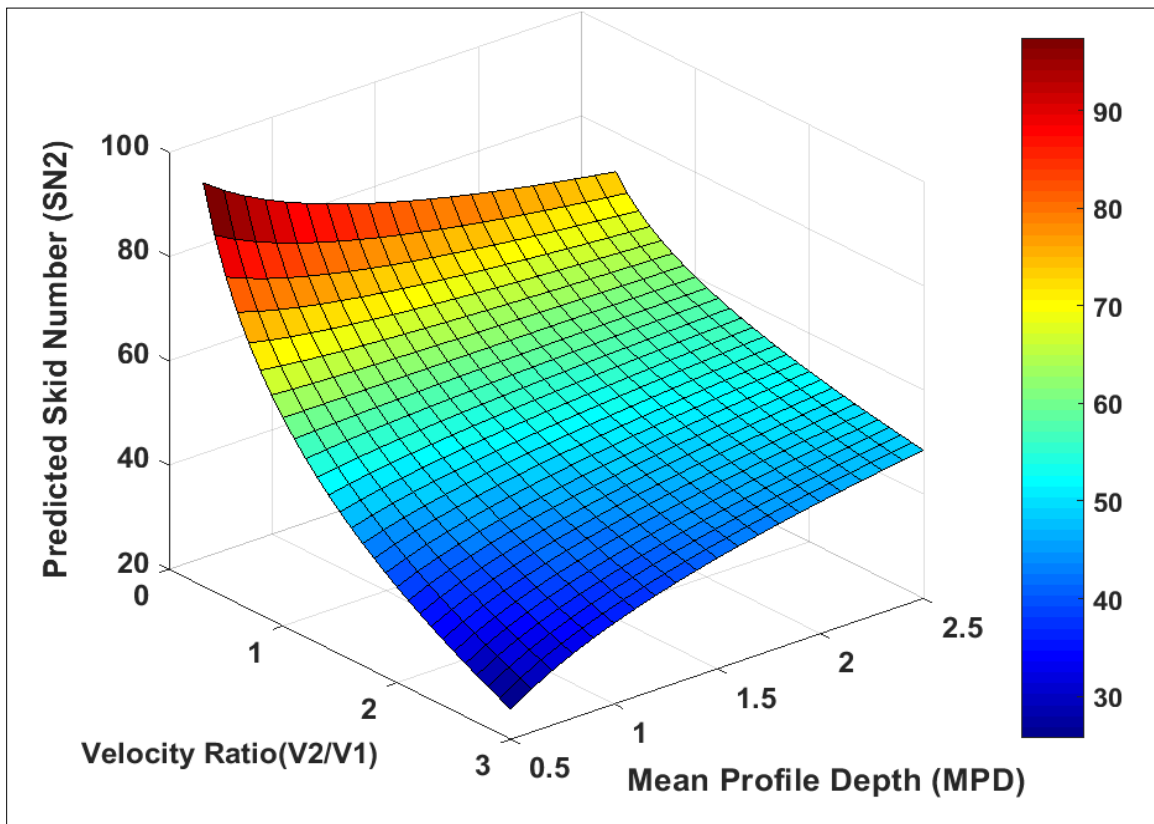
Models	General	Seal coat	HMA	Concrete
Adjusted R -Square	0.94	0.86	0.92	0.96
Residual Standard Error	2.95	2.78	4.02	3.17
Number of Observations	201	113	69	26
Prediction Interval (95 percent confidence)	$\pm 5.7$	$\pm 5.6$	$\pm 6.98$	$\pm 5.6$

## Sensitivity Analysis of the Model

The proposed prediction model presented in Figure 53 is a function of three input parameters; measured skid resistance ( $SN_1$ ) at a given speed ( $V_1$ ) and a desired reference speed ( $V_2$ ) at which the skid number needs to be calculated ( $SN_2$ ), and mean profile depth (MPD) of the test surface. The velocity ratio ( $V_2/V_1$ ) term combines both speeds (i.e.,  $V_1$  and  $V_2$ ). Each of these input parameters affects the predicted skid number ( $SN_2$ ). A sensitivity analysis was performed to study the effect of input parameters on the predicted skid number. The MATLAB software was used to create a three dimension surface plot to show the variation in predicted skid number ( $SN_2$ ) due to the change in each input parameters.<sup>69</sup> The results of the sensitivity analysis are shown in Figure 67 through Figure 69.

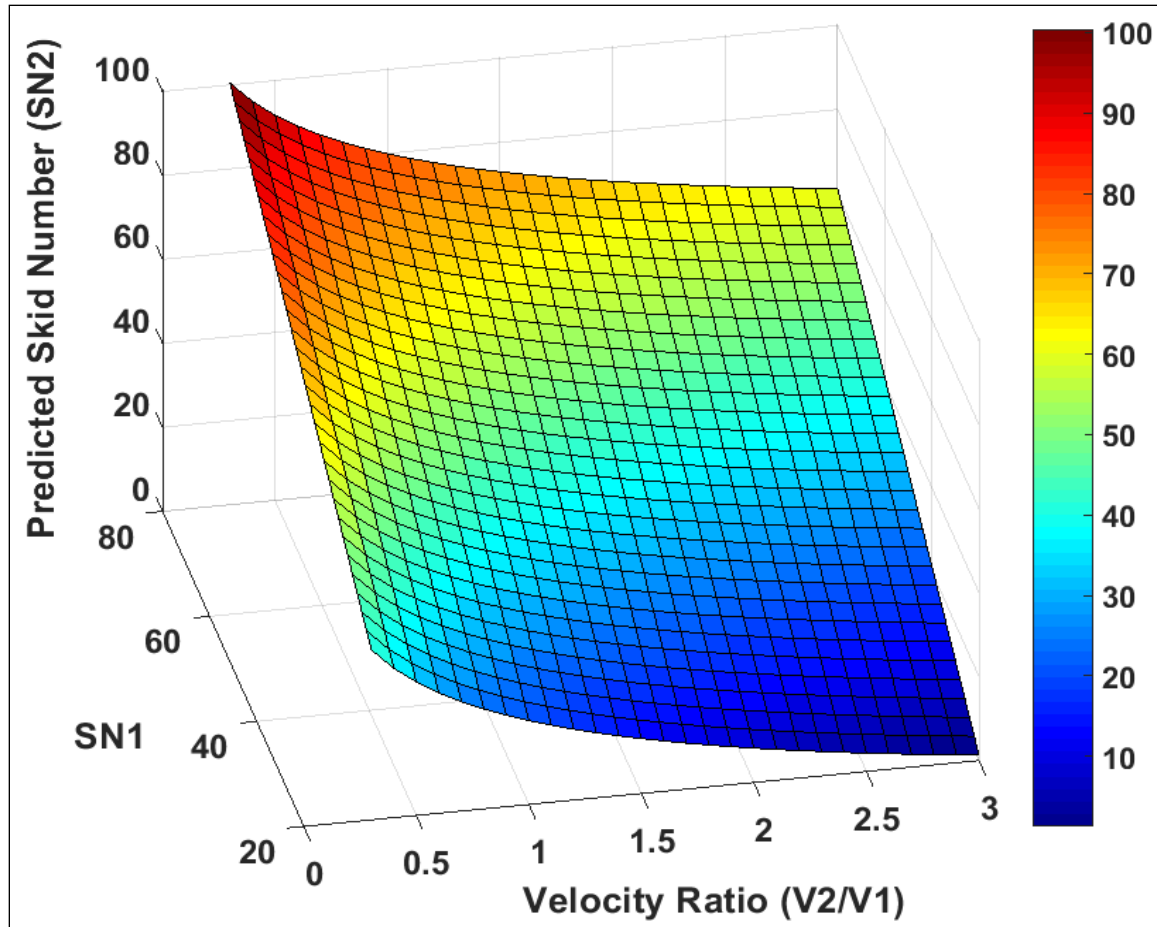
Figure 67 shows an example of variation in predicted skid number ( $SN_2$ ) with velocity ratio ( $V_2/V_1$ ), and MPD. In this particular example, the measured skid number ( $SN_1$ ) was maintained constant at 60. The results demonstrated that  $SN_2$  was higher than  $SN_1$  (i.e., 60) when the velocity ratio ( $V_2/V_1$ ) was less than one (i.e., the reference speed [ $V_2$ ] is lower than the test speed [ $V_1$ ]), and  $SN_2$  was lower than  $SN_1$  (i.e., 60) when the velocity ratio ( $V_2/V_1$ ) was greater than one (i.e., the reference speed [ $V_2$ ] is higher than test speed [ $V_1$ ]). These findings are in good agreement with the change in skid number with test speed as

shown in Figure 46 through Figure 48. In addition, Figure 67 shows that the MPD affects the change in  $SN_2$  with velocity ratio. The  $SN_2$  was higher than  $SN_1$  when the velocity ratio ( $V_2/V_1$ ) was smaller than one at various MPD values; however, the difference between  $SN_2$  and  $SN_1$  was higher at low MPD compared to the difference at high MPD. Similarly, The  $SN_2$  was lower than  $SN_1$  when the velocity ratio ( $V_2/V_1$ ) was greater than one at various MPD values and the difference between  $SN_2$  and  $SN_1$  was higher at low MPD compared to the difference at high MPD. These results are consistent with the observations from the field (Figure 49) where the skid number speed gradient ( $G_v$ ) decreased with the increase in MPD.



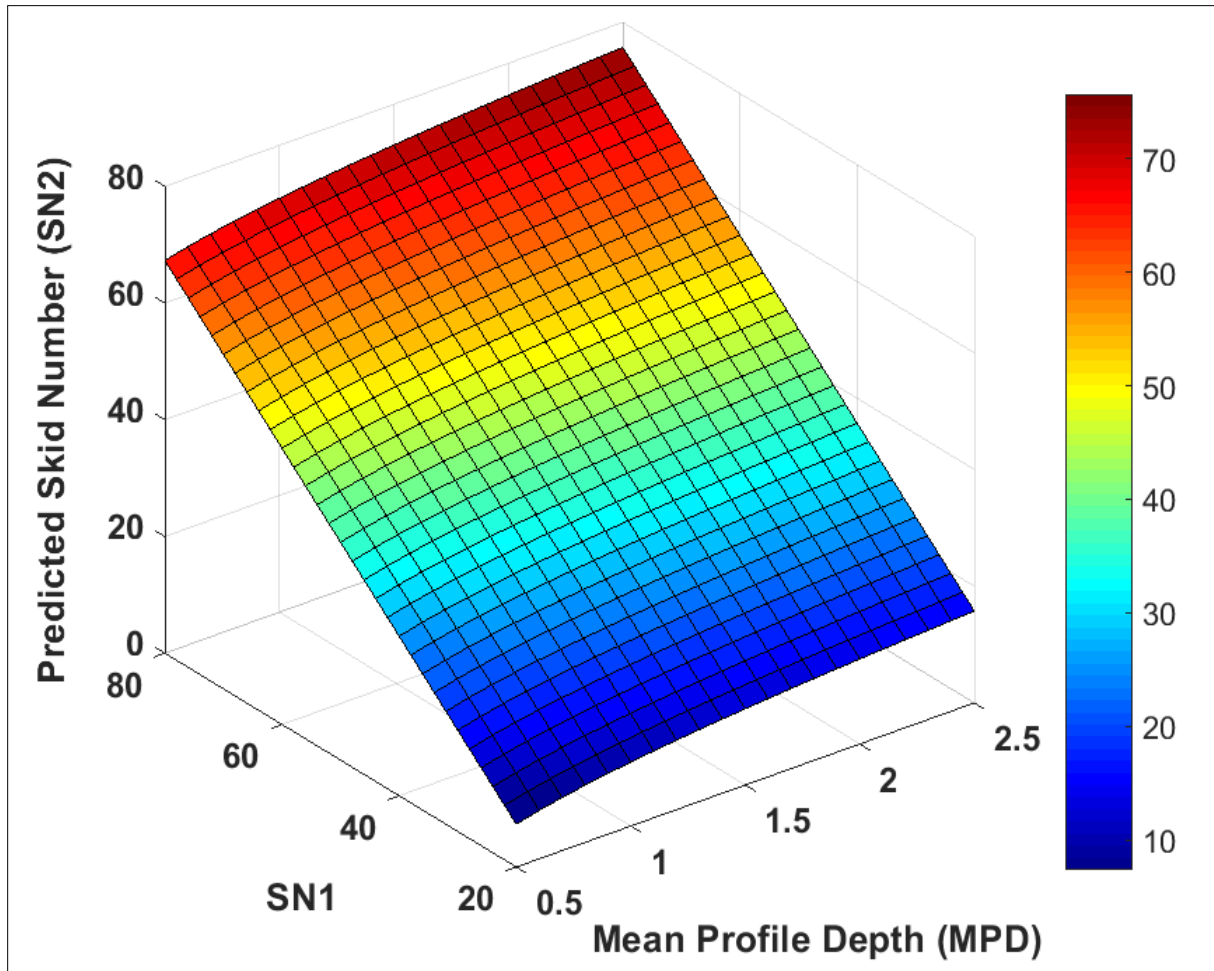
**Figure 67. Change in Predicted Skid Number with Velocity Ratio and Mean Profile Depth**  
(Note: The  $SN_1$  is Maintained Constant at 60 mph)

Figure 68 shows an example of variation in predicted skid number ( $SN_2$ ) with velocity ratio ( $V_2/V_1$ ), and measured skid number ( $SN_1$ ). In this example, the MPD was maintained constant at 1.5 mm. The results demonstrated that the predicted skid number ( $SN_2$ ) increased with measured skid number ( $SN_1$ ).  $SN_2$  had a linear relationship with  $SN_1$  while the  $SN_2$  had a nonlinear relationship with the velocity ratio.



**Figure 68. Change in Predicted Skid Number with Velocity Ratio and Measured Skid Number**  
(Note: The MPD is Maintained Constant at 1.5 mm)

Figure 69 shows an example of variation in predicted skid number ( $SN_2$ ) with velocity ratio ( $V_2/V_1$ ), and mean profile depth (MPD). In this example, the velocity ratio ( $V_2/V_1$ ) was maintained constant at 1.5. At this velocity ratio, the  $SN_2$  is always lower than  $SN_1$ . The results of Figure 69 demonstrate that the difference between  $SN_2$  and  $SN_1$  is lower at higher MPD compared to low MPD. These results are consistent with the field measurements presented in Figure 49.



**Figure 69. Change in Predicted Skid Number with Measured Skid Number and Mean Profile Depth**  
 (Note: The Velocity Ratio is Maintained Constant at 1.5)

### Development of Alternative Approach

The research team also developed an alternative model to predict skid as a function of macrotexture (i.e., mean texture depth), microtexture (i.e., DFT<sub>20</sub>), and speed. This model is proposed to estimate the skid number at various speeds if the skid trailer is not available or difficult to use (e.g., bridge deck) and when the laser profiler is not available. This model is developed based on 108 skid data points collected from 22 test sections where both microtexture and macrotexture data are available. The results of the previous section and the findings of the literature demonstrated that rate of change of pavement friction with speed depends on surface macrotexture, while the magnitude of friction is dictated by surface microtexture and many previous studies have shown that the skid number of a pavement surface can be predicted at a given speed if both the macrotexture and microtexture are known for the pavement surface.<sup>12, 19, 42, 70</sup>

Figure 70 shows the change in skid number with speed for two test sections; one with high macrotexture (2.29 mm) and the other with low macrotexture (0.56 mm). These two sections have comparable microtexture or DFT<sub>20</sub>. The skid resistance decreased with speed for both sections; however, the test section with low macrotexture had a steeper slope compared to the test section with higher macrotexture. The macrotexture controls the rate of change of skid number as found in the previous section of this study and in previous research studies.<sup>2</sup>

Figure 71 shows the change of skid number with speed for two test sections; one with higher microtexture (DFT<sub>20</sub> = 0.63) and the other with lower microtexture (DFT<sub>20</sub> = 0.52). These two test sections have comparable macrotexture (1.22 mm and 1.30 mm, respectively). These two sections showed comparable slopes (i.e., rate of change in skid number with speed). The section with higher microtexture had higher skid number when compared to the section with low microtexture. This was in agreement with previous findings where the microtexture was found to dictate the magnitude of skid number for pavement surfaces.<sup>2</sup>

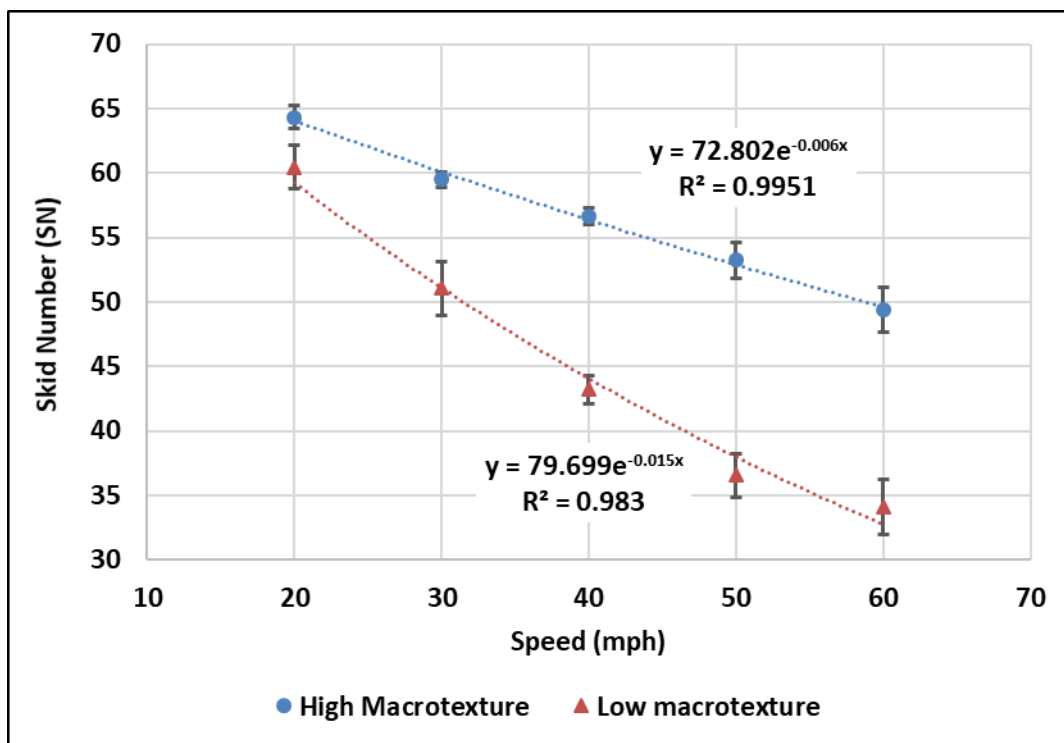
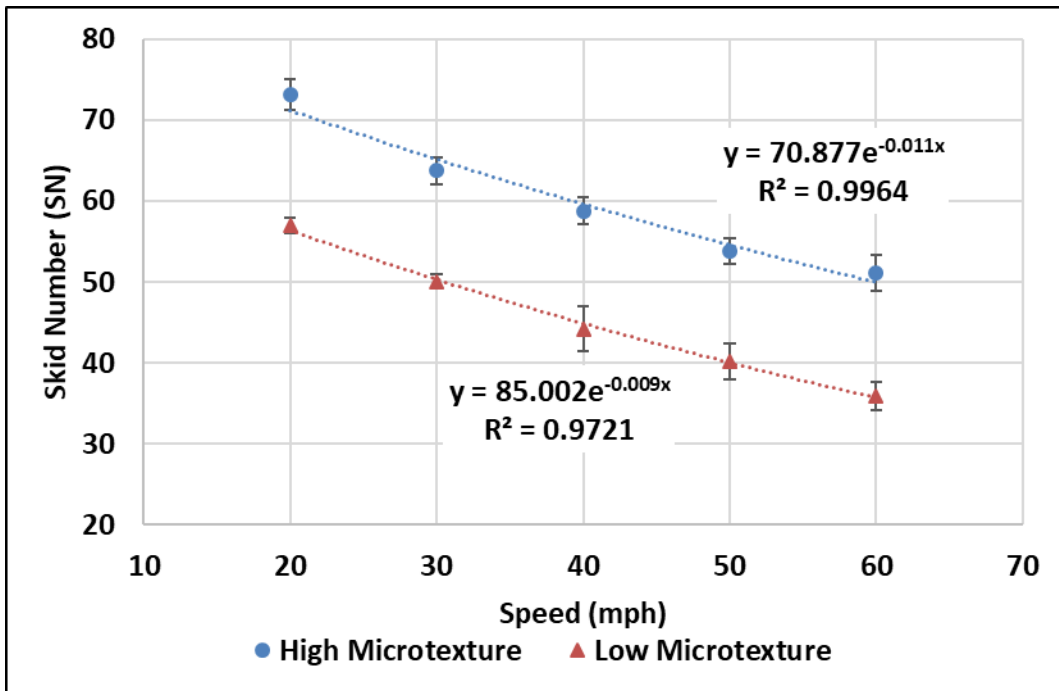


Figure 70. Change of SN with Speed for Sections with Low and High Macrotexture.



**Figure 71. Typical Change of Measured SN with Speed for Test Sections with Lower and Higher Microtexture.**

The research team used the microtexture ( $DFT_{20}$  values) and macrotexture (mean texture depth) and developed a statistical-based model to predict the skid number at various speeds. The equation in Figure 72 presents the proposed model for skid number as a function of speed and surface microtexture and macrotexture.

$$SN = 157.733 DFT_{20} e^{\left(\frac{-0.309(V/40)}{MTD}\right)} - 9.631$$

where,

$DFT_{20}$  = the coefficient of friction measured at speed of 20 km/h

MTD = the mean texture depth measured in mm

V = the speed measured in mph

**Figure 72. Model for Alternative Approach of Skid Number Prediction**

Figure 73 shows the correlation between predicted and measured skid number at various test speeds for the test sections. The results demonstrate that there is a very good correlation ( $R^2 = 0.83$ ) between predicted and measured skid numbers. The model provides a prediction interval of  $\pm 9.6$  at 95 percent confidence level. A diagnostic check was performed on the developed model as shown in Figure 74. The residuals were normally distributed with no significant skewness or bias and there is no pattern for the residuals as the measured skid number changes.

The results showed that prediction interval of this model is wider ( $\pm 9.6$ ) compared to the developed general model to describe the change in skid number with speed ( $\pm 5.7$ ) presented in Figure 53. The accuracy of the latter is better than the former since the skid level is measured using the skid trailer and the change in skid number with speed is assessed using macrotexture while the former estimate both the skid level and change with speed using microtexture and macrotexture. It should be noted that there is no previous model available in the literature that can be used to estimate skid number at various speeds using only pavement texture information. Also, it should be clear that this model (Figure 72) is not proposed to replace the model developed to describe the change in skid number with speed (Figure 53). The alternative model (Figure 72) is proposed when the skid trailer and laser profile are not available or cannot be used.

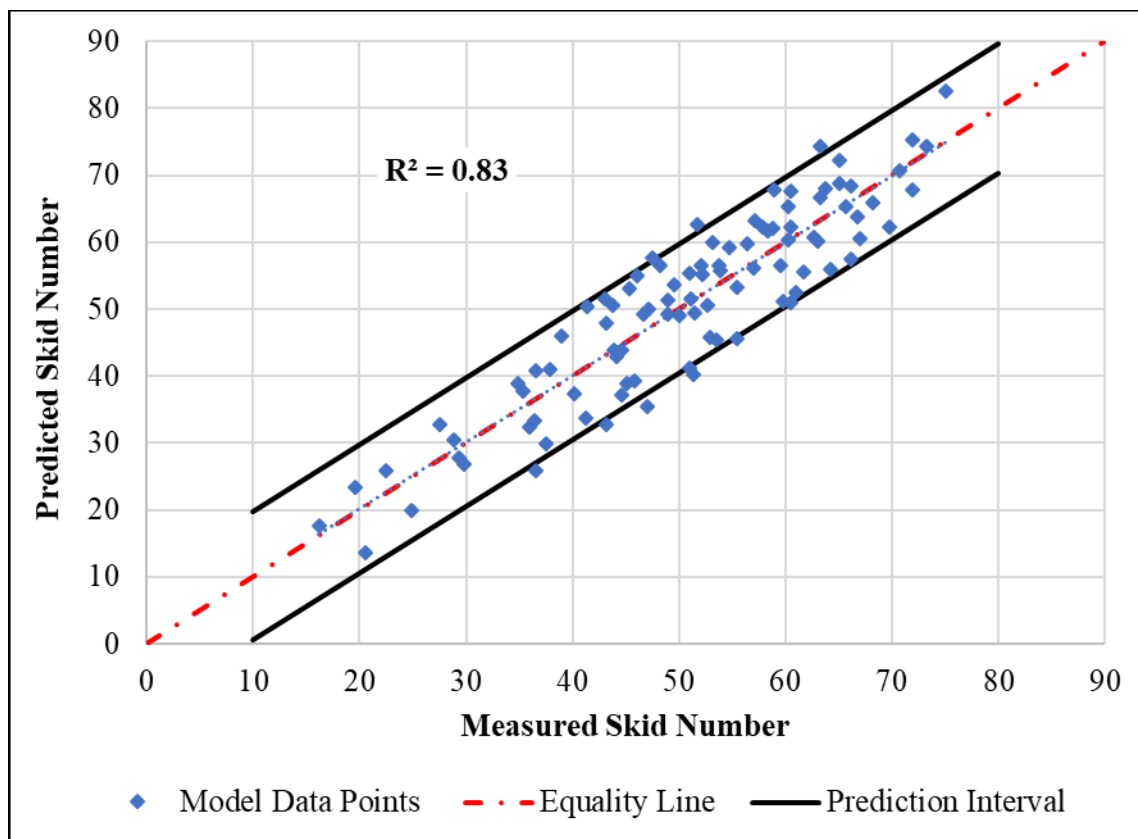


**Figure 73. Relationship between Measured and Calculated Skid Number at Different Speeds**

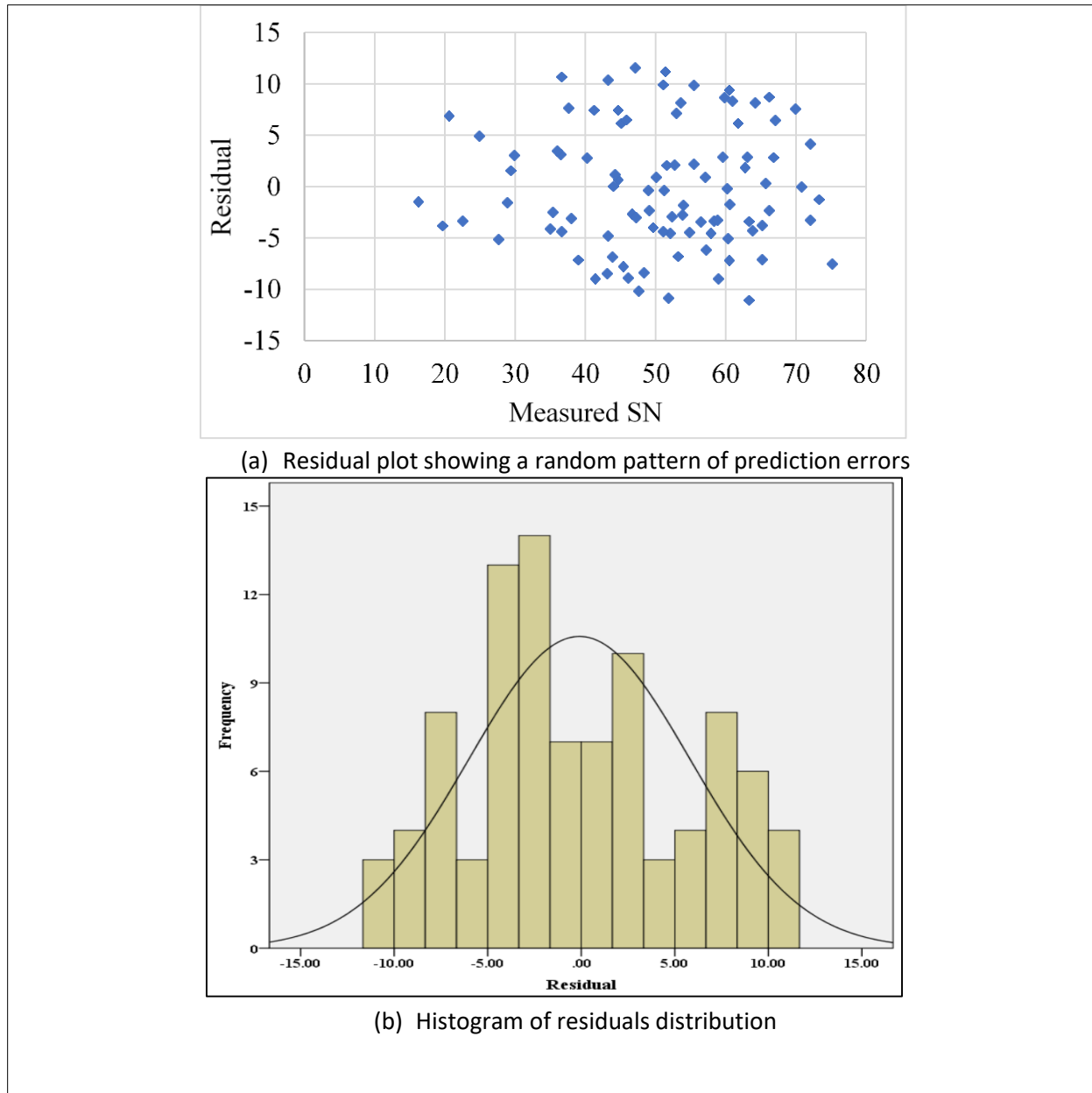


Figure 74. Diagnostic Check of the Normality of the Developed Model



## Chapter 5

# Development of Skid Prediction Software

### Overview

This chapter presents the development of an excel-based visual basic application to facilitate the use of the proposed skid model (Figure 53) developed in this study. The excel-based software simplifies the analysis and enables ITD engineers to use the developed skid prediction model to convert skid number measurements collected at any speed between 20 mph and 60 mph to a corresponding value at a reference speed (e.g., 40 mph). The software can be used to import the skid measurements at various test speeds and MPD data as recorded by the ITD pavement friction tester and use such information to calculate the skid number at a reference speed specified by the user. The software removes the erroneous data and displays the average skid number and MPD measured along the test section as well as the calculated skid number at the desired speed. By default, the desired reference speed is set at 40 mph, but the user can change it to any other speed as needed. Figure 75 shows the interface of the software.

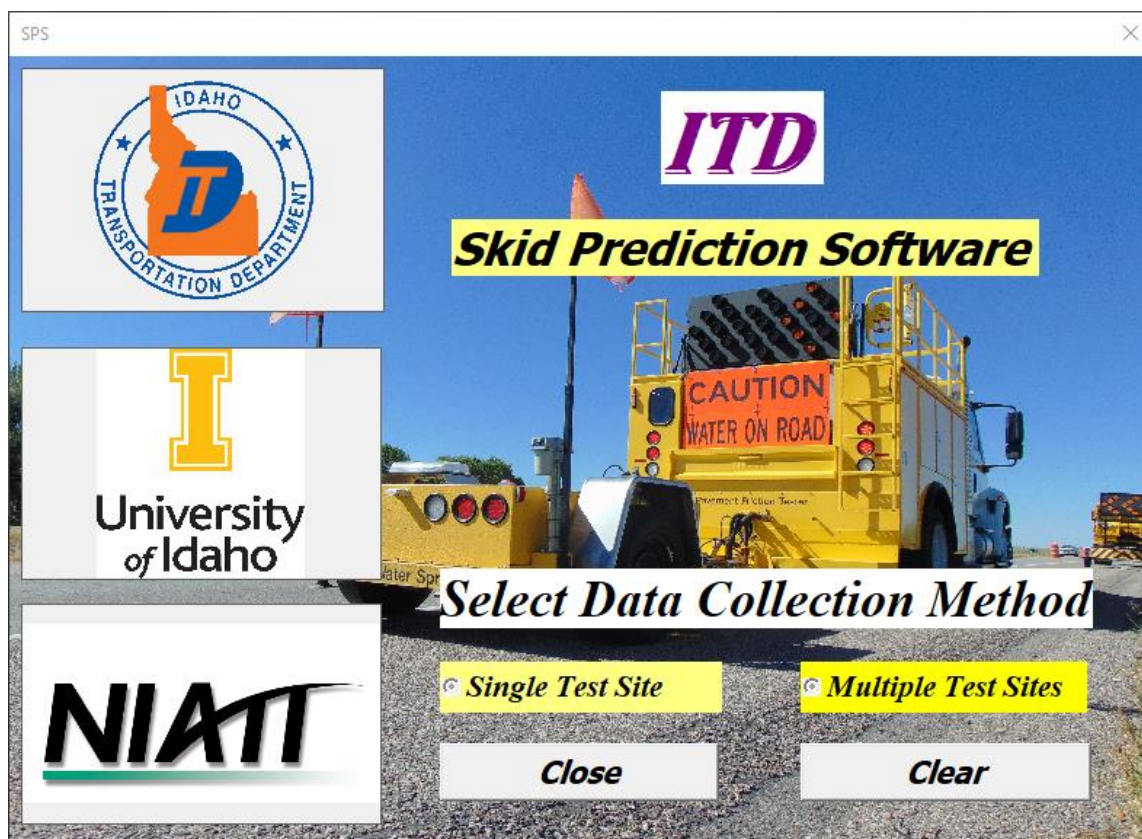


Figure 75. Skid Prediction Software Interface

As shown in Figure 75, there are two modes for running the software depending on the type of data collected and objective of the skid measurements; single test site or multiple test sites. These two options are discussed in this section.

## Single Test Site

The interface for the single test site mode is shown in Figure 76. The user should select this mode under the following circumstances:

- If the objective of the skid testing is to collect several skid friction and texture measurements (e.g., 7 or 10 measurements along the test section) to calculate a representative value for skid number and MPD at a reference speed, and
- If the test surface has the same characteristics (i.e., surface type, mix design, material properties, texture pattern, etc.).

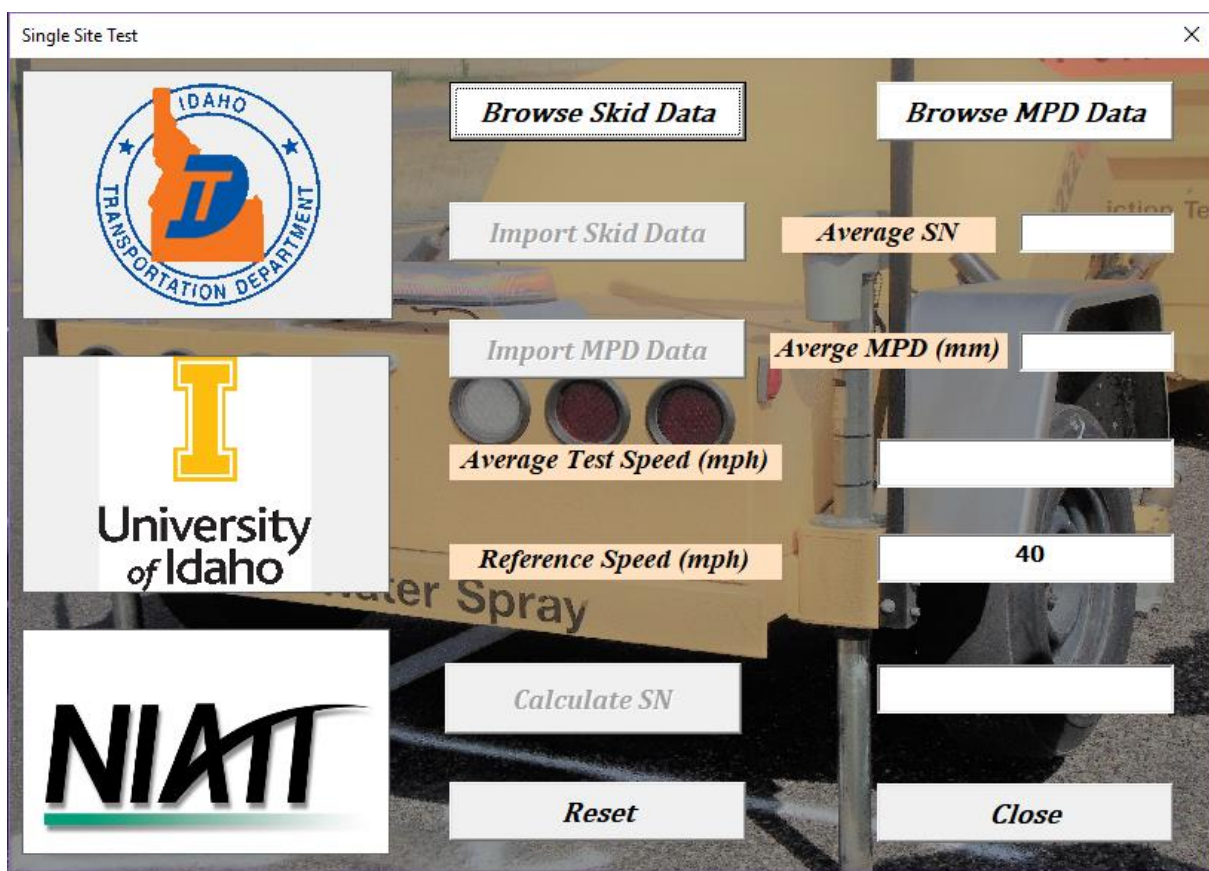


Figure 76. Interface of the Single Test Site Mode

**Command Buttons**

There are several command buttons in the software that are coded to perform specific functions (Figure 76). The command buttons and their respective functions are summarized in Table 8.

**Table 8. Command Buttons and Their Function**

Command	Functions
Browse Skid data	Browse and select skid measurement data collected using the skid trailer
Browse MPD data	Browse and select the mean profile depth measurement data collected using the laser sensor installed on the skid truck
Import Skid Data	Import the selected skid data file into excel, remove the outliers (highly deviated data) and calculate the average skid number
Import MPD Data	Import the selected texture data file into excel, remove the outliers (highly deviated data) and calculate the average MPD
Calculate SN	Calculate the skid number at the reference speed provided by a user using the prediction model (Equation 4.1) embedded in the software
Reset	Clear all the commands and inputs and restore the software to the initial status to run additional analysis
Close	Close the program

**Software Outputs**

Table 9 summarizes the main outcomes of the single test site mode that include 1) average skid number, 2) average MPD, 3) average test speed, and 4) reference speed, and 5) calculated skid number. Appendix E provides an example of single test site skid analysis.

**Table 9. Single Test Site Mode Outputs**

<b>Output</b>	<b>Definition</b>
Average SN	Display the average skid number for various skid number measurements imported into the software. This is the $SN_1$ parameter used in equation for general model presented in Figure 53.
Average MPD (mm)	Display the average mean profile depth (mm) for various MPD measurements imported into the software. This is the MPD input parameter used in general model equation presented in Figure 53. It should be noted that the MPD is measured in inches by the laser sensor and it is converted to mm in the software.
Average Test Speed (mph)	Display the average test speed at which the skid numbers were measured using the skid trailer. It is expressed in mile per hour. This is the $V_1$ input parameter used in general model equation presented in Figure 53.
Reference Speed (mph)	This is where the reference speed is specified by the user. The predicted skid number is calculated at the reference speed. It is expressed in mile per hour. This is the $V_2$ input parameter used in the general model equation presented in Figure 53.
Calculated Skid Number	Display the skid number calculated from the prediction model embedded in the software. This is the $SN_2$ parameter used in the general model equation presented in Figure 53.

## Multiple Test Site

The interface for the multiple test sites mode is shown in Figure 77. The user should select this mode if the objective is to collect continuous friction and texture measurements which is the typical practice at ITD. This mode has similar command buttons and outputs to the single test site mode. A user can browse and import the skid and MPD data into the software as recorded by the skid friction tester. Also, the user can specify the reference speed. A default value of 40 mph (current reference speed used by ITD) is selected. Upon importing the skid and texture data and specifying the reference speed, the skid number can be calculated at the reference speed by selecting “Calculate Skid Number” command button. One major difference between the single and multiple test sites interface is the output display of predicted skid number. While the single test site mode displays the predicted skid number in the interface itself, the multiple test sites interface allows the user to save and export the results into a separate excel file. This is useful to a user because the output results from the multiple sites interface consist of multiple rows and columns of data unlike a single value as in single site analysis. After completing the analysis, the user has the option either to run another calculation or quit the application as indicated by the command buttons in the software.

Figure 78 shows a typical input file (skid number) measured using the ITD skid friction tester. Similar file is obtained for MPD. Figure 79 displays typical output of the multiple test sites mode in excel format. The output files include the station number, milepost, test speed, measured skid number at the test speed, mean profile depth, adjusted mean profile depth which is the mean profile depth corresponding to the location of skid number measurement, and finally the predicted skid number at the desired reference speed set by a user. Appendix E provides an example of multiple test sites skid analysis.

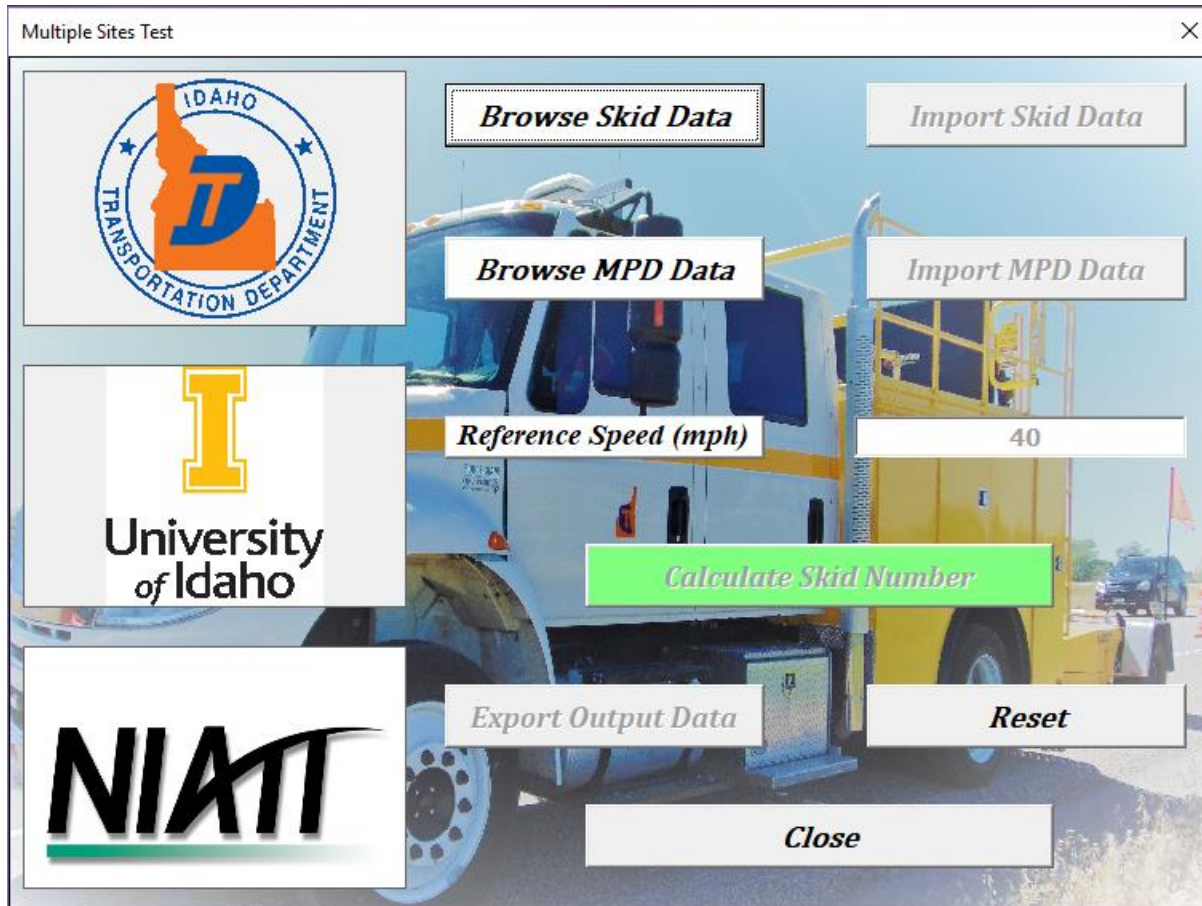


Figure 77. Interface of the Multiple Test Sites Mode

**Figure 78. Typical Input File (SN) for the Software Obtained from Skid Truck**

File	Home	Insert	Draw	Page Layout	Formulas	Data	Review	View	Developer	Help	Search	
Clipboard		Font			Alignment			Number			Conditional Formatting	
O9		X	Y	Z							Table	
1	Station Number	Mile Post	Speed	Measured SN	Mean Profile Depth	DMI	Adjusted MPD	Predicted SN				
2	0	30.422	21.6	38.8	0.125	30.522	0.125	34.21				
3	1	30.922	28.1	45.6	0.125	30.622	0.123	42.87				
4	2	31.422	22.3	41.1	0.123	30.722	0.12	36.44				
5	3	31.922	33.9	36.1	0.122	30.822	0.119	34.74				
6	4	32.422	34.6	40.1	0.123	30.922	0.121	38.93				

### **Figure 79. Output of the Multiple Test Site Mode**

## **Chapter 6**

# **Conclusions and Recommendations**

### **Summary**

The Idaho Transportation Department (ITD) measures skid number at 40 mph to ensure adequate friction level for pavements in Idaho. Since the skid number changes with the testing speed, it is important to collect the skid number measurements at a reference speed (e.g., 40 mph). However, field operations may not permit the collection of skid resistance at the reference speed. This study aimed to develop a method that can be used to convert the skid number collected at any speed between 20 mph and 60 mph to the corresponding skid number at a reference speed.

The researchers measured the frictional characteristics of 34 various pavement sections including hot mix asphalt, seal coat, and concrete. The skid number was measured at five different speeds (e.g., 20, 30, 40, 50, and 60 mph) using a locked wheel skid trailer with a smooth tire. In addition, the researchers measured the mean profile depth (MPD) of the test sites using a laser profiler and sand patch test. The microtexture was quantified indirectly by measuring the coefficient of friction using a portable dynamic friction tester (DFT). The results demonstrated that there is a logarithmic relationship between measured skid number and testing speed. Based on the collected data in this study, the researchers developed a statistical based model to describe the change in skid number with speed. The model utilizes the MPD data and skid number measurements at a given speed and calculates the skid number at a reference speed specified by the user. The predicted skid number values correlated well with the measured ones. The model was further validated with skid data from additional eight test sites that were not used in the model development. Good correlation was also found between the measured and predicted skid numbers for the validation sites.

The researcher developed an Excel-based utility that can be used to import the skid measurements and texture data collected by the ITD pavement friction tester and use the statistical model to calculate the skid number at a reference speed. The outcome of this study shall assist ITD pavement engineers to collect skid measurements at a safe speed (i.e., lower than 40 mph) when field operations do not allow data collection at the standard test speed (i.e., 40 mph). In addition, some interstate highways have posted speed limit up to 80 mph and the skid measurements are still collected at 40 mph which impose hazard to motorists and ITD staff. The skid number can be collected at higher speed (e.g., 60 mph) and converted to the corresponding values at a reference speed (e.g., 40 mph). Such practice would improve the safety of the ITD skid crew and motorists. In addition, it can expedite the data collection since the skid can be collected at higher speeds especially on interstate highways.

## Findings

This section summarizes the main findings of various components of the research study.

### Skid and Texture Data Analysis

- Seal coat test sections had relatively higher skid resistance and macrotexture compared to HMA and concrete test sections. The higher mean profile depth of the seal coat test sections contributed to the higher skid number. The seal coat test sections were found to be statistically different from HMA pavements in terms of macrotexture and skid resistance. In addition, there was no significant difference between HMA and concrete surfaces. All test sections (seal coat, HMA, and concrete) had comparable microtexture.
- A strong linear correlation ( $R^2 = 0.95$ ) was found between the mean profile depth measured using a laser sensor attached to the skid truck and mean texture depth measured using the sand patch test. Such correlation can be used to estimate the mean profile depth from the mean texture depth data. The laser sensor has several advantages over the sand patch test since it provides continuous data collected for texture data and doesn't record traffic control. The sand patch test is relatively cheaper but can be used to measure the macrotexture at only limited spots since it requires lane closure.
- In general, a logarithmic trend was found between the measured skid number and test speed. Although the  $R^2$  for the logarithmic relationship was higher than 0.9, the linear trend between measured skid resistance and test speed also provided higher  $R^2$  as well. The  $R^2$  for the logarithmic trend was higher than the linear trend for HMA and concrete sections, while the linear trend had higher  $R^2$  for the seal coat sections. Both correlation trends were observed and cited in the literature.
- The skid number decreased with the test speed for all test sections. The rate of change in skid number was a function of the macrotexture of the test sections. Sections with higher macrotexture showed low reduction in skid resistance with speed compared to sections with low macrotexture that had steeper decrease in skid with speed.
- The skid number had a fair correlation with the macrotexture; however, it should be noted that skid number is a function of both macrotexture and microtexture. This study concerned with the change in skid number with speed which was found to be controlled by the macrotexture. The results are in good agreement with the findings of previous research studies.
- The test sections evaluated in this study had comparable microtexture. The coefficient of friction measured using the DFT device at 20 km/hr, which is used to indirectly describe the microtexture, ranged from 0.51 to 0.67. Higher microtexture contribute to higher skid number. The microtexture was not significant in affecting the change in skid number with speed.

### **Development of Skid Prediction Model**

- A general statistical-based model was proposed to describe the change of skid number with speed of various surfaces including seal coat, HMA, and concrete. In addition, separate models were developed for each pavement surface. Such models were a function of measured skid number value ( $SN_1$ ), a ratio of reference to test speed ( $V_2/V_1$ ) and surface mean profile depth. The statistical analysis of measured and predicted skid values for model development and validation concluded that the general model is recommended to describe the change in skid number with speed.
- The results demonstrated a strong correlation between the predicted skid number and the measured ones. Most of the validation points were within the 95 percent prediction intervals of the proposed model. These results clearly demonstrate that the model can be used to describe the change in skid number with speed as a function of mean profile depth. In addition, the results showed that skid number speed gradient decreased with the increase in MPD. The predicted skid number had a linear positive relationship with the measured skid number when the mean profile depth is kept constant while predicted skid number had nonlinear relationship with the velocity ratio.
- This study also proposed an alternative model to predict skid number as a function of macrotexture (i.e., mean texture depth), microtexture (i.e.,  $DFT_{20}$ ), at a given speed between 20 mph and 60 mph. The results demonstrate that there is a very good correlation ( $R^2 = 0.83$ ) between predicted and measured skid number. It should be noted that there is no previous model available in the literature that can be used to estimate skid number at various speeds using only pavement texture information. Also, this model is proposed to estimate the skid number at various speeds if only the skid trailer is not available or difficult to use (e.g., bridge deck).

### **Development of a Skid Prediction Software**

- An Excel-based utility was developed on a visual basic platform to facilitate the process of analyzing the friction and texture data collected using the ITD pavement friction tester and calculating the skid number at a reference speed. The software is used to extract the needed information and values from the raw data files and consider the reference speed specified by the user to estimate the skid number at this speed.
- The software removes erroneous data, provides warning for the wrong inputs by the user, gives the user the option to re-import the data, and uses the proposed model to predict the skid number at a desired reference speed. The output from the software is displayed in the interface itself for the single test site analysis whereas it provides an option to the user to save the outputs from the software in excel formats for the multiple test sites mode.

## **Recommendations for Future Research**

- ITD can use the developed model to convert the skid number collected at any speed between 20 mph and 60 mph to the corresponding skid number at a reference speed. Meanwhile, it is recommended that ITD to check the model results against the measured skid numbers during their skid collection operations to determine if any revision is needed.
- Test sections with a wider range of microtexture can be included to investigate the effects of microtexture on the change of skid number with speed. Meanwhile, the microtexture mostly governs the magnitude of pavement friction which is incorporated in the measured skid number used in the model. Furthermore, previous research studies demonstrate that change in skid with speed is influenced by the macrotexture or MPD and not microtexture.
- Generate a database for the aggregate properties used in pavement construction in the state. Such database includes aggregate texture and its resistance to abrasion and polishing. Such data can be used to predict skid resistance performance over time.
- Develop skid prediction models that can be used in the mix design stage to ensure adequate skid resistance over the service life of pavements. Such model shall utilize aggregate properties and mix design and predict skid number over time.
- Additional skid resistance data can be collected to examine the effect of traffic level on skid resistance for various pavement surfaces (e.g., seal coat, HMA, concrete).
- Study the effect of studded tires on skid resistance of various HMA mix types. Such research study can assist ITD to construct pavements with better resistance to deterioration caused by studded tires and improved skid resistance.

## References

1. Noyce, D. A., Bahia, H. U., Yambó, J. M. & Kim, G. *Incorporating Road Safety into Pavement Management: Maximizing Asphalt Pavement Surface Friction for Road Safety Improvements.* Midwest Regional University Transportation Center (2005).
2. Hall, J. W., Kelly L. Smith & Paul Christopher Littleton. Texturing of concrete pavements. *NCHRP, Transportation Res. Board 634*, (2008).
3. Flitsch, G., McGhee, K., Izeppi, E. D. L. & Najafi, S. *The Little Book of Tire Pavement Friction.* (Pavement Surface Properties Consortium1, 2012).
4. Åström, H. & Wallman, C.-G. Friction Measurement Methods And The Correlation Between Road Friction And Traffic Safety: A Literature Review. *Digit. Vetenskapliga Ark. vti* (2001).
5. Corsello, P. Evaluation of surface friction guidelines for Washington state highways. *Defense Technical Information Center* (University of Seattle, Seattle, 1993).
6. Fuentes, L. G. Investigation of the Factors Influencing Skid Resistance and the International Friction Index. (Department of Civil and Environmental Engineering, University of South Florida, 2009).
7. Kulakowski, B. T. Mathematical Model of Skid Resistance as a Function of Speed. *Transp. Res. Rec. J. Transp. Res. Board* 26–32 (1991).
8. Chowdhury, M. A., Khalil, M. K., Nuruzzaman, D. M. & Rahaman, M. L. The effect of sliding speed and normal load on friction and wear property of aluminum. *Int. J. Mech. Mechatron. Eng* 11, 53–57 (2011).
9. Bowden, F. P. & Tabor, D. *The Friction and lubrication of solids.* Oxford University Press (1950). doi:10.1002/asl
10. Schallamach, A. How does rubber slide? *Wear* 17, 301–312 (1971).
11. Bitelli, G., Simone, A., Girardi, F. & Lantieri, C. Laser Scanning on Road Pavements: A New Approach for Characterizing Surface Texture. *Sensors* 12, 9110–9128 (2012).
12. Kassem, E., Awed, A., Masad, E. A. & Little, D. N. Development of Predictive Model for Skid Loss of Asphalt Pavements. *Transp. Res. Rec. J. Transp. Res. Board* 2372, 83–96 (2013).
13. Cairney, P. Skid Resistance and Crashes: A Review of the Literature. *Transp. Res. Rec. J. Transp. Res. Board* (1997).
14. Moyer, R. A. Historical background of skid resistance measurement-American experience. in *Al-Rayhanee, 1st international skid prevention conference, Charlottesville, Virginia* (1959).
15. Shahin, M. Y. *Pavement management for airports, roads, and parking lots.* (1994).
16. Li, S. Consideration in Developing a Network Pavement Inventory Friction Test Program for a State Highway Agency. *J. Test. Eval.* 33, (2005).
17. Federal Aviation Administration. *Measurement of Runway Friction Characteristics on Wet, Icy or Snow Covered Runways.* (1971).
18. Ragland, D., Chan, C. & Oh, S. M. Evaluation of Traffic and Environment Effects on Skid Resistance and Safety Performance of Rubberized Open-grade Asphalt Concrete Soon Mi Oh , David R . Ragland , Ching-Yao Chan UCB-ITS-PRR-2010-14. 0003, (2010).
19. Hall, J. W. et al. Guide for pavement friction. *NCHRP, Trasnsportation Res. Board* 1, 43 (2009).
20. Dunford, A. Friction and the texture of aggregate particles used in the road surface course.

- (2013).
- 21. Al-Assi, M. & Kassem, E. Evaluation of Adhesion and Hysteresis Friction of Rubber–Pavement System. *Appl. Sci.* **7**, 1029 (2017).
  - 22. Jayawickrama, P. & Thomas, B. Correction of field skid measurements for seasonal variations in Texas. *Transp. Res. Rec. J. Transp. Res. Board* 147–154 (1998).
  - 23. Luo, Y. Effect of Pavement Temperature on Frictional Properties of Hot Mix Asphalt Pavement Surfaces at Virginia Smart Road. *MSc. Thesis., Virginia Polytechnic Inst. State Univ.* (2003).
  - 24. Moore, D. F. The Friction of Pneumatic Tyres. *Transp. Res. Rec. J. Transp. Res. Board* (1975).
  - 25. Beautru, Y., Kane, M., Cerezo, V. & Do, M.-T. Effect of thin water film on tire/road friction. in *Young Researchers Seminar (YRS 2011)* (2011).
  - 26. Harwood, D. ., Blackburn, R. ., Kulakowski, B. . & Kibler, D. . *Wet weather exposure measures. Federal Highway Administration* (1998).
  - 27. Horne, W. B. & Buhlmann, F. A method for rating the skid resistance and micro/macrotecture characteristics of wet pavements. in *Frictional Interaction of Tire and Pavement* (ASTM International, 1983).
  - 28. Henry, J. J. *Evaluation of pavement friction characteristics*. 291, (Transportation Research Board, 2000).
  - 29. American Society of Testing and Materials (ASTM) E524-08 . Standard Specification for Standard Smooth Tire for Pavement Skid-Resistance Tests. *ASTM Int. West Conshohocken, PA* (2015).
  - 30. American Society of Testing and Materials (ASTM) E501-08. Standard Specification for Standard Rib Tire for Pavement Skid-Resistance Tests. *ASTM Int. West Conshohocken, PA* (2015).
  - 31. American Socciety of Testing and Materials (ASTM) E274 / E274M-15. Standard Test Method for Skid Resistance of Paved Surfaces Using a Full-Scale Tire. *ASTM Int. West Conshohocken, PA* (2015).
  - 32. American Society of Testing and Materials (ASTM) E670-09. Standard Test Method for Testing Side Force Friction on Paved Surfaces Using the Mu-Meter. *ASTM Int. West Conshohocken, PA* (2015).
  - 33. American Society of Testing and Materials (ASTM) E1551-16. Standard Specification for a Size 4.00-8 Smooth Tread Friction Test Tire. *ASTM Int. West Conshohocken, PA* (2016).
  - 34. American Society of Testing and Materials (ASTM) E1859 / E1859M-11. Standard Test Method for Friction Coefficient Measurements Between Tire and Pavement Using a Variable Slip Technique. *ASTM Int. West Conshohocken, PA* (2015).
  - 35. American Society of Testing and Materials (ASTM) E303-93. Standard Test Method for Measuring Surface Frictional Properties Using the British Pendulum Tester. *ASTM Int. West Conshohocken, PA* (2018).
  - 36. Martino, M. M. & Weissmann, J. *Evaluation of Seal Coat Performance Using Macro-texture Measurements*. (Citeseer, 2008).
  - 37. Lu, Q., Steven, B. & No, F. Friction testing of pavement preservation treatments: literature review. *Compare* (1971).
  - 38. Saito, K., Horiguchi, T., Kasahara, A., Abe, H. & Henry, J. J. Development of portable tester for

- measuring skid resistance and its speed dependency on pavement surfaces. *Transp. Res. Rec.* 1536, 45–51 (1996).
39. Aldagari, S., Al-Assi, M., Kassem, E., Chowdhury, A. & Masad, E. Prediction Models for Skid Resistance of Asphalt Pavements and Seal Coat. *Transp. Res. Rec. J. Transp. Res. Board* (2018).
40. American Society of Testing and Materials (ASTM) E1911-09ae1. Standard Test Method for Measuring Paved Surface Frictional Properties Using the Dynamic Friction Tester. *ASTM Int. West Conshohocken, PA* (2018).
41. American Society of Testing and Materials (ASTM) E2157-15. Standard Test Method for Measuring Pavement Macrotexture Properties Using the Circular Track Meter. *ASTM Int. West Conshohocken, PA* (2015).
42. Masad, E., Rezaei, A., Chowdhury, A. & Freeman, T. J. *Field evaluation of asphalt mixture skid resistance and its relationship to aggregate characteristics*. (Texas Transportation Institute, 2010).
43. Abe, H., Tamai, A., Henry, J. J. & Wambold, J. Measurement of Pavement Macrotexture with Circular Texture Meter. *Transp. Res. Rec. J. Transp. Res. Board* 1764, 201–209 (2001).
44. Hanson, D. I. & Prowell, B. D. *Evaluation of circular texture meter for measuring surface texture of pavements*. (The Center, 2004).
45. Mataei, B., Zakeri, H., Zahedi, M. & Nejad, F. M. Pavement friction and skid resistance measurement methods: a literature review. *Open J. Civ. Eng* 6, 537 (2016).
46. American Society of Testing and Materials (ASTM) E965-15. Standard Test Method for Measuring Pavement Macrotexture Depth Using a Volumetric Technique. *ASTM Int. West Conshohocken, PA* (2015).
47. Lebans, M. A. & Troyer, B. *Porous asphalt pavement performance in cold regions*. 12, (Citeseer, 2012).
48. Cybernetics, I. Skid\Friction Testing System. *Pennsylvania Department of Transportation* (2000).
49. Zimmer, R. & Fernando, E. Evaluation of Skid Measurements Used by TxDOT: Technical Report. 7, (2013).
50. Poorbaugh, J. Idaho Transportation System Pavement Performance-2017 Report. (2017).
51. Moyer, R. A. Motor Vehicle Operating Costs, Road Roughness and Slipperiness of Various Bituminous and Portland Cement Concrete Surfaces. *Highw. Res. Board Proc.* 22, (1943).
52. Byrd, T. *MacDonald and Lewis Training Course: Skid Resistance Measurements and Design, Instructor Notebook*. US Department of Transportation, Federal Highway Administration, and National Highway Institute 10, (1981).
53. Rizenbergs, R. L., Burchett, J. L. & Napier, C. T. Skid resistance of pavements. in *Skid resistance of highway pavements* (ASTM International, 1973).
54. Leu, M. C. & Henry, J. J. Prediction of skid resistance as a function of speed from pavement texture measurements. *Transp. Res. Rec.* 666, 7–13 (1978).
55. Jackson, N. M. *Harmonization of texture and skid-resistance measurements*. 32224, (University of North Florida, 2008).
56. Flintsch, G., de León Izeppi, E., McGhee, K. & Najafi, S. Speed adjustment factors for locked-wheel skid trailer measurements. *Transp. Res. Rec. J. Transp. Res. Board* 117–123 (2010).

57. Henry, J. J. Tire wet-pavement traction measurement: A state-of-the-art review. in *The tire pavement interface* (ASTM International, 1986).
58. Henry, J. J. & Wambold, J. C. Use of smooth-treaded test tire in evaluating skid resistance. *Transp. Res. Rec.* (1992).
59. American Society of Testing and Materials (ASTM) E1845-15. Standard Practice for Calculating Pavement Macrotexture Mean Profile Depth. *ASTM Int. West Conshohocken, PA* (2015).
60. American Society of Testing and Materials (ASTM) E867-06. Standard Terminology Relating to Vehicle-Pavement Systems. *ASTM Int. West Conshohocken, PA* (2012).
61. Yaacob, H., Hassan, N. A., Hainin, M. R. & Rosli, M. F. Comparison of sand patch test and multi laser profiler in pavement surface measurement. *J. Teknol.* 70, (2014).
62. Hao, X., Sha, A., Sun, Z., Li, W. & Zhao, H. Evaluation and comparison of real-time laser and electric sand-patch pavement texture-depth measurement methods. *J. Transp. Eng.* 142, 4016022 (2016).
63. China, S. & James, D. E. Comparison of laser-based and sand patch measurements of pavement surface macrotexture. *J. Transp. Eng.* 138, 176–181 (2011).
64. Praticò, F. G. & Vaiana, R. A study on the relationship between mean texture depth and mean profile depth of asphalt pavements. *Constr. Build. Mater.* 101, 72–79 (2015).
65. RStudio, I. RStudio: Integrated Development for R. (2015).
66. Murray, L., Nguyen, H., Lee, Y.-F., Remmenga, M. D. & Smith, D. W. Variance inflation factors in regression models with dummy variables. (2012).
67. O'brien, R. M. A caution regarding rules of thumb for variance inflation factors. *Qual. Quant.* 41, 673–690 (2007).
68. Statistics Solution. *Homoscedasticity [WWW Document]. Retrieved from website.* (2013). Available at: <https://www.statisticssolutions.com/homoscedasticity/>. (Accessed: 2nd December 2019)
69. MATLAB. version 7.10.0 (R2010a). (2010).
70. Kassem, E., Masad, E., Awed, A. & Little, D. Laboratory Evaluation of Friction Loss and Compactability of Asphalt Mixtures. *Texas Transp. Inst.* (2012).

## Appendix A Test Data

**Table A.1. Skid Measurement Data**

<b>Section ID</b>	<b>Test Speed (mph)</b>	<b>Average SN</b>	<b>Standard Deviation of SN</b>
1	20	75.09	0.95
1	30	71.97	1.11
1	40	66.49	1.33
1	50	60.37	1.48
1	60	50.97	6.12
2	20	63.31	1.49
2	30	55.16	1.75
2	40	49.64	1.47
2	50	45.24	2.59
2	60	39.36	2.65
3	20	62.69	2.39
3	30	47.15	3.11
3	40	37.91	3.25
3	50	36.41	2.45
3	60	29.87	2.89
4	20	60.31	1.94
4	30	52.33	2.67
4	40	44.92	3.60
4	50	40.90	6.69
4	60	37.91	4.61
5	20	69.83	1.88
5	30	60.45	3.02
5	40	50.50	3.28
5	50	44.60	1.28
5	60	43.60	3.05
6	20	63.52	2.09
6	30	56.38	2.20
6	40	49.60	1.07
6	50	43.19	1.72
7	20	57.40	0.94
7	30	50.47	0.86
7	40	43.59	2.77
7	50	39.46	2.20
7	60	35.55	1.76

**Table A.1. Skid Measurement Data (continued)**

<b>Section ID</b>	<b>Test Speed (mph)</b>	<b>Average SN</b>	<b>Standard Deviation of SN</b>
8	20	70.72	0.49
8	30	65.66	1.19
8	40	60.20	1.08
8	50	53.88	2.06
8	60	50.45	2.78
9	20	66.17	0.82
9	30	59.78	1.55
9	40	53.52	1.73
9	50	51.37	1.58
9	60	44.86	3.44
10	20	60.46	1.67
10	30	52.02	2.08
10	40	43.21	1.10
10	50	36.54	1.68
10	60	33.05	2.13
11	20	66.99	1.75
11	30	55.54	1.19
11	40	44.70	1.08
11	50	38.94	2.06
11	60	31.37	1.88
12	20	50.26	2.01
12	30	35.45	2.14
12	40	29.23	2.96
12	50	17.23	2.02
12	60	15.00	1.76
13	20	64.31	0.90
13	30	59.49	0.59
13	40	56.62	0.64
13	50	53.23	1.36
13	60	49.39	1.71
14	20	68.26	1.50
14	30	60.93	1.90
14	40	54.88	1.92
14	50	47.13	1.20
14	60	41.28	2.29

**Table A.1. Skid Measurement Data (continued)**

<b>Section ID</b>	<b>Test Speed (mph)</b>	<b>Average SN</b>	<b>Standard Deviation of SN</b>
15	20	71.98	1.07
15	30	66.74	0.93
15	40	63.33	1.07
15	50	59.43	0.85
15	60	56.00	1.98
16	20	51.73	6.45
16	30	33.58	4.29
16	40	30.39	4.45
16	50	24.67	2.82
16	60	21.97	3.99
17	20	64.14	0.97
17	30	53.25	1.49
17	40	44.61	2.12
17	50	38.16	1.90
17	60	36.53	3.56
18	20	52.09	1.43
18	30	51.34	0.98
18	40	47.13	0.75
18	50	45.37	1.24
19	20	67.18	0.96
19	30	60.99	0.88
19	40	54.41	0.92
19	50	47.96	1.44
19	60	42.45	1.99
20	20	57.81	1.35
20	30	43.82	1.52
20	40	32.54	2.14
20	50	24.57	3.07
20	60	22.50	3.85
21	20	48.97	4.57
21	30	34.90	1.70
21	40	23.90	2.46
21	50	19.60	2.77
21	60	16.18	1.92

**Table A.1. Skid Measurement Data (continued)**

<b>Section ID</b>	<b>Test Speed (mph)</b>	<b>Average SN</b>	<b>Standard Deviation of SN</b>
22	20	65.20	0.75
22	30	60.72	0.68
22	40	57.50	0.94
22	50	53.74	1.02
22	60	49.39	1.81
23	20	65.93	12.63
23	30	61.93	12.00
23	40	53.60	13.44
23	50	49.07	12.05
23	60	41.13	10.75
24	20	65.08	2.09
24	30	58.32	2.80
24	40	52.25	1.63
24	50	46.60	2.08
24	60	43.95	2.67
25	20	73.20	1.94
25	30	63.74	1.64
25	40	58.78	1.63
25	50	53.80	1.54
25	60	51.17	2.24
26	20	65.11	1.51
26	30	60.45	2.48
26	40	57.11	2.22
26	50	54.78	1.64
26	60	50.98	5.35
27	40	31.30	0.78
27	50	26.00	3.02
27	60	21.10	3.82
28	40	50.27	4.12
28	50	48.53	1.23
28	60	42.87	0.91

**Table A.1. Skid Measurement Data (continued)**

<b>Section ID</b>	<b>Test Speed (mph)</b>	<b>Average SN</b>	<b>Standard Deviation of SN</b>
<b>29</b>	40	49.65	1.08
<b>29</b>	50	44.40	1.39
<b>29</b>	60	41.05	0.77
<b>30</b>	40	59.80	1.00
<b>30</b>	50	56.65	1.32
<b>30</b>	60	51.85	0.92
<b>31</b>	40	44.03	3.98
<b>31</b>	50	39.03	3.37
<b>31</b>	60	34.03	4.05
<b>32</b>	20	57.78	4.16
<b>32</b>	30	44.93	2.58
<b>32</b>	40	38.45	4.28
<b>33</b>	20	61.73	3.31
<b>33</b>	30	61.55	3.89
<b>33</b>	40	56.70	2.02
<b>33</b>	50	55.13	1.25
<b>33</b>	60	51.80	1.36
<b>34</b>	40	44.30	1.26
<b>34</b>	50	37.73	2.64
<b>34</b>	60	32.90	1.37

**Table A.2. Texture Measurement Data**

<b>Section ID</b>	<b>MPD (mm)</b>	<b>MTD (mm)</b>	<b>DFT<sub>20</sub></b>
<b>1</b>	1.194	1.196	0.69
<b>2</b>	1.232	1.249	0.62
<b>3</b>	0.648	0.601	0.62
<b>4</b>	1.162	1.334	0.55
<b>5</b>	1.016	0.862	0.55
<b>6</b>	1.105	1.059	0.58
<b>7</b>	1.016	0.893	0.52
<b>8</b>	1.634	1.322	0.59
<b>9</b>	1.008	1.001	0.52
<b>10</b>	0.576	0.555	0.55
<b>11</b>	0.720	0.469	0.62
<b>12</b>	0.508	0.277	0.64
<b>13</b>	2.269	2.287	0.6
<b>14</b>	0.821	0.827	0.57
<b>15</b>	2.040	1.904	0.55
<b>16</b>	0.525	0.418	0.61
<b>17</b>	0.660	0.587	0.58
<b>18</b>	1.651	1.415	0.57
<b>19</b>	1.718	1.635	
<b>20</b>	0.645	0.561	0.65
<b>21</b>	0.598	0.514	0.55
<b>22</b>	1.848	1.765	
<b>23</b>	1.249	1.166	
<b>24</b>	1.124	1.040	0.6
<b>25</b>	1.328	1.245	0.63
<b>26</b>	1.810	1.727	0.58
<b>27</b>	2.311		
<b>28</b>	2.515		
<b>29</b>	2.388		
<b>30</b>	2.489		
<b>31</b>	1.778		
<b>32</b>	2.032		
<b>33</b>	2.235		
<b>34</b>	1.854		

## Appendix B

### Data for Model Development and Validation

**Table B.1. Model Development Data**

<b>Section ID</b>	<b>V1</b>	<b>SN1</b>	<b>MPD</b>	<b>V2</b>	<b>SN2</b>
1	20	75.09	1.19	30	71.97
1	20	75.09	1.19	40	66.49
1	20	75.09	1.19	50	60.37
1	20	75.09	1.19	60	50.97
2	20	63.31	1.23	30	55.16
2	20	63.31	1.23	40	49.64
2	20	63.31	1.23	50	45.24
2	20	63.31	1.23	60	39.36
3	20	62.69	0.65	30	47.15
3	20	62.69	0.65	40	37.91
3	20	62.69	0.65	50	36.41
3	20	62.69	0.65	60	29.87
4	20	60.31	1.16	30	52.33
4	20	60.31	1.16	40	44.92
4	20	60.31	1.16	50	40.90
4	20	60.31	1.16	60	37.91
5	20	69.83	1.02	30	60.45
5	20	69.83	1.02	40	50.50
5	20	69.83	1.02	50	44.60
5	20	69.83	1.02	60	43.60
6	20	63.52	1.10	30	56.38
6	20	63.52	1.10	40	49.60
6	20	63.52	1.10	50	43.19
8	20	70.72	1.63	30	65.66
8	20	70.72	1.63	40	60.20
8	20	70.72	1.63	50	53.88
8	20	70.72	1.63	60	50.45
9	20	66.17	1.01	30	59.78
9	20	66.17	1.01	40	53.52
9	20	66.17	1.01	50	51.37
9	20	66.17	1.01	60	44.86
10	20	60.46	0.58	30	52.02
10	20	60.46	0.58	40	43.21
10	20	60.46	0.58	50	36.54
11	20	66.99	0.72	30	55.54
11	20	66.99	0.72	40	44.70
11	20	66.99	0.72	50	38.94
11	20	66.99	0.72	60	31.37

**Table B.1. Model Development Data (continued)**

<b>Section ID</b>	<b>V1</b>	<b>SN1</b>	<b>MPD</b>	<b>V2</b>	<b>SN2</b>
14	20	68.26	0.82	30	60.93
14	20	68.26	0.82	40	54.88
14	20	68.26	0.82	50	47.13
14	20	68.26	0.82	60	41.28
16	20	51.73	0.52	30	33.58
16	20	51.73	0.52	40	30.39
16	20	51.73	0.52	50	24.67
16	20	51.73	0.52	60	21.97
17	20	64.14	0.66	30	53.25
17	20	64.14	0.66	40	44.61
17	20	64.14	0.66	50	38.16
17	20	64.14	0.66	60	36.53
19	20	67.18	1.72	30	60.99
19	20	67.18	1.72	40	54.41
19	20	67.18	1.72	50	47.96
19	20	67.18	1.72	60	42.45
21	20	48.97	0.60	30	34.90
21	20	48.97	0.60	40	23.90
21	20	48.97	0.60	50	19.60
21	20	48.97	0.60	60	16.18
22	20	65.20	1.85	30	60.72
22	20	65.20	1.85	40	57.50
22	20	65.20	1.85	50	53.74
22	20	65.20	1.85	60	49.39
24	20	65.08	1.12	30	58.32
24	20	65.08	1.12	40	52.25
24	20	65.08	1.12	50	46.60
24	20	65.08	1.12	60	43.95
26	20	65.11	1.81	30	60.45
26	20	65.11	1.81	40	57.11
26	20	65.11	1.81	50	54.78
26	20	65.11	1.81	60	50.98
33	20	61.73	2.24	30	61.55
33	20	61.73	2.24	40	56.70
33	20	61.73	2.24	50	55.13
33	20	61.73	2.24	60	51.80
1	30	71.97	1.19	40	66.49
1	30	71.97	1.19	50	60.37
1	30	71.97	1.19	60	50.97

**Table B.1. Model Development Data (continued)**

<b>Section ID</b>	<b>V1</b>	<b>SN1</b>	<b>MPD</b>	<b>V2</b>	<b>SN2</b>
2	30	55.16	1.23	40	49.64
2	30	55.16	1.23	50	45.24
2	30	55.16	1.23	60	39.36
3	30	47.15	0.65	40	37.91
3	30	47.15	0.65	50	36.41
3	30	47.15	0.65	60	29.87
4	30	52.33	1.16	40	44.92
4	30	52.33	1.16	50	40.90
4	30	52.33	1.16	60	37.91
5	30	60.45	1.02	40	50.50
5	30	60.45	1.02	50	44.60
5	30	60.45	1.02	60	43.60
6	30	56.38	1.10	40	49.60
6	30	56.38	1.10	50	43.19
8	30	65.66	1.63	40	60.20
8	30	65.66	1.63	50	53.88
8	30	65.66	1.63	60	50.45
9	30	59.78	1.01	40	53.52
9	30	59.78	1.01	50	51.37
9	30	59.78	1.01	60	44.86
10	30	52.02	0.58	40	43.21
10	30	52.02	0.58	50	36.54
10	30	52.02	0.58	60	33.05
11	30	55.54	0.72	40	44.70
11	30	55.54	0.72	50	38.94
11	30	55.54	0.72	60	31.37
14	30	60.93	0.82	40	54.88
14	30	60.93	0.82	50	47.13
14	30	60.93	0.82	60	41.28
16	30	33.58	0.52	40	30.39
16	30	33.58	0.52	50	24.67
16	30	33.58	0.52	60	21.97
17	30	53.25	0.66	40	44.61
17	30	53.25	0.66	50	38.16
17	30	53.25	0.66	60	36.53
19	30	60.99	1.72	40	54.41
19	30	60.99	1.72	50	47.96
19	30	60.99	1.72	60	42.45

**Table B.1. Model Development Data (continued)**

Section ID	V1	SN1	MPD	V2	SN2
21	30	34.90	0.60	40	23.90
21	30	34.90	0.60	50	19.60
21	30	34.90	0.60	60	16.18
22	30	60.72	1.85	40	57.50
22	30	60.72	1.85	50	53.74
22	30	60.72	1.85	60	49.39
24	30	58.32	1.12	40	52.25
24	30	58.32	1.12	50	46.60
24	30	58.32	1.12	60	43.95
26	30	60.45	1.81	40	57.11
26	30	60.45	1.81	50	54.78
26	30	60.45	1.81	60	50.98
33	30	61.55	2.24	40	56.70
33	30	61.55	2.24	50	55.13
33	30	61.55	2.24	60	51.80
1	40	66.49	1.19	50	60.37
1	40	66.49	1.19	60	50.97
2	40	49.64	1.23	50	45.24
2	40	49.64	1.23	60	39.36
3	40	37.91	0.65	50	36.41
3	40	37.91	0.65	60	29.87
4	40	44.92	1.16	50	40.90
4	40	44.92	1.16	60	37.91
5	40	50.50	1.02	50	44.60
5	40	50.50	1.02	60	43.60
6	40	49.60	1.10	50	43.19
8	40	60.20	1.63	50	53.88
8	40	60.20	1.63	60	50.45
9	40	53.52	1.01	50	51.37
9	40	53.52	1.01	60	44.86
10	40	43.21	0.58	50	36.54
10	40	43.21	0.58	60	33.05
11	40	44.70	0.72	50	38.94
11	40	44.70	0.72	60	31.37
14	40	54.88	0.82	50	47.13
14	40	54.88	0.82	60	41.28
16	40	30.39	0.52	50	24.67
16	40	30.39	0.52	60	21.97

**Table B.1. Model Development Data (continued)**

<b>Section ID</b>	<b>V1</b>	<b>SN1</b>	<b>MPD</b>	<b>V2</b>	<b>SN2</b>
17	40	44.61	0.66	50	38.16
17	40	44.61	0.66	60	36.53
19	40	54.41	1.72	50	47.96
19	40	54.41	1.72	60	42.45
21	40	23.90	0.60	50	19.60
21	40	23.90	0.60	60	16.18
22	40	57.50	1.85	50	53.74
22	40	57.50	1.85	60	49.39
24	40	52.25	1.12	50	46.60
24	40	52.25	1.12	60	43.95
26	40	57.11	1.81	50	54.78
26	40	57.11	1.81	60	50.98
27	40	31.30	2.31	50	26.00
27	40	31.30	2.31	60	21.10
28	40	50.27	2.51	50	48.53
28	40	50.27	2.51	60	42.87
30	40	59.80	2.49	50	56.65
30	40	59.80	2.49	60	51.85
31	40	44.03	1.78	50	39.03
31	40	44.03	1.78	60	34.03
33	40	56.70	2.24	50	55.13
33	40	56.70	2.24	60	51.80
34	40	44.30	1.85	50	37.73
34	40	44.30	1.85	60	32.90
1	50	60.37	1.19	60	50.97
2	50	45.24	1.23	60	39.36
3	50	36.41	0.65	60	29.87
4	50	40.90	1.16	60	37.91
5	50	44.60	1.02	60	43.60
8	50	53.88	1.63	60	50.45
9	50	51.37	1.01	60	44.86
10	50	36.54	0.58	60	33.05
11	50	38.94	0.72	60	31.37
14	50	47.13	0.82	60	41.28
16	50	24.67	0.52	60	21.97
17	50	38.16	0.66	60	36.53
19	50	47.96	1.72	60	42.45
21	50	19.60	0.60	60	16.18
22	50	53.74	1.85	60	49.39

**Table B.1. Model Development Data (continued)**

<b>Section ID</b>	<b>V1</b>	<b>SN1</b>	<b>MPD</b>	<b>V2</b>	<b>SN2</b>
24	50	46.60	1.12	60	43.95
26	50	54.78	1.81	60	50.98
27	50	26.00	2.31	60	21.10
28	50	48.53	2.51	60	42.87
30	50	56.65	2.49	60	51.85
31	50	39.03	1.78	60	34.03
33	50	55.13	2.24	60	51.80
34	50	37.73	1.85	60	32.90

**Table B.2. Model Validation Data**

<b>V1</b>	<b>SN1</b>	<b>MPD</b>	<b>V2</b>	<b>SN2</b>
20	57.40	1.02	40	43.59
30	50.47	1.02	40	43.59
50	39.46	1.02	40	43.59
60	35.55	1.02	40	43.59
20	50.26	0.51	40	29.23
30	35.45	0.51	40	29.23
50	17.23	0.51	40	29.23
60	15.00	0.51	40	29.23
20	64.31	2.27	40	56.62
30	59.49	2.27	40	56.62
50	53.23	2.27	40	56.62
60	49.39	2.27	40	56.62
20	71.98	2.04	40	63.33
30	66.74	2.04	40	63.33
50	59.43	2.04	40	63.33
60	56.00	2.04	40	63.33
20	52.09	1.65	40	47.13
30	51.34	1.65	40	47.13
50	45.37	1.65	40	47.13
20	57.81	0.64	40	32.54
30	43.82	0.64	40	32.54
50	24.57	0.64	40	32.54
60	22.50	0.64	40	32.54
20	65.93	1.25	40	53.60
30	61.93	1.25	40	53.60
50	49.07	1.25	40	53.60
60	41.13	1.25	40	53.60
20	73.20	1.33	40	58.78
30	63.74	1.33	40	58.78
50	53.80	1.33	40	58.78
60	51.17	1.33	40	58.78
50	44.40	2.39	40	49.65
60	41.05	2.39	40	49.65
20	57.78	2.03	40	38.45
30	44.93	2.03	40	38.45



## Appendix C

### Relation between SN And MPD

#### HMA Sections

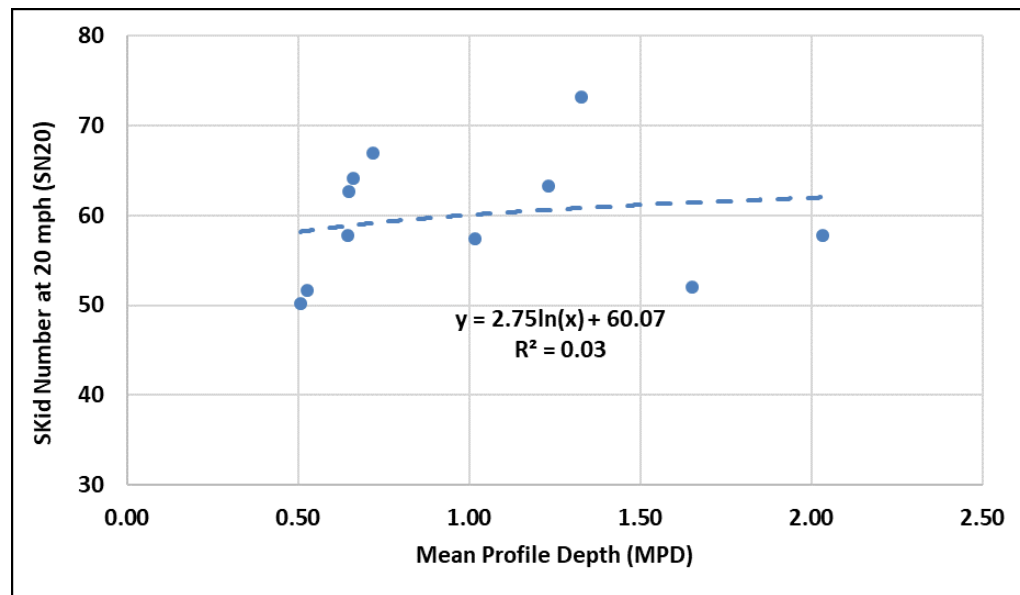


Figure C.1. Relationship between Skid Number at 20 mph (SN20) and Mean Profile Depth

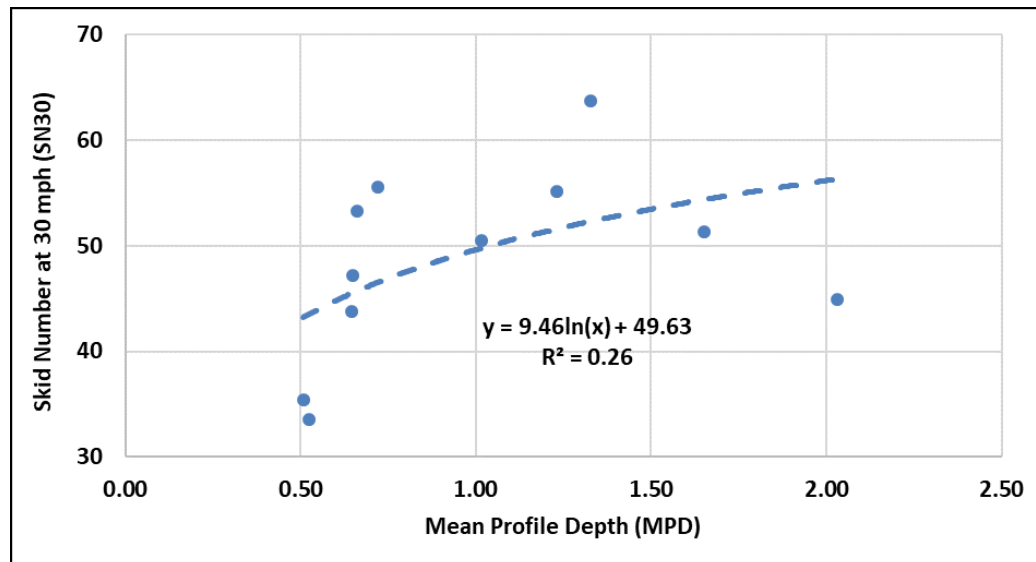


Figure C.2. Relationship between Skid Number at 30 mph (SN30) and Mean Profile Depth

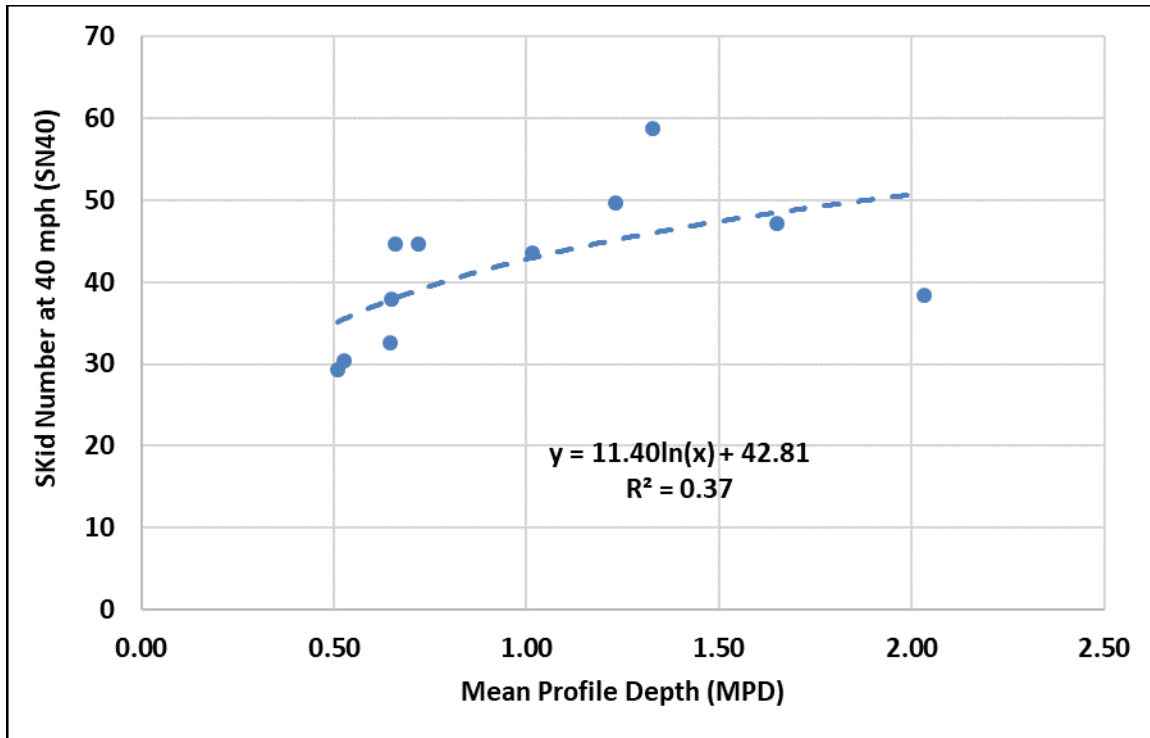


Figure C.3. Relationship between Skid Number at 40 mph (SN40) and Mean Profile Depth

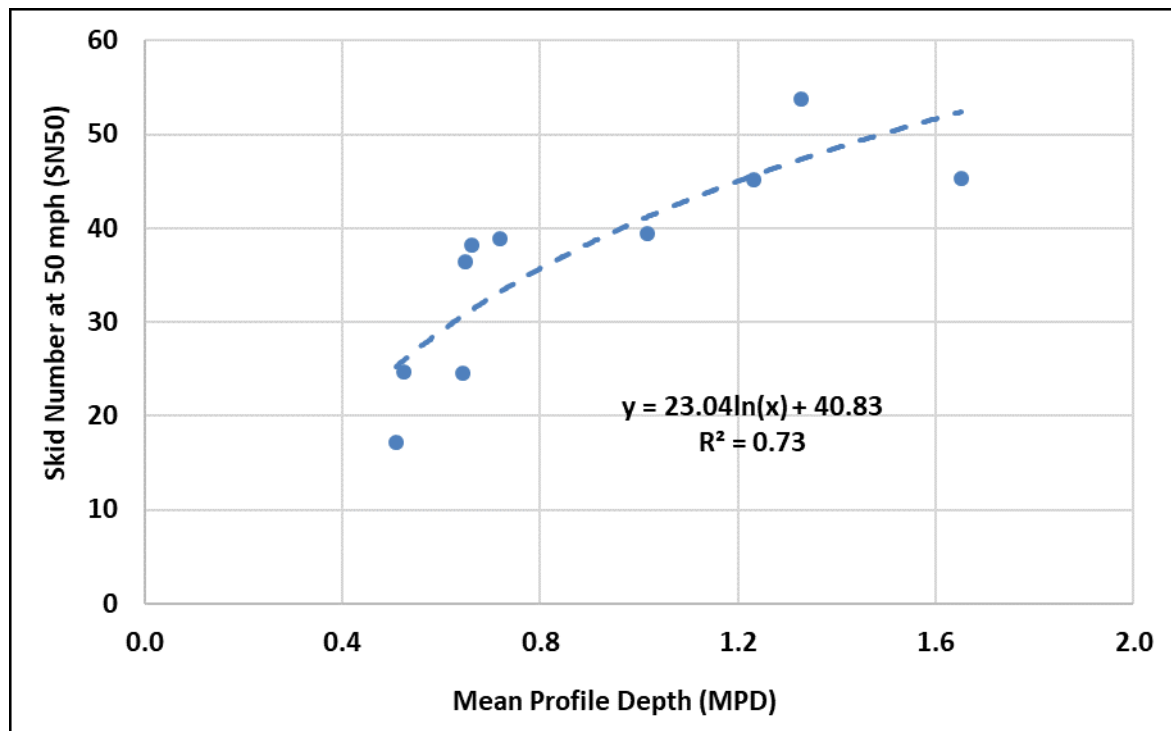


Figure C.4. Relationship between Skid Number at 50 mph (SN50) and Mean Profile Depth

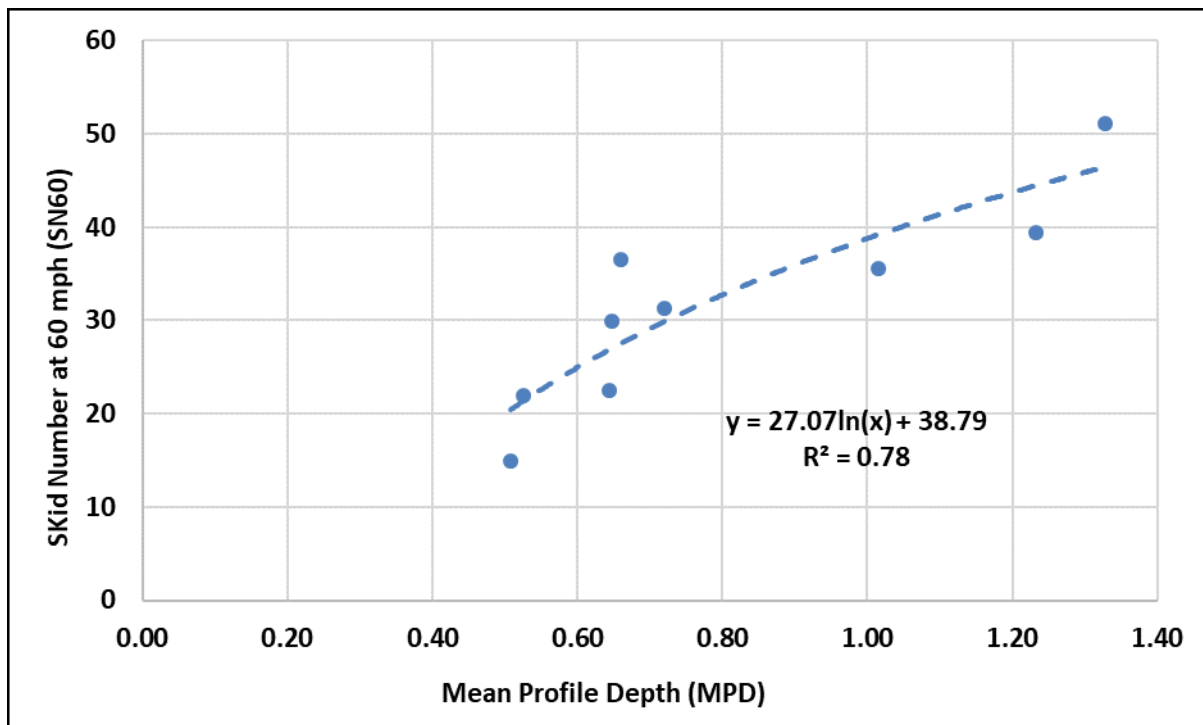


Figure C.5. Relationship between Skid Number at 60 mph (SN60) and Mean Profile Depth

## Seal Coat Sections

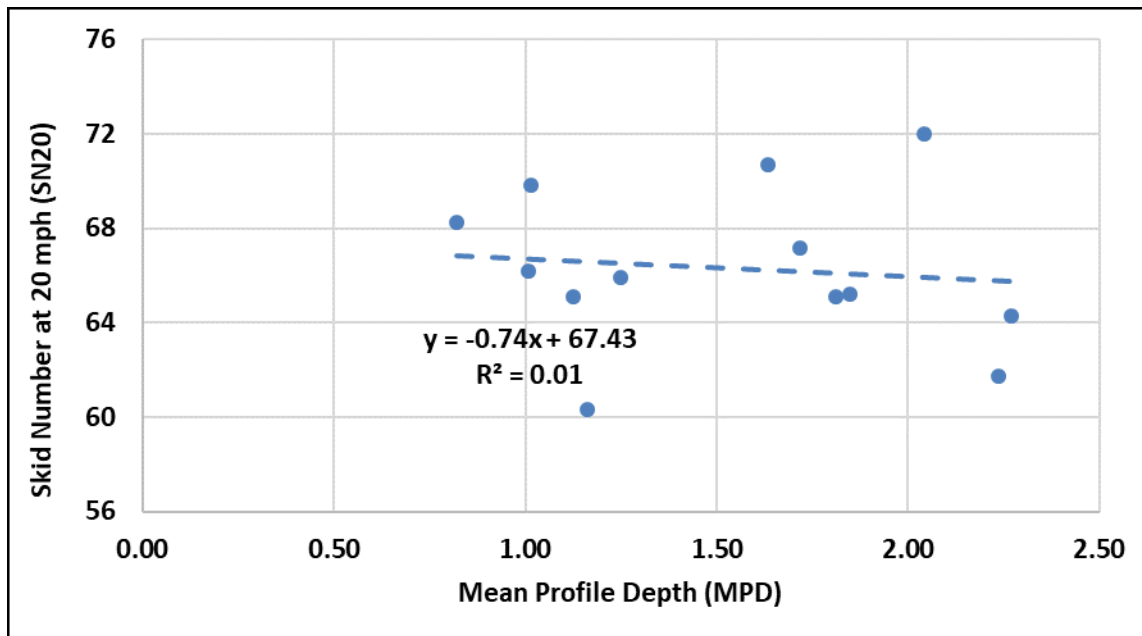


Figure C.6. Relationship between Skid Number at 20 mph (SN20) and Mean Profile Depth

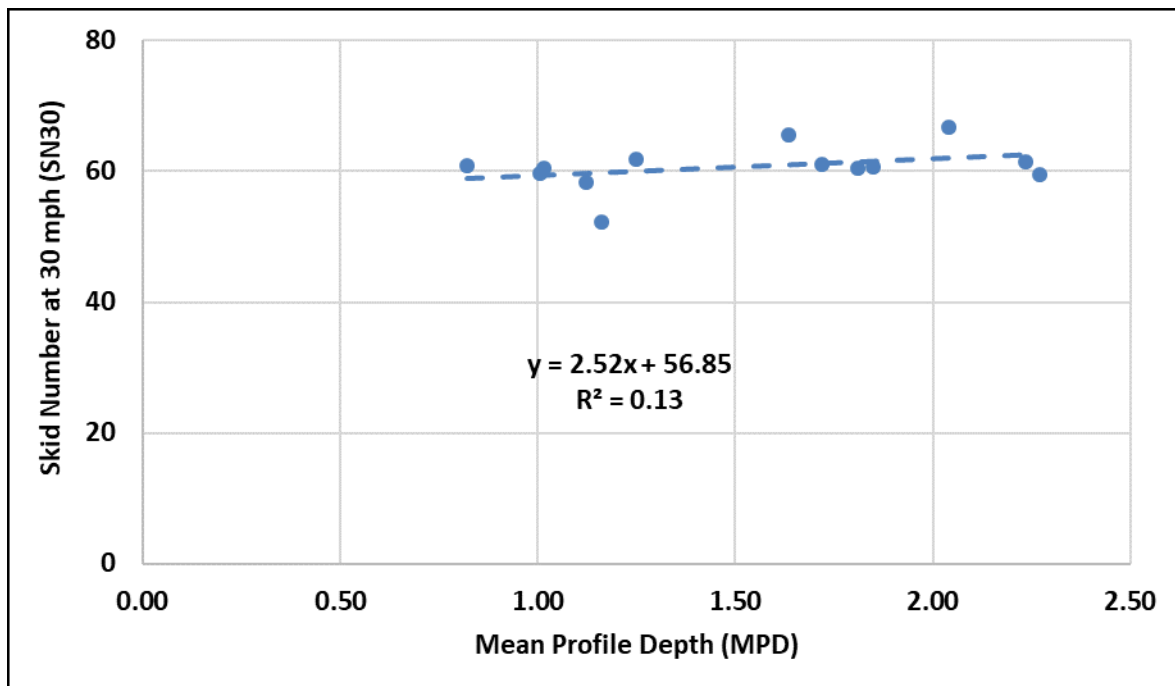


Figure C.7. Relationship between Skid Number at 30 mph (SN30) and Mean Profile Depth

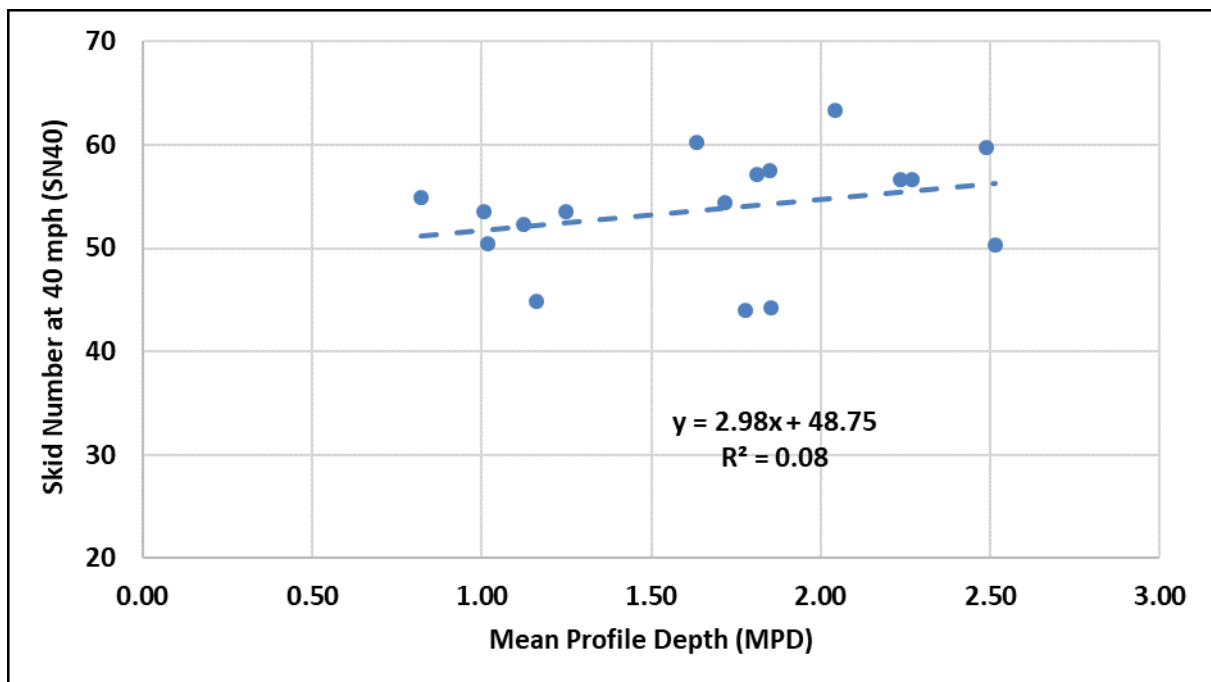


Figure C.8. Relationship between Skid Number at 40 mph (SN40) and Mean Profile Depth

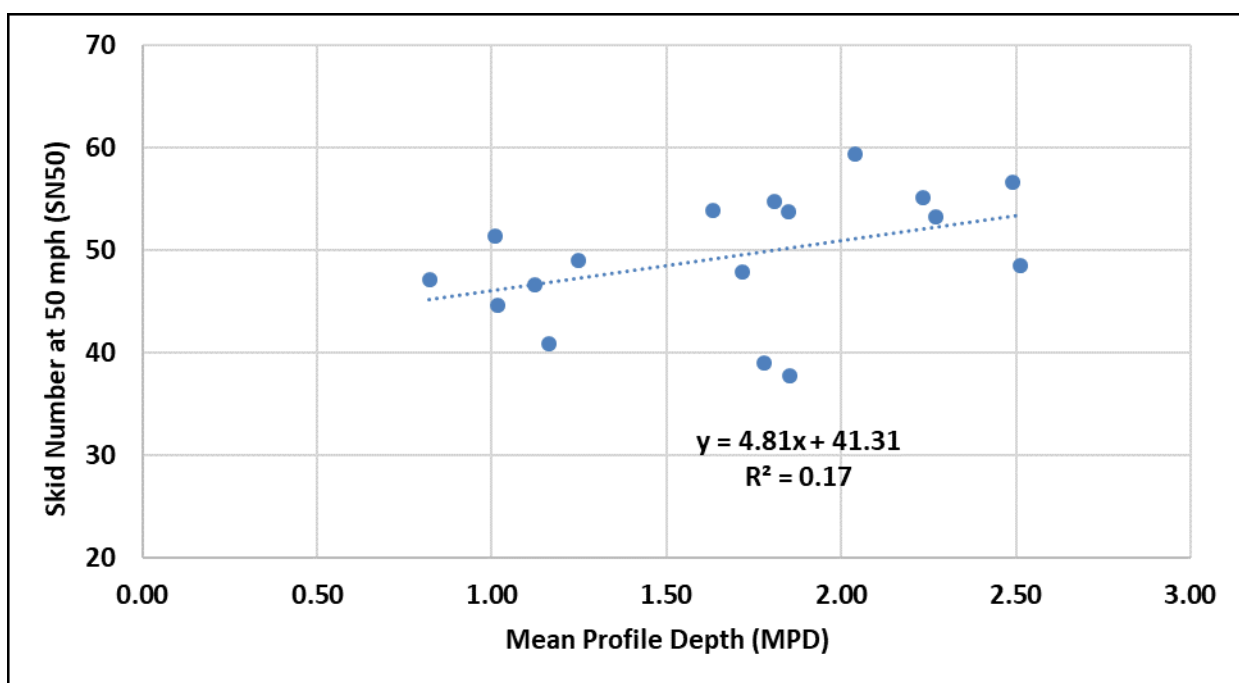


Figure C.9. Relationship between Skid Number at 50 mph (SN50) and Mean Profile Depth

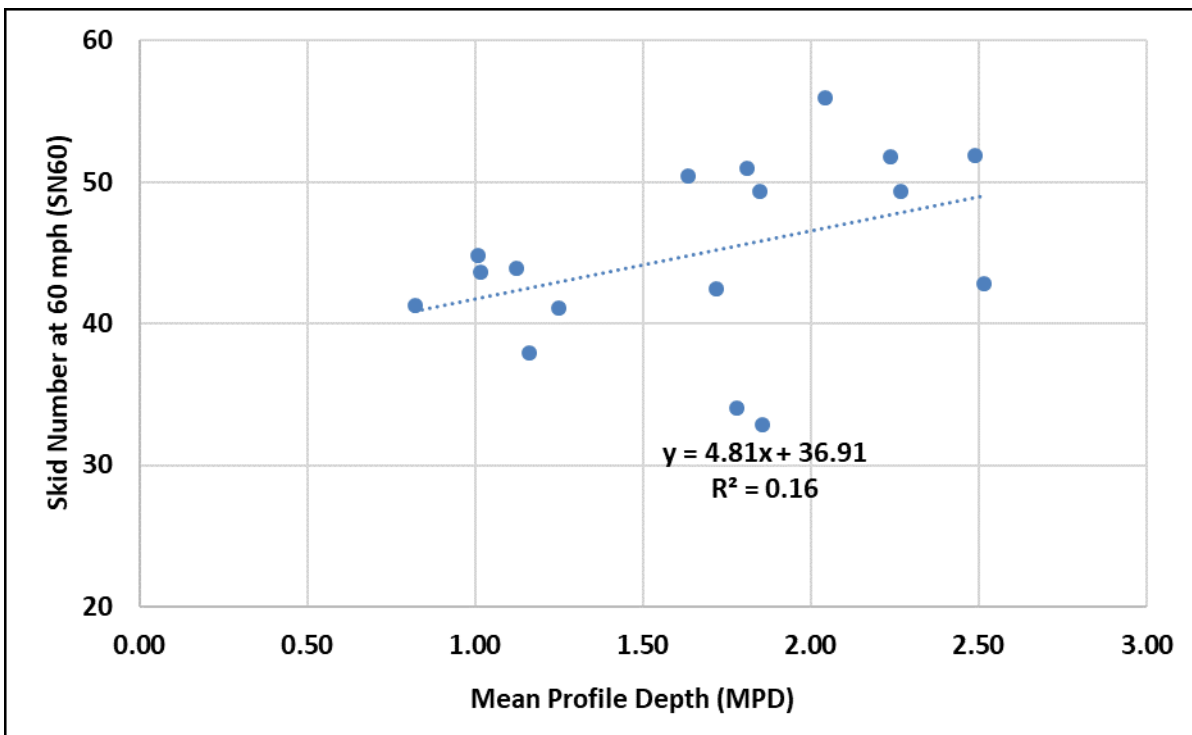


Figure C.10. Relationship between Skid Number at 60 Mph (SN60) and Mean Profile Depth

## Appendix D

### Relation Between Skid Number (SN) And $DFT_{20}$

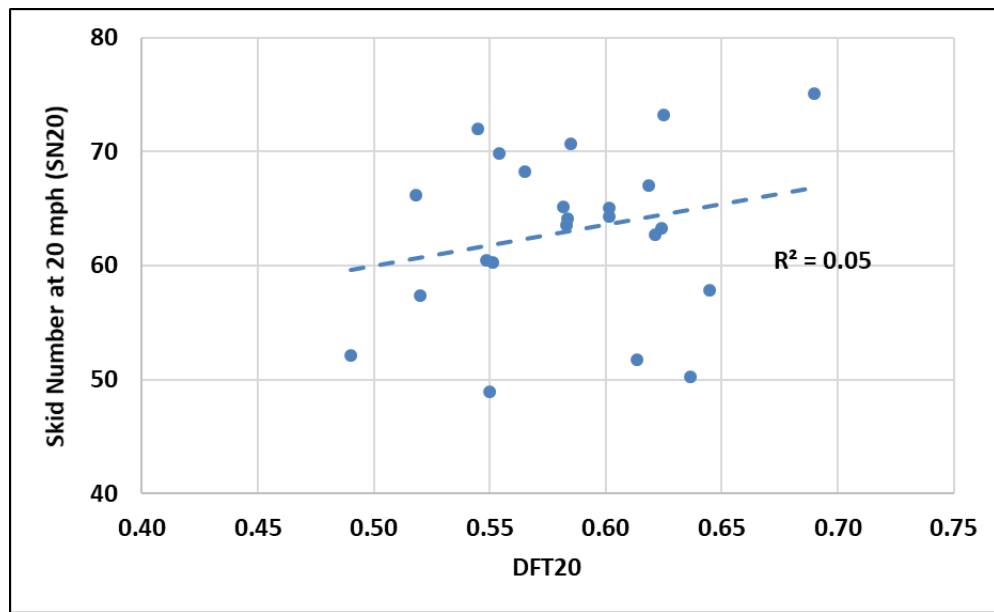


Figure D.1. Relationship between Skid Number at 20 mph (SN20) and  $DFT_{20}$

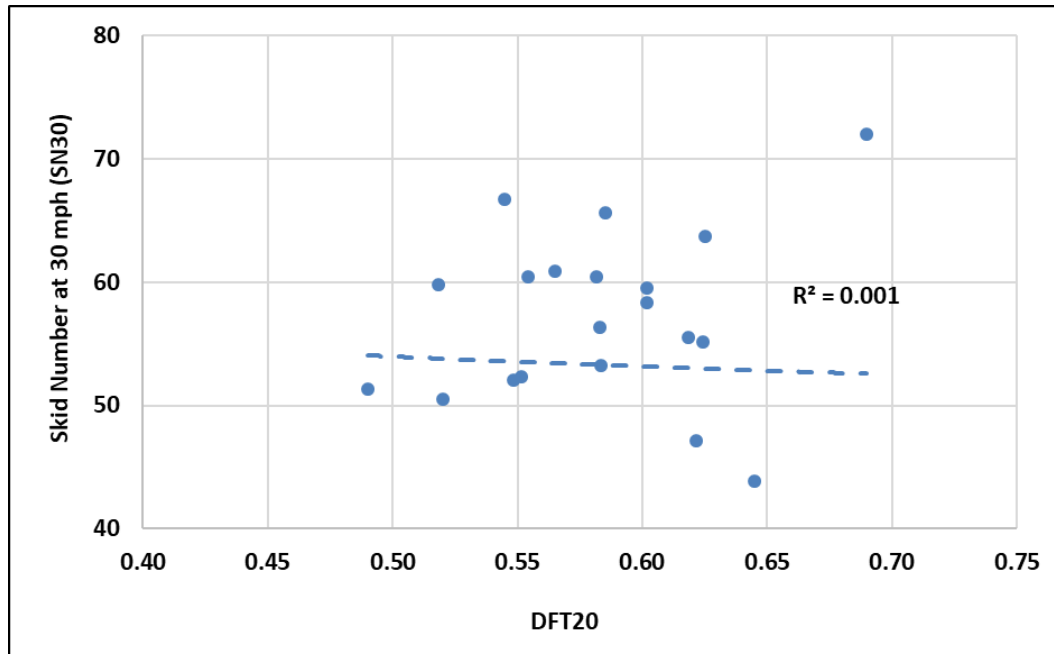


Figure D.2. Relationship between Skid Number at 30 mph (SN30) and  $DFT_{20}$

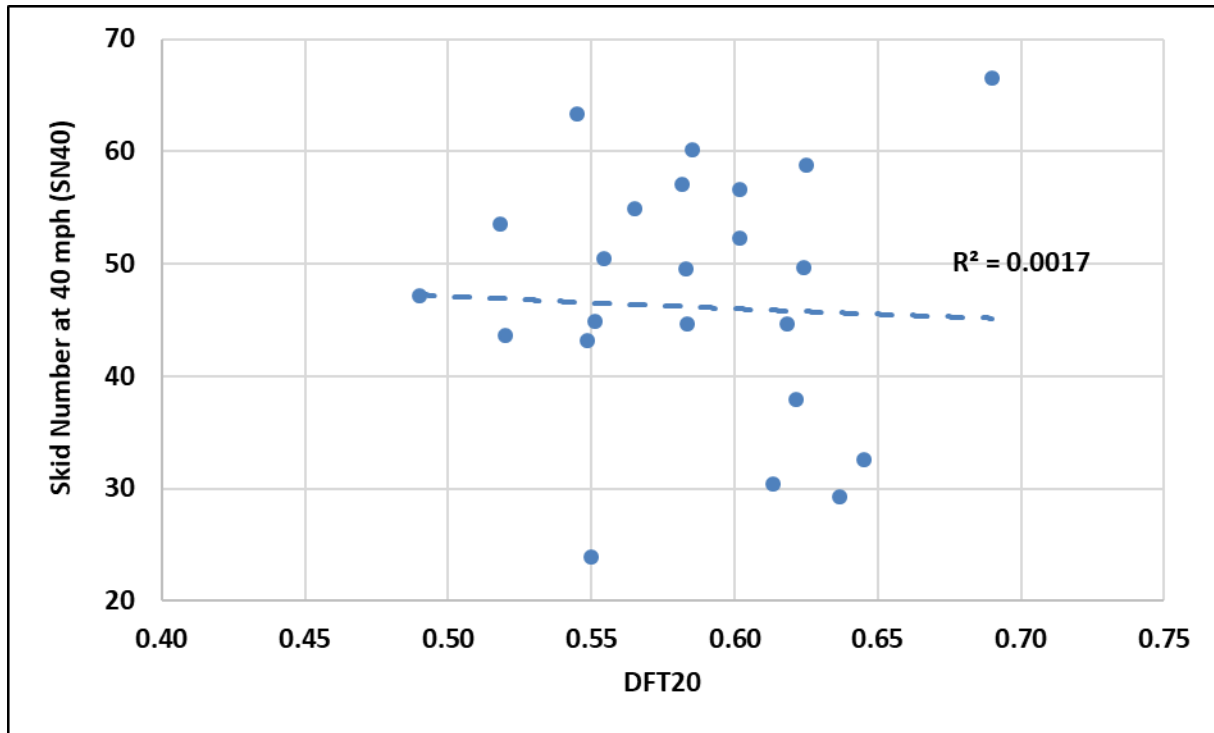


Figure D.3. Relationship between Skid Number at 40 mph (SN40) and DFT<sub>20</sub>

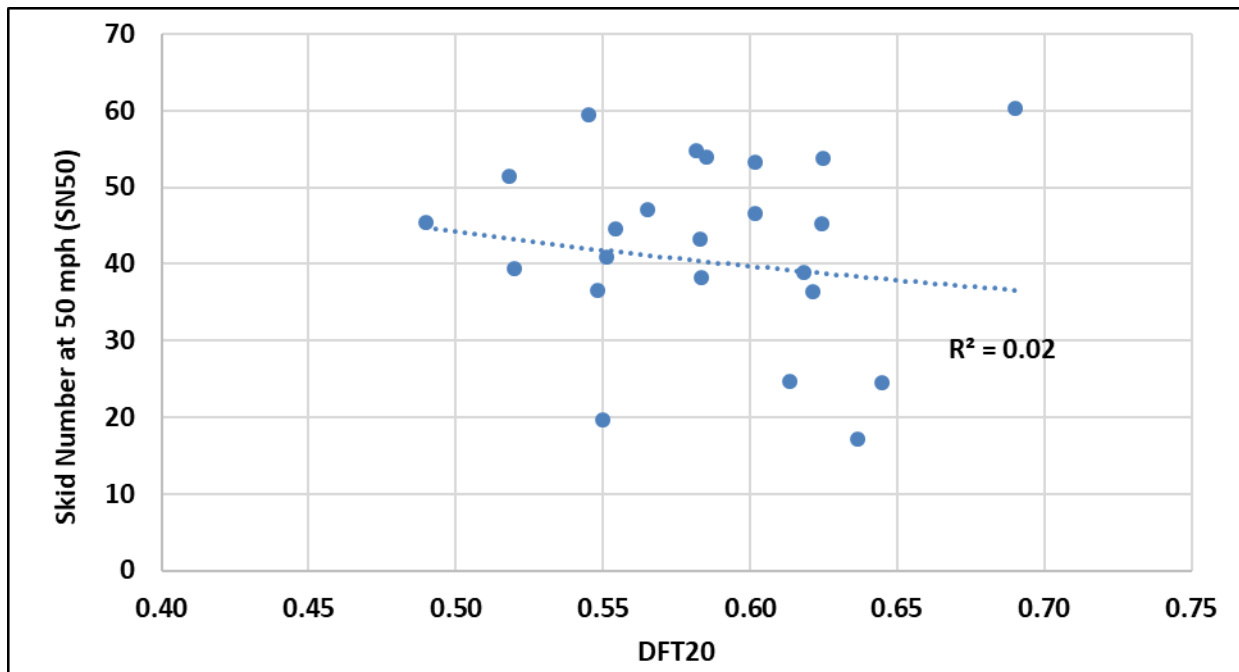


Figure D.4. Relationship between Skid Number at 50 mph (SN50) And DFT<sub>20</sub>

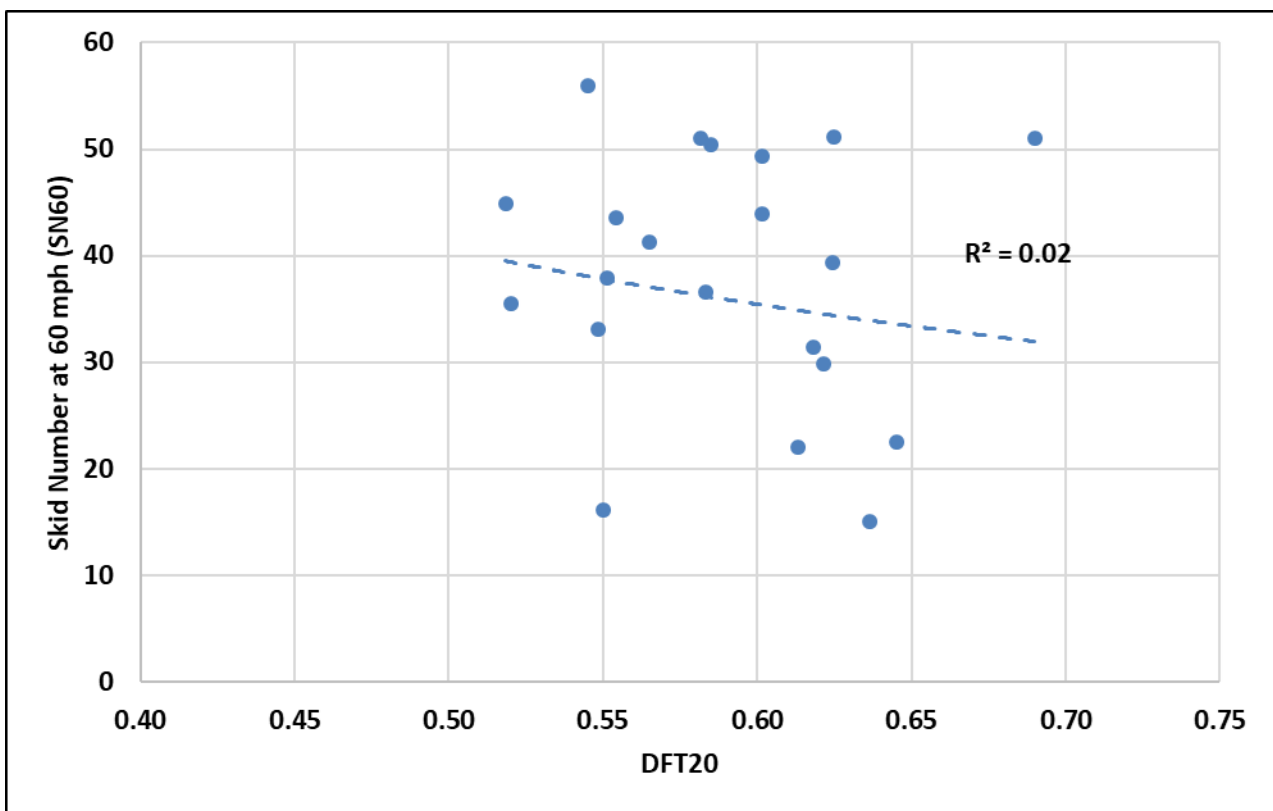


Figure D.5. Relationship between Skid Number at 60 mph (SN60) and  $DFT_{20}$



## Appendix E

### Skid Software Examples

#### Single Test Site Mode

##### 1. Step 1

This is the interface of the software. The user has two options to either select Single Test Site option or Multiple Test Site option. Figure F.1 highlights the selection of “Single Test Site” option. The “Clear” command button resets the selection and allows the user to make another selection. The “Close” command button is used to close the application.

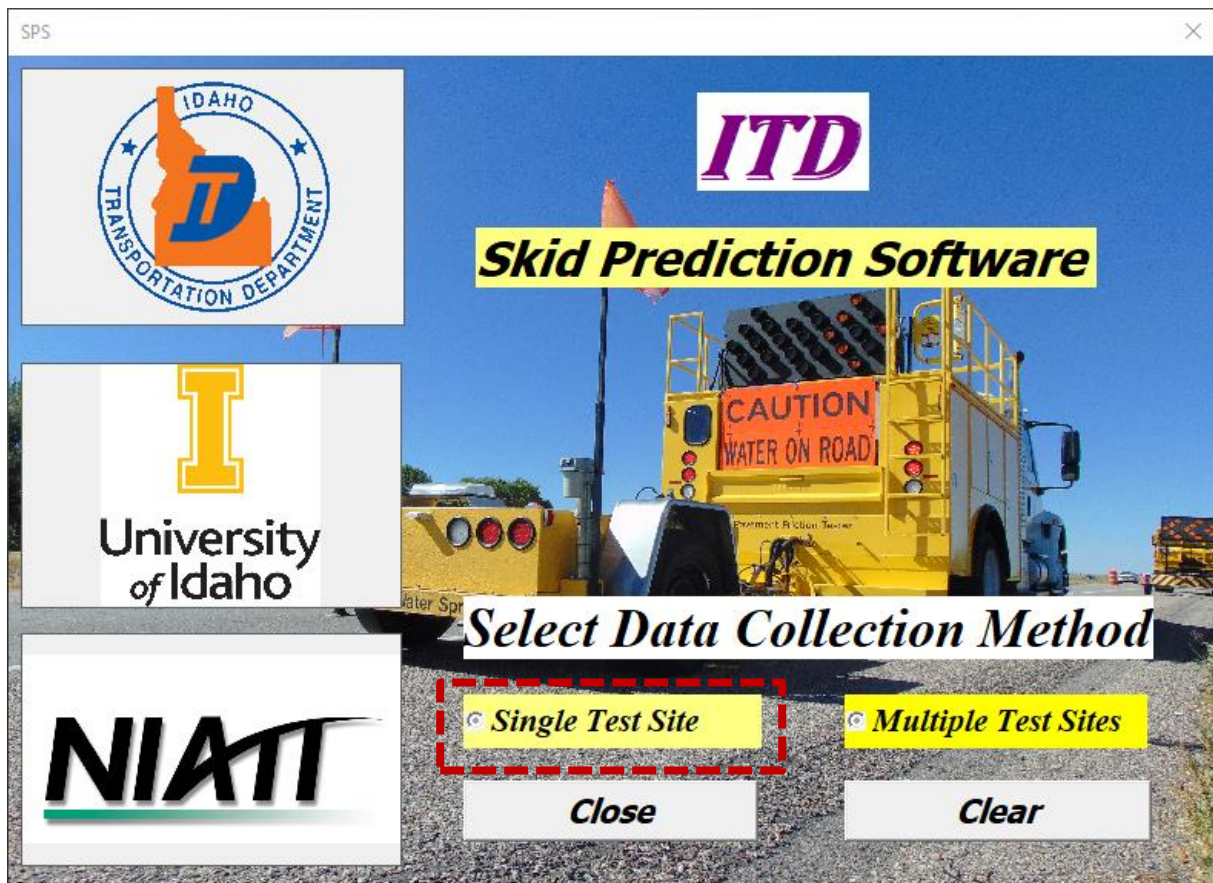


Figure F.1. “Single Test Site” Mode

## 2. Step 2

After the “**Single Test Site**” is selected, the interface in Figure F.2 can be used by the user to perform all steps for skid number prediction in the Single Test Site mode. First, the user needs to import the skid data collected using the skid trailer by selecting the “**Browse Skid Data**” command button. This button allows the user to browse the files and select the appropriate skid data file.

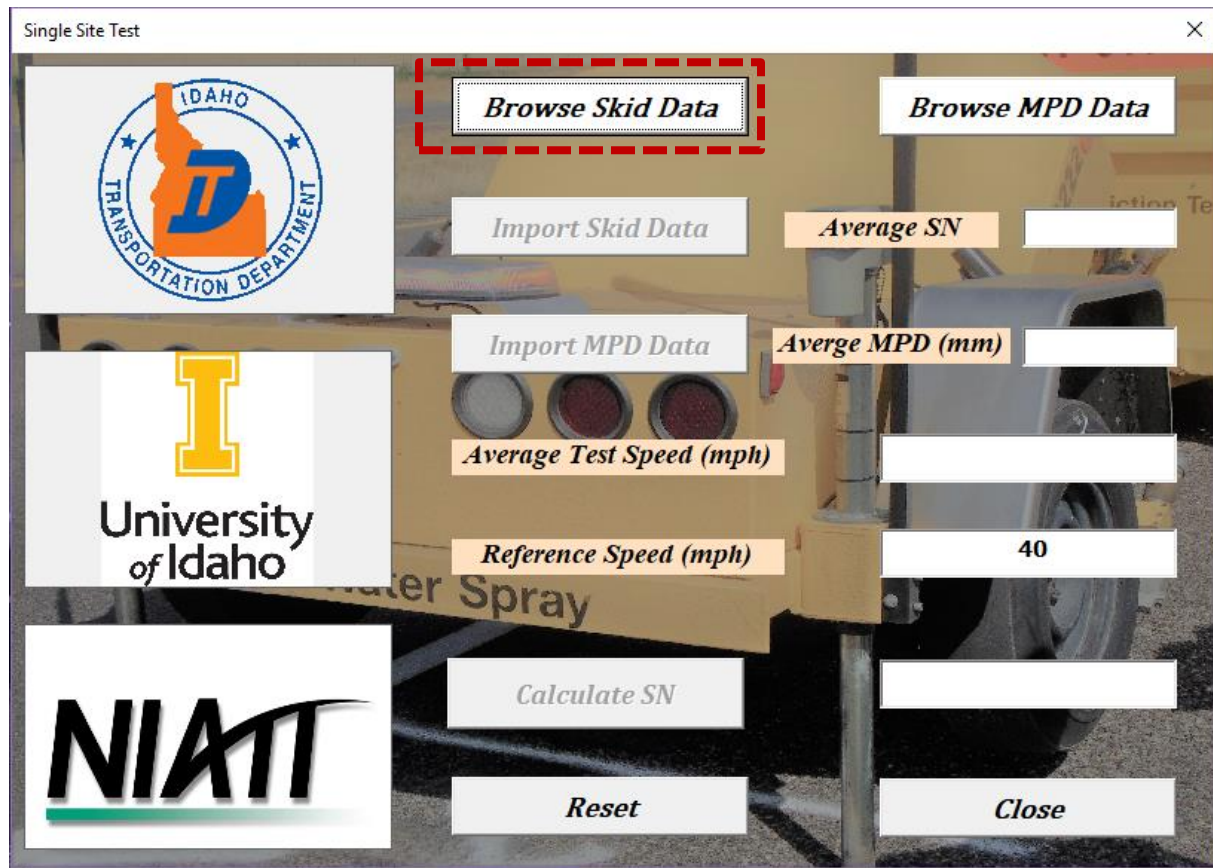


Figure F.2. Browsing Skid Data

### 3. Step 3

After the user selects the “**Browse Skid Data**” command button in Step 2, a dialog box (Figure F.3) opens to allow the user to locate and select the skid data files. After the user makes the selection, the user needs to click the “**Open**” button highlighted in red in Figure F.3 to complete the selection of the skid data.

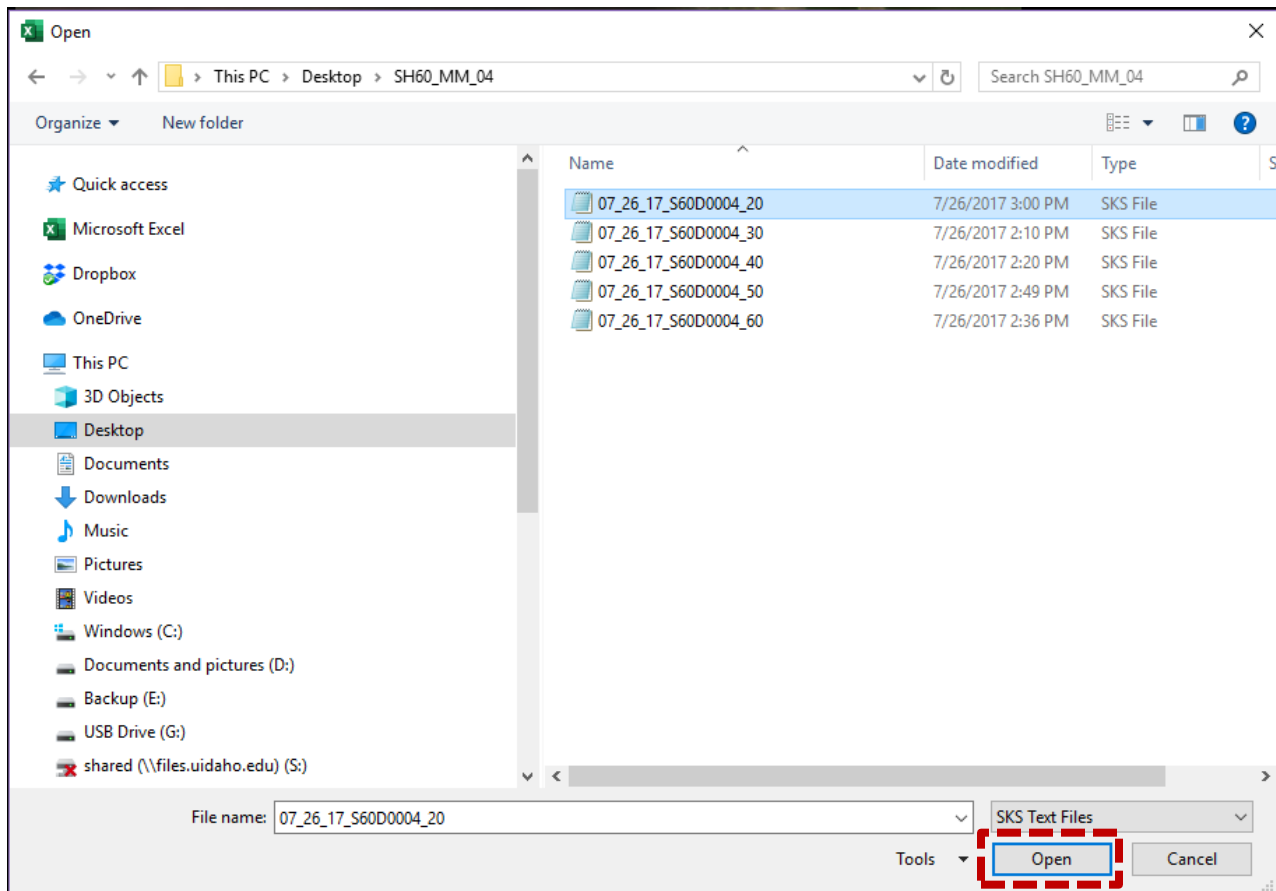


Figure F.3. Selecting Skid Data File

4. Step 4

The user needs to click the “**Browse MPD Data**” command button to select the MPD data. The “**Browse MPD Data**” command button is highlighted in red in Figure F.4. This button allows the user to locate and select the texture data files recorded by the laser sensor installed on the skid truck.

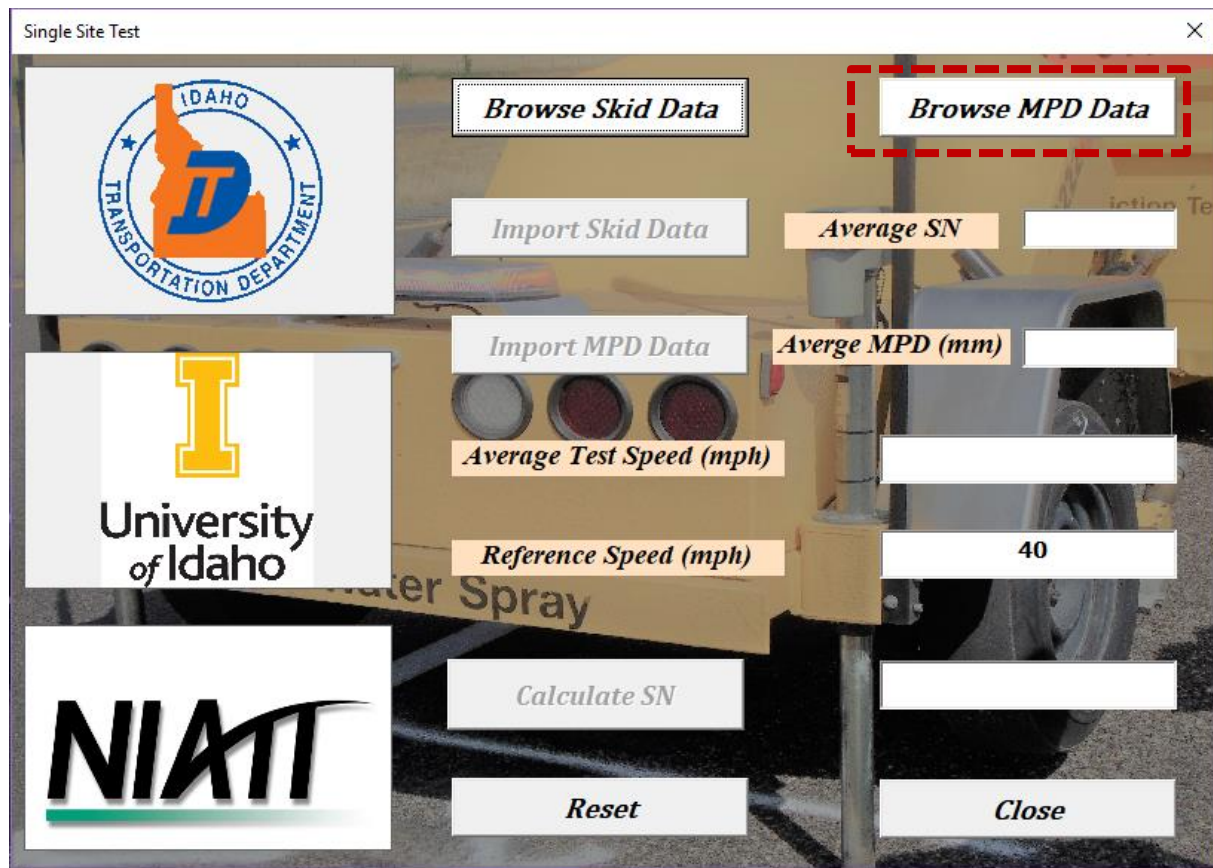


Figure F.4. Browsing MPD Data

## 5. Step 5

After the user selects the “**Browse MPD Data**” command button in Step 4, a dialog box (Figure F.5) opens to enable the user to locate and select the skid data files. After the user makes the selection, the user needs to click the “**Open**” button highlighted in red in Figure F.4 to complete the selection of the texture data. The user can select the desired MPD data file from the list of available skid data files.

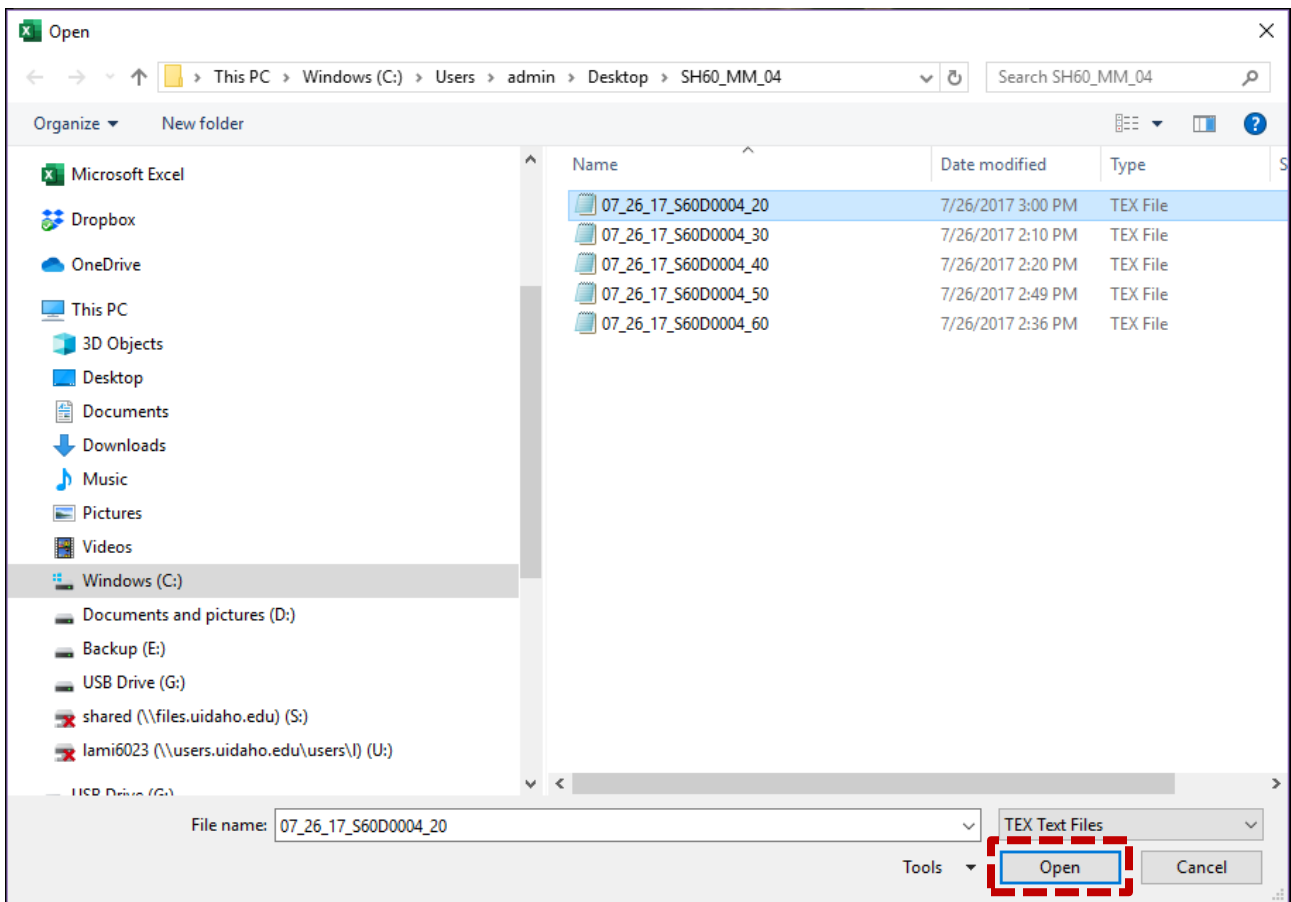


Figure F.5. Selecting MPD Data File

6. Step 6

Once the selection of skid and texture data is completed, both command buttons; “**Browse Skid Data**” and “**Browse MPD Data**”, are highlighted in green as shown in Figure F.6.

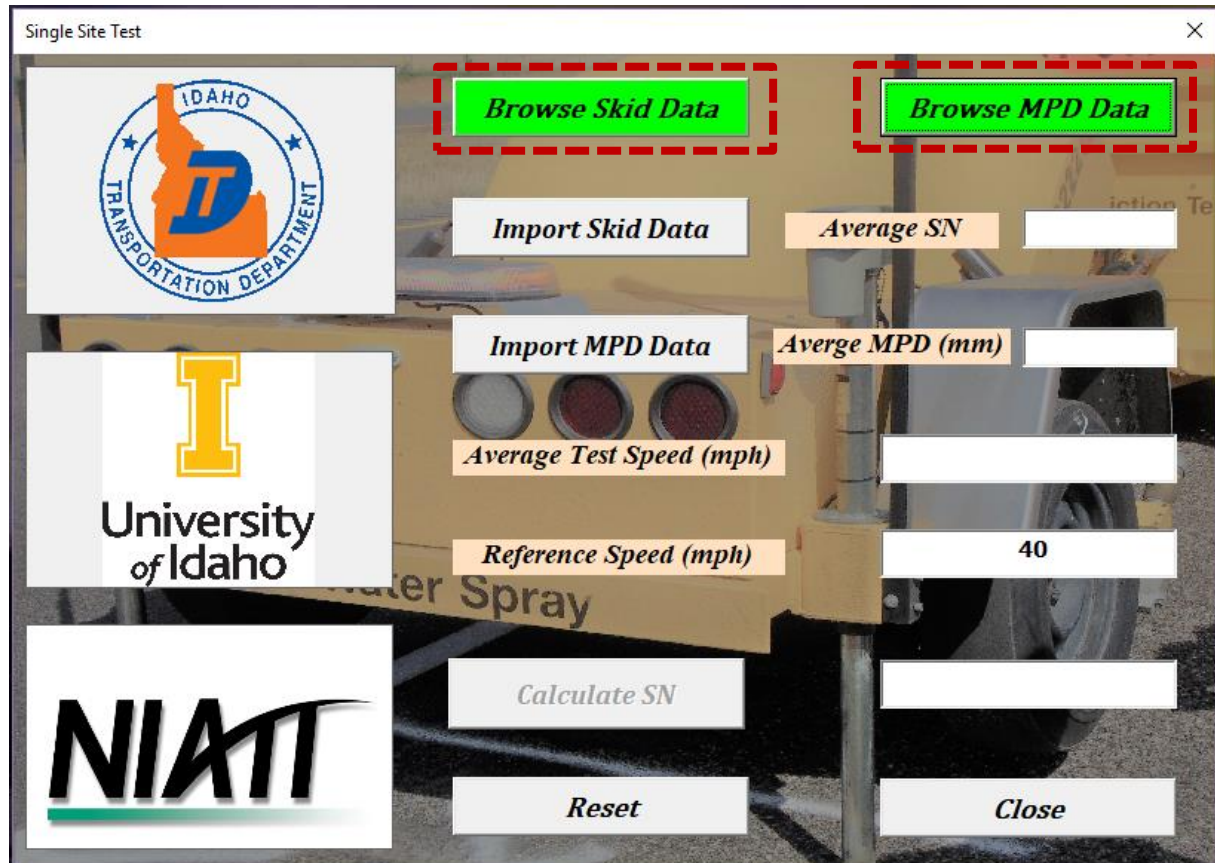


Figure F.6. Completing Skid and Texture Data Selection

## 7. Step 7

After the user selects the skid data file, the user needs to import the data to the software by selecting “Import Skid Data” command button. The average value of the uploaded skid data for the Single Site Test is calculated and reported as shown in Figure F.7.

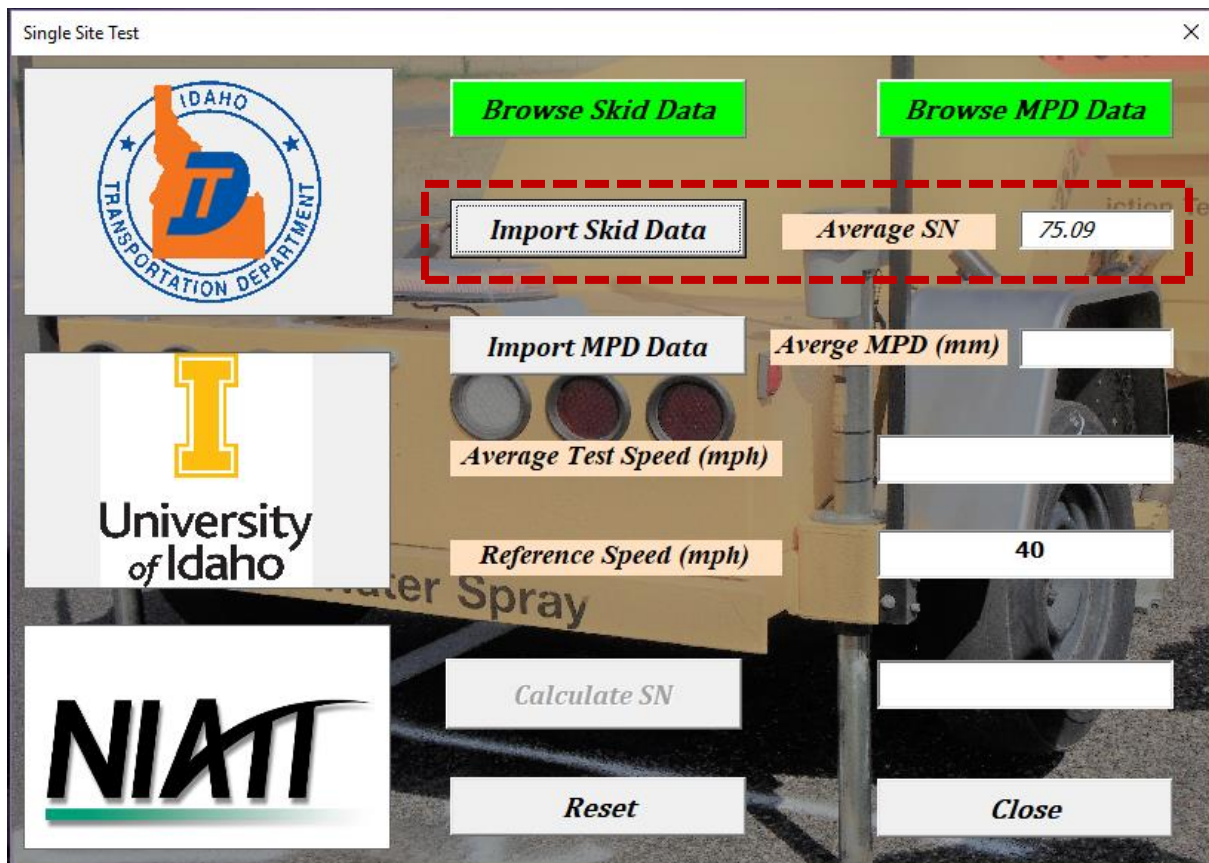


Figure F.7. Importing Skid Data to the software

## 8. Step 8

Similar to the skid data, after the user selects the texture data file, the user needs to import the data to the software by selecting “**Import MPD Data**” command button. The average value of the uploaded MPD data for the Single Site Test is calculated and reported as shown in Figure F.8. Upon importing the MPD data, the user is allowed to enter and specify the reference speed. The default value of the reference speed is set at 40 mph but the user can change this value as needed. The current practice at ITD is to measure the skid number at a reference speed of 40 mph.

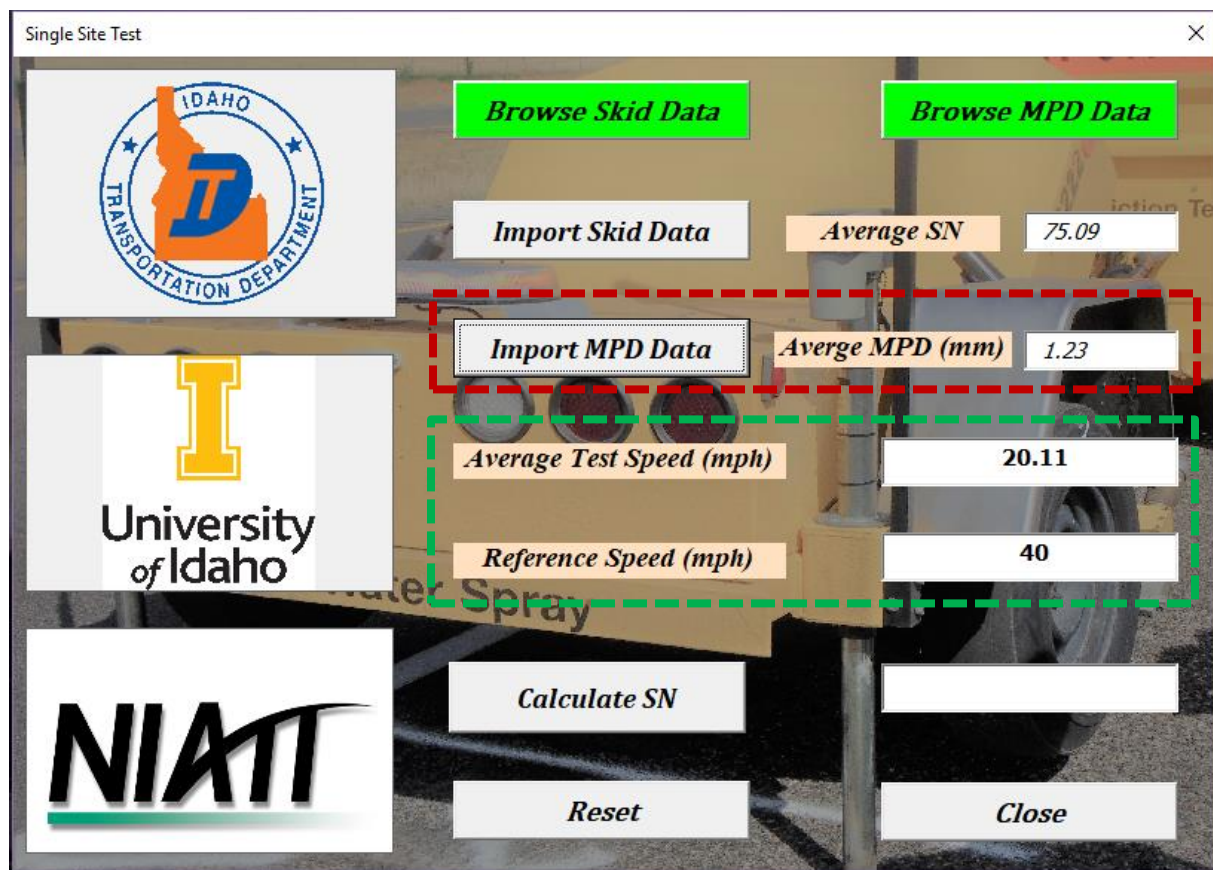


Figure F.8. Importing MPD Data and Specifying the Reference Speed

### 9. Step 9

After the user specifies the reference speed, the “Calculate SN” command button becomes active. The user can select this command to calculate the skid number at the reference desired speed. The calculated skid number is displayed as shown in Figure F.9.

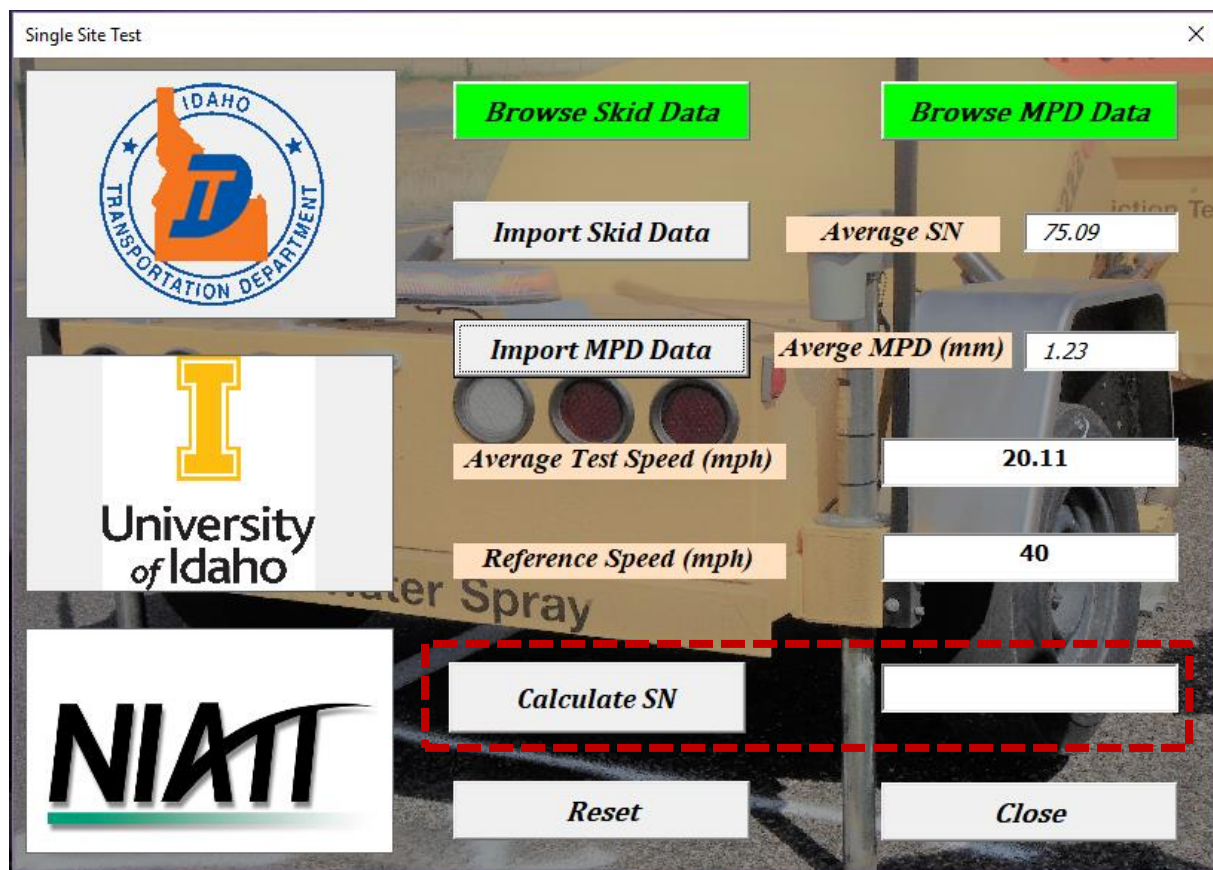


Figure F.9. Calculation of Skid Number at the Reference Speed

10. Step 10

If the user wants to perform additional analyses, the “Reset” command button (Figure F.10) is used to delete all imported skid and texture data. The user needs to repeat the above steps to select new data.

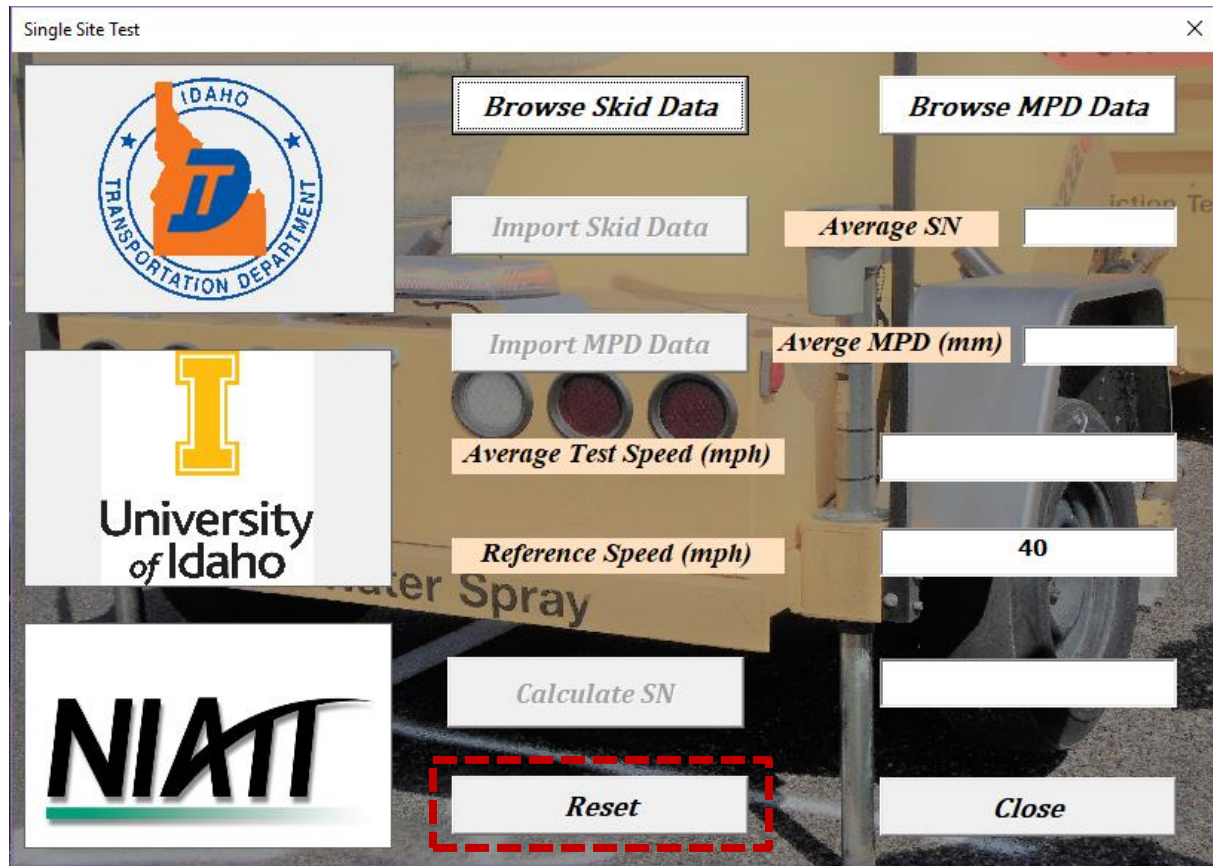


Figure F.10. Resetting the Software to Initial Conditions

## 11. Step 11

The user can return to the main software interface (Figure F.1) by selecting the “Close” command button as shown in Figure F.11. The user can either close the software or run the software again in different modes; Single Test Site or Multiple Test Sites.

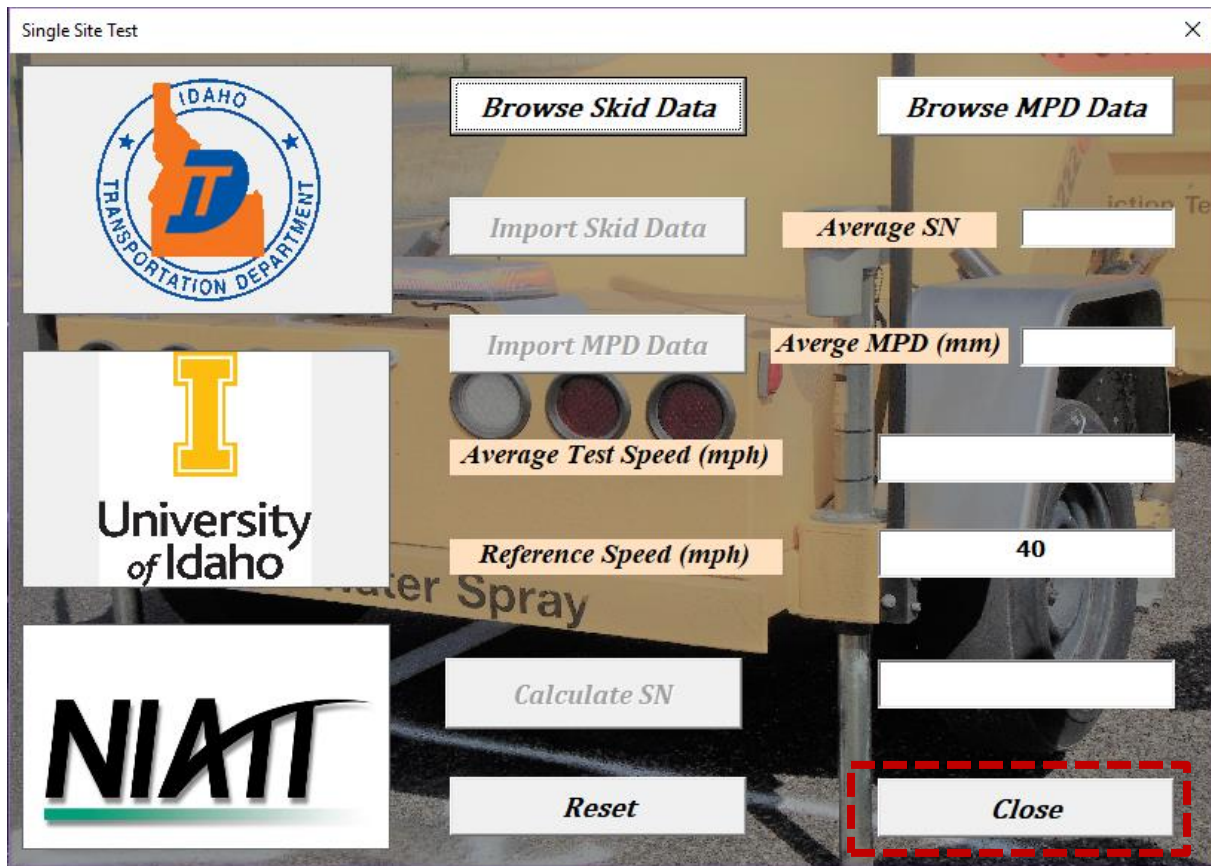


Figure F.11. Closing the Single Test Site Test Mode

## Multiple Test Site Mode

### 1. Step 1

Figure F.12 shows the main interface of the software. The user has two options to either select Single Test Site option or Multiple Test Sites option. Figure F.12 highlights the selection of “**Multiple Test Sites**” option. The “**Clear**” command button resets the selection and allow user to make another selection. The “**Close**” command button is used to close the application.

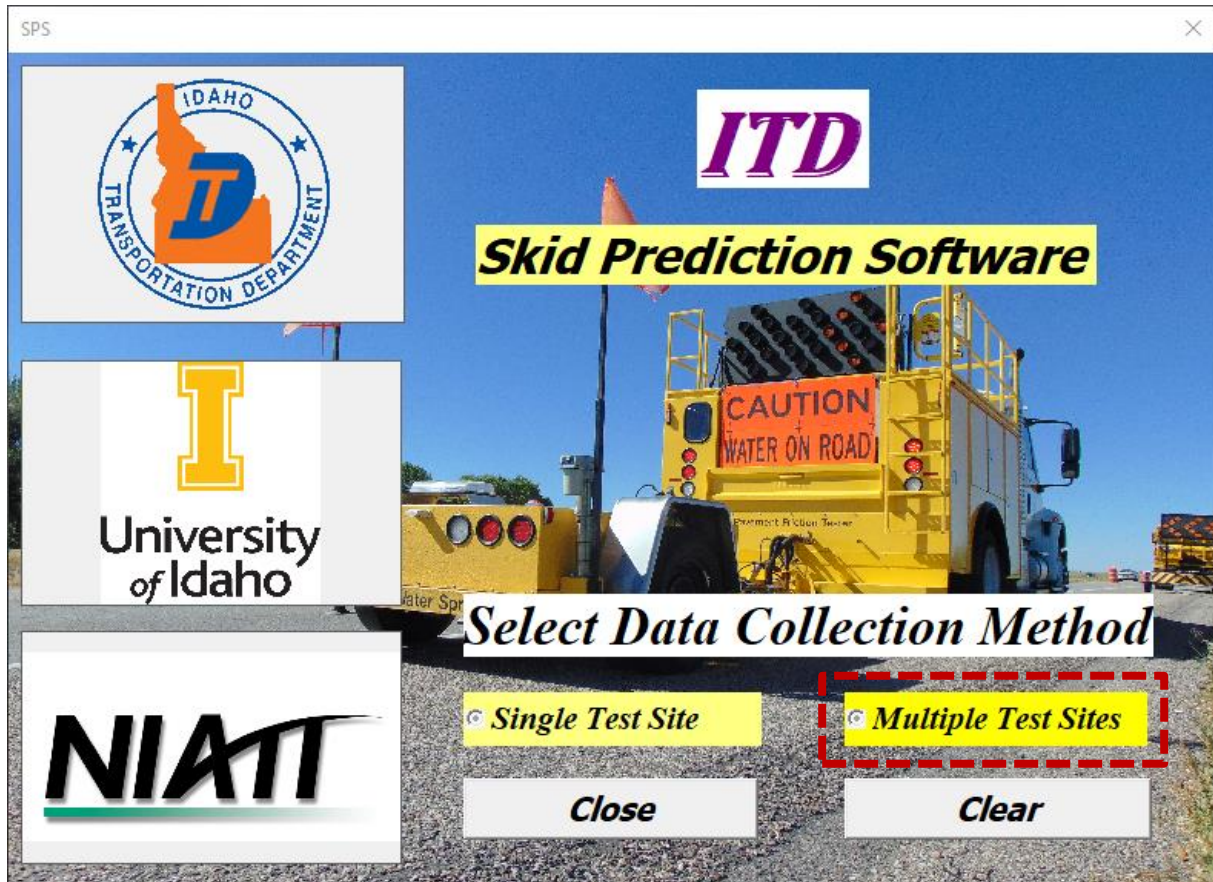


Figure F.12. “Multiple Test Site” Mode

## 2. Step 2

After the “**Multiple Test Sites**” mode is selected, the interface in Figure F.13 can be used by the user to perform all steps for skid number prediction under the Multiple Test Sites mode. First, the user needs to import the skid data collected using the skid trailer by selecting the “**Browse Skid Data**” command button. This button allows the user to browse the files and select appropriate skid data file.

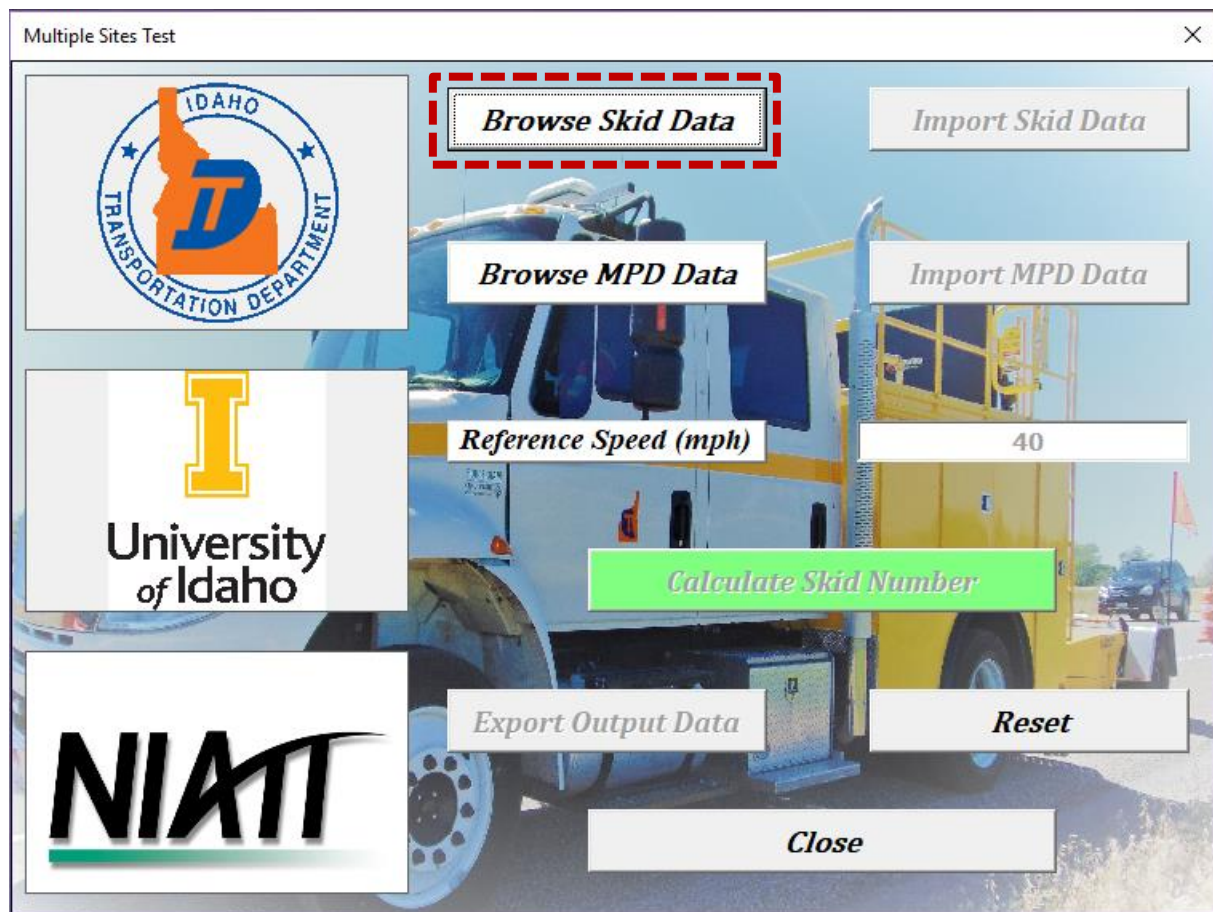


Figure F.13. Browsing Skid Data File

### 3. Step 3

After the user selects the “**Browse Skid Data**” command button in Step 2, a dialog box (Figure F.14) opens to allow the user to locate and select the skid data files. After the user makes the selection, the user needs to click the “**Open**” button highlighted in red in Figure F.14 to complete the selection of the skid data.

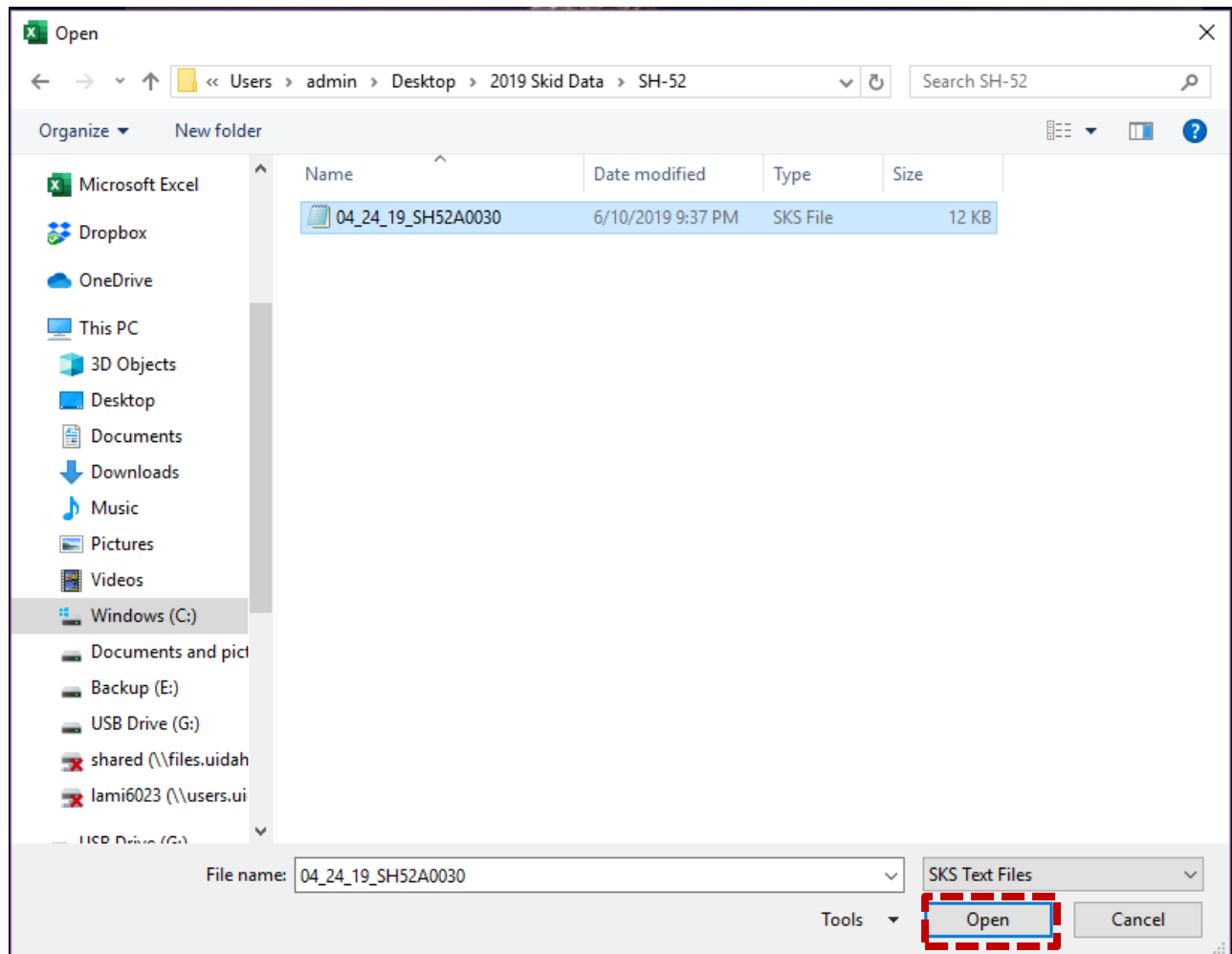


Figure F.14. Selecting Skid Data File

#### 4. Step 4

After the selection of skid data file, the user can import the skid data into the software by selecting the “Import Skid Data” command button. The “Import Skid Data” command button is highlighted in Figure F.15. After importing the skid data, the “Browse Skid Data” button turns into green as shown in Figure F.15.

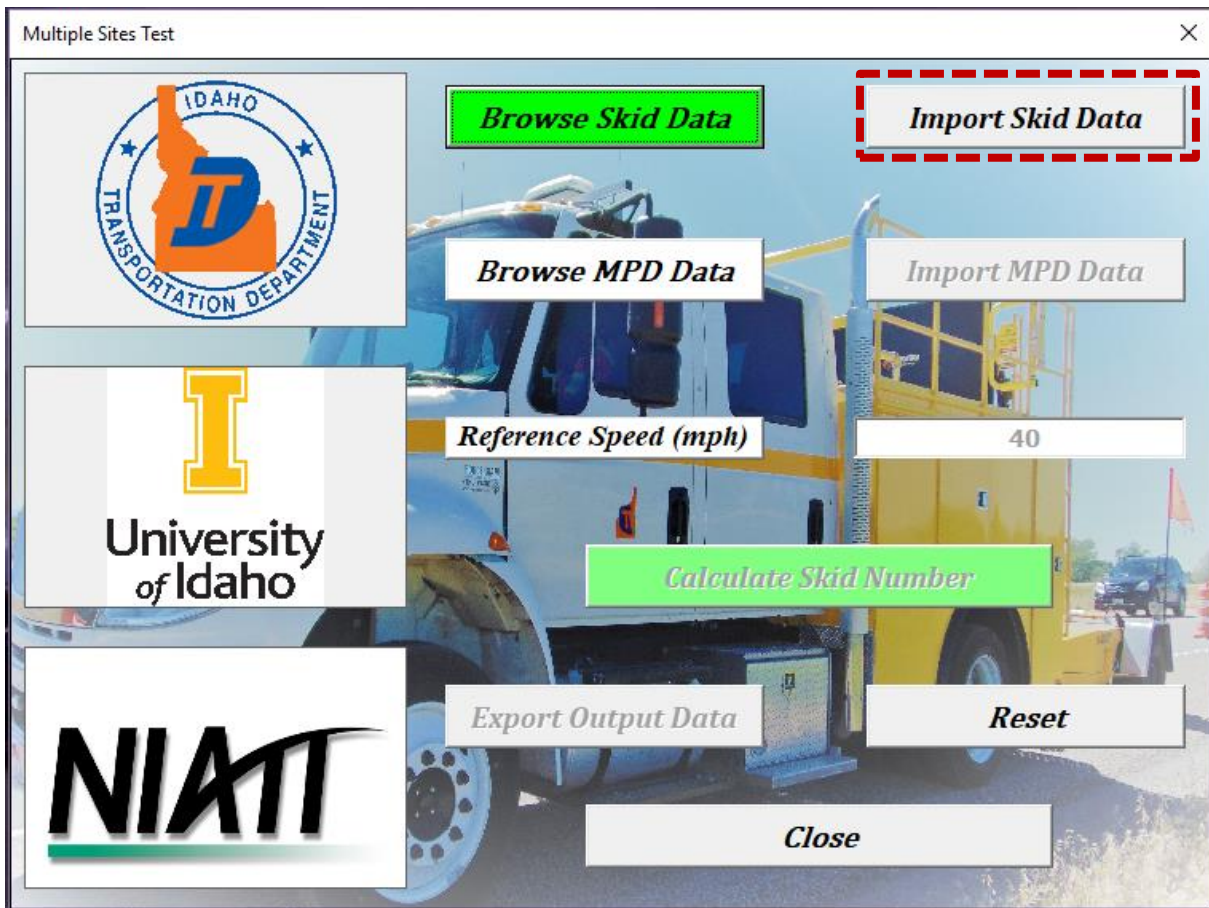


Figure F.15. Importing Skid Data

5. Step 5

The user needs to click the “Browse MPD Data” to select the MPD data. The “Browse MPD Data” command button is highlighted in red in Figure F.16. This button allows the user to locate and select the texture data files recorded by the laser sensor installed on the skid truck.

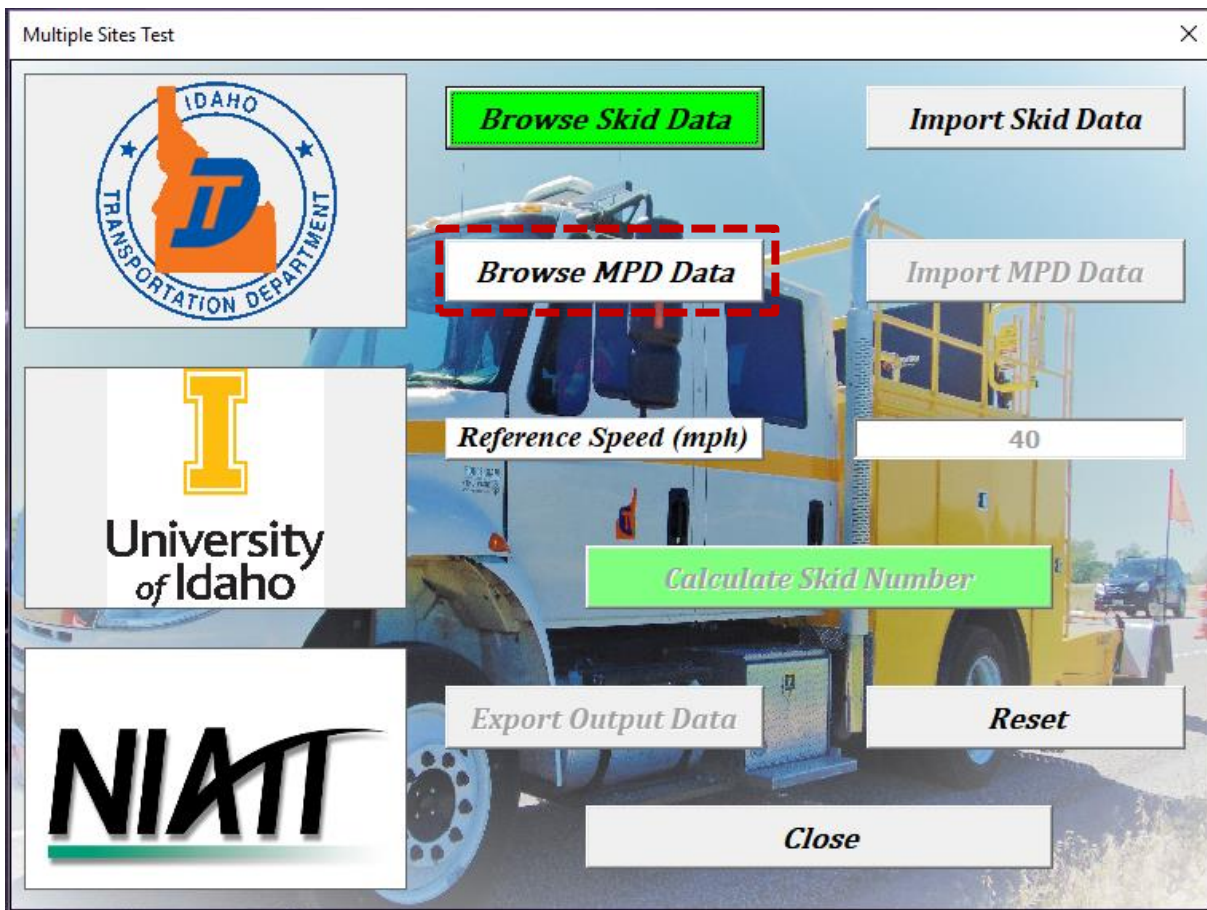


Figure F.16. Selecting the MPD Data File

## 6. Step 6

After the user selects the “**Browse MPD Data**” command button in Step 5, a dialog box (Figure F.17) opens to allow the user to locate and select the MPD data files. After the user makes the selection, the user needs to click the “**Open**” button highlighted in red in Figure F.17 to complete the selection of the MPD data.

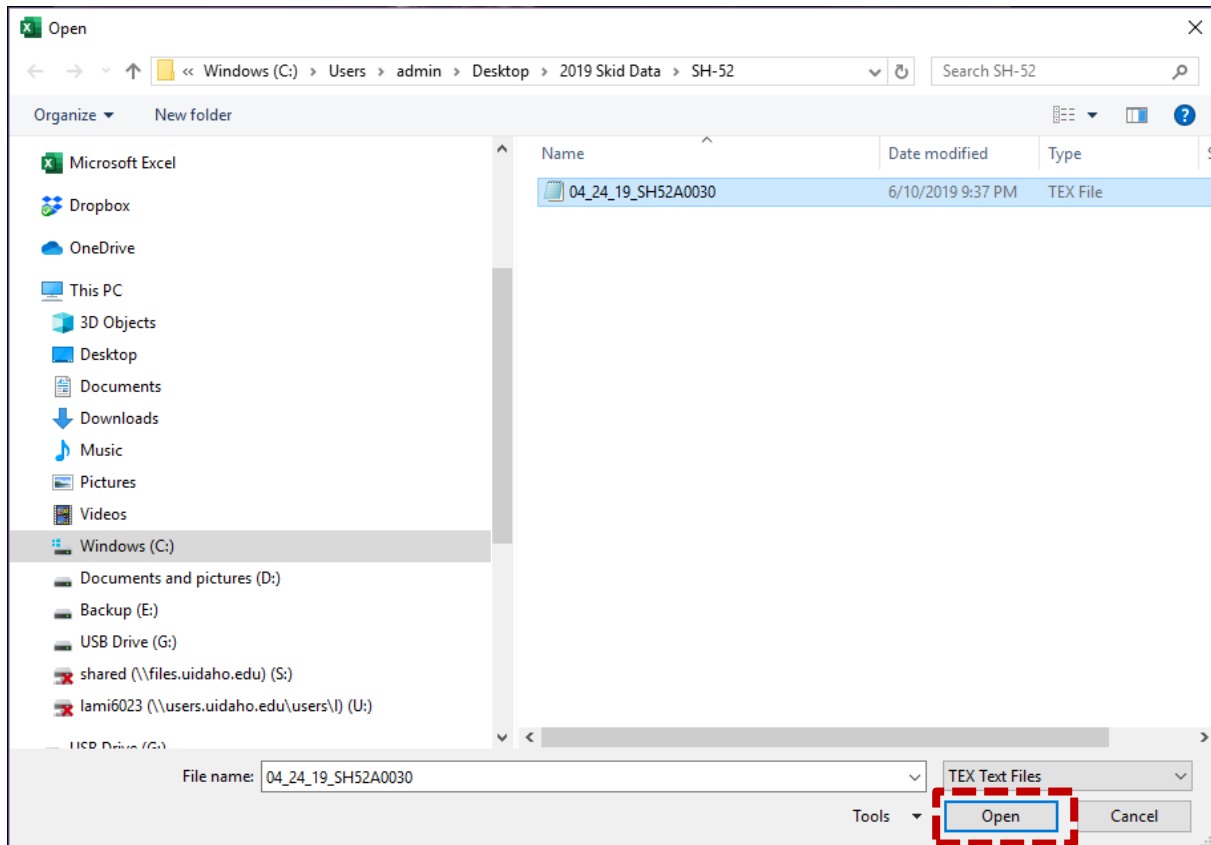
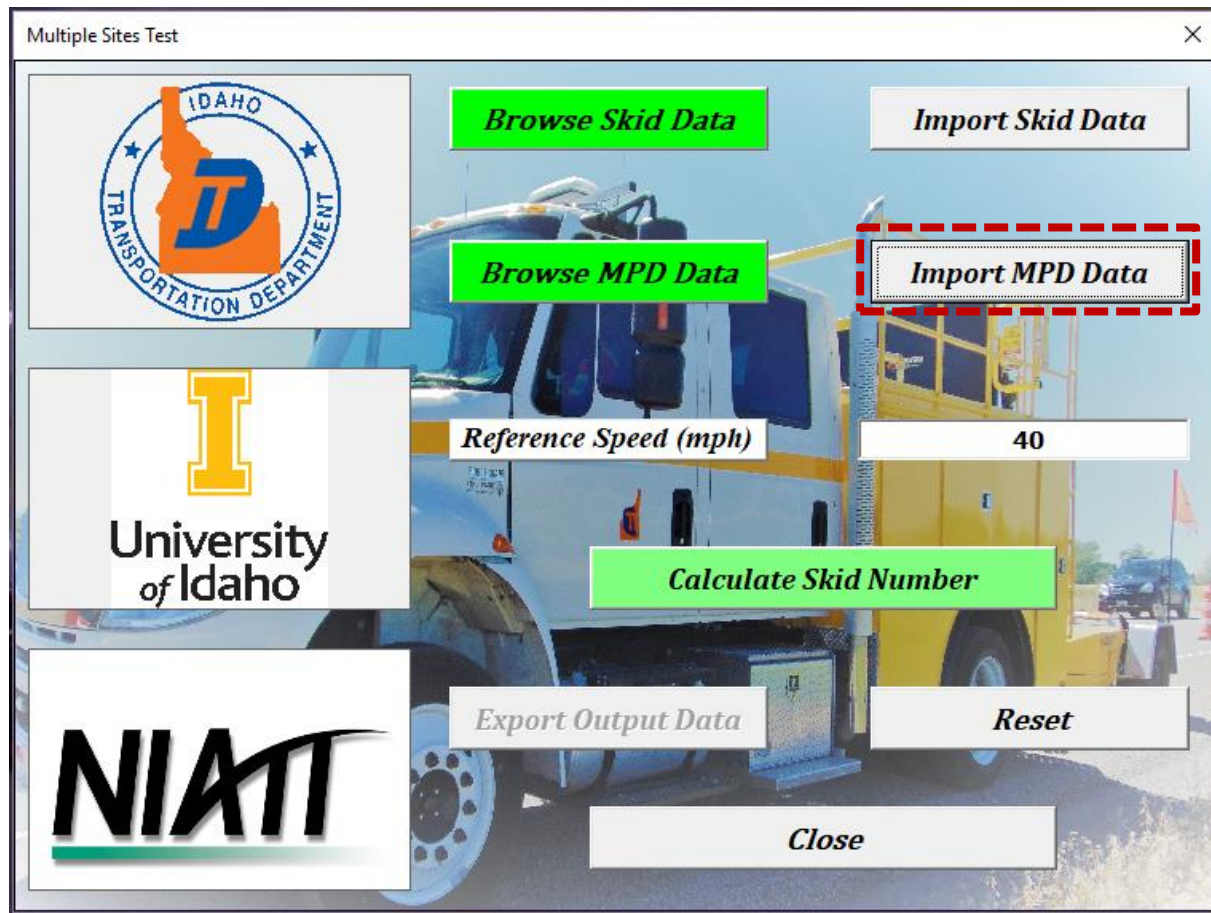


Figure F.17. Selecting the MPD Data File

## 7. Step 7

Similar to the skid data, after the user selects the texture data file, the user needs to import the data to the software by selecting “**Import MPD Data**” command button. After importing the MPD data, the “**Browse MPD Data**” button turns into green as shown in Figure F.18. Upon importing the MPD data, the user is allowed to enter and specify the reference speed. The default value of the reference speed is set at 40 mph but the user can change this value as needed. The current practice at ITD is to measure the skid number at a reference speed of 40 mph.



**Figure F.18. Importing MPD Data**

### 8. Step 8

After the user specifies the reference speed, the “Calculate Skid Number” command button becomes active. After the user specifies the reference speed, the “Calculate Skid Number” command button becomes active (Figure F.19). The user can select this command to calculate the skid number at the reference desired speed. The calculated skid number for various test sections can be exported to an excel sheet using “Export Output Data” command button (Figure F.19).

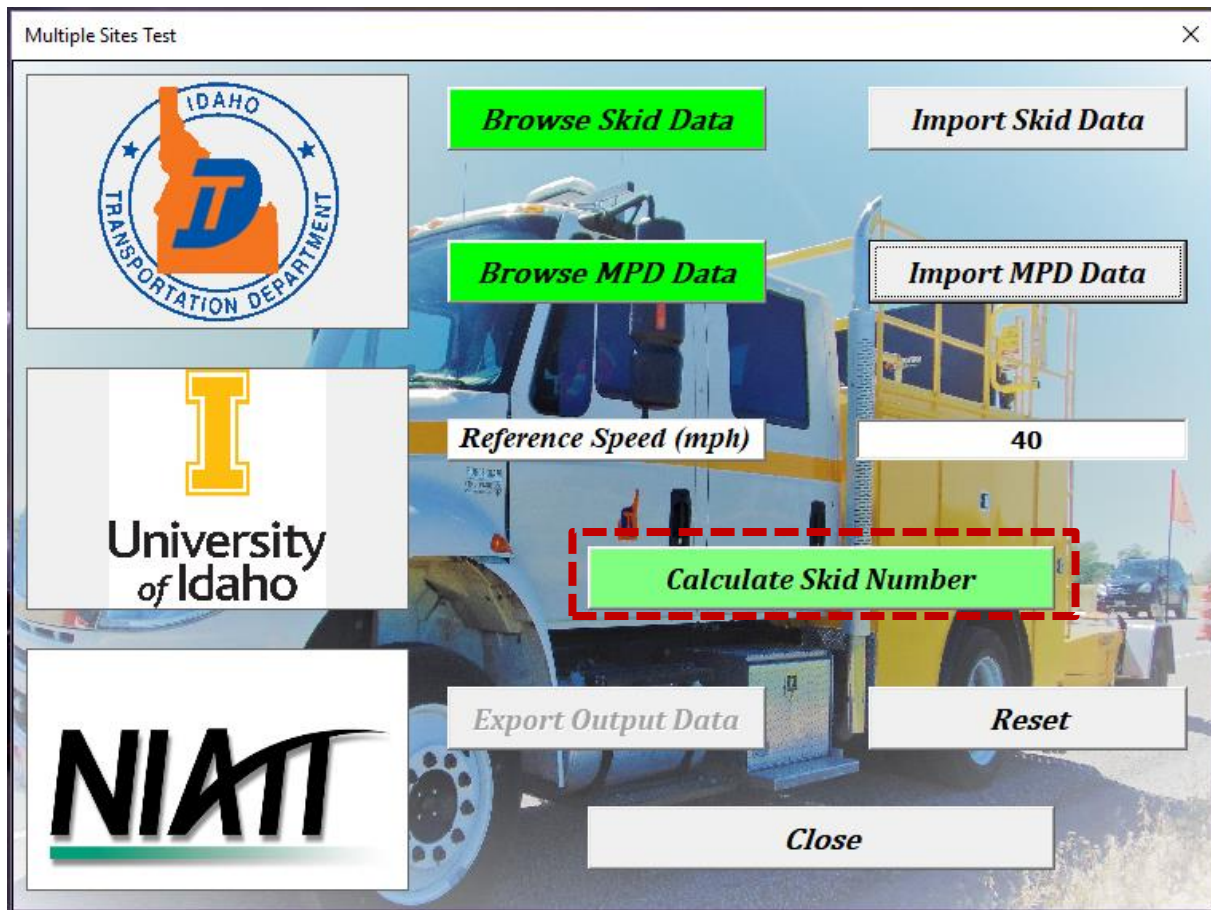
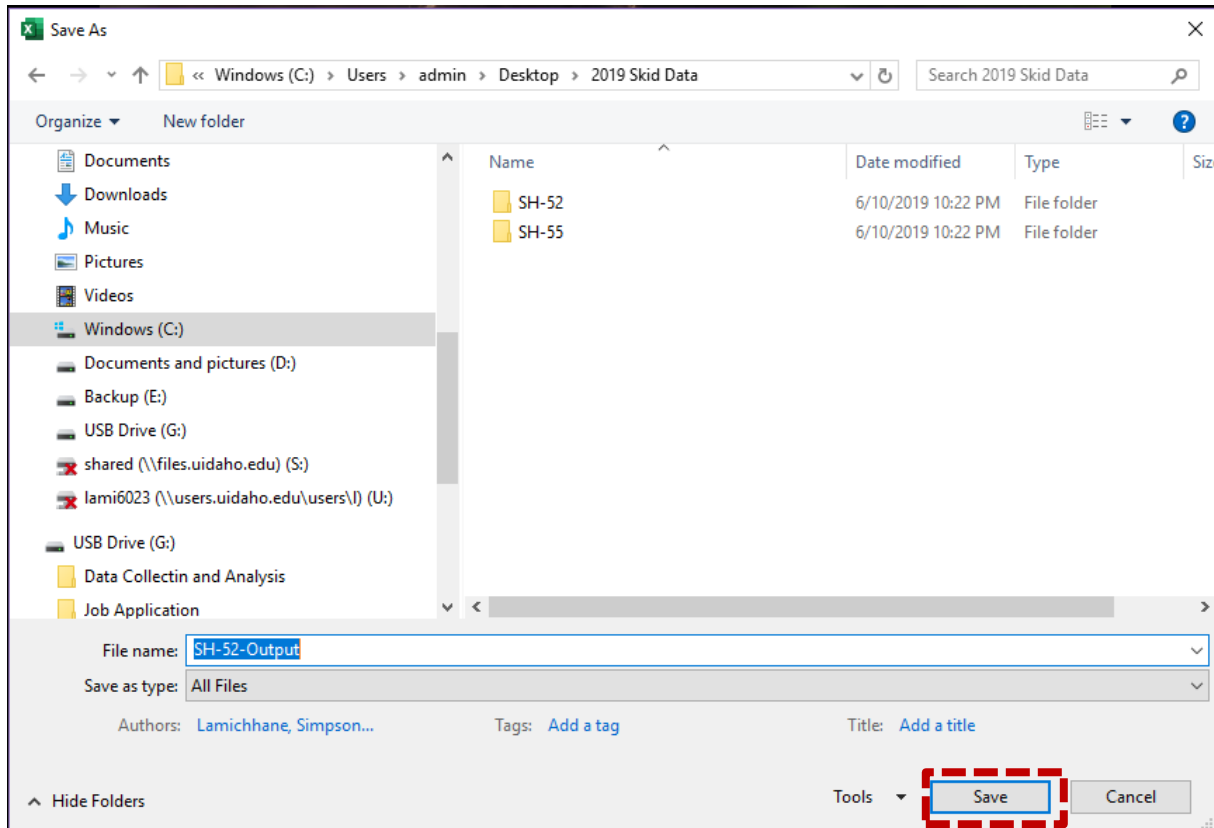


Figure F.19. Skid Number Calculation

## 9. Step 9

After the user selects the “**Export Output Data**” command button (Figure F.19), a dialog box is open to allow the user to save the output file as shown in Figure F.20. After the user selects the location and name for the output file, the user needs to select the “**Save**” button as highlighted in red in Figure F.20.



**Figure F.20. Exporting and Saving the Output Data**

## 10. Step 10

If the user wants to perform additional analyses, the “Reset” command button (Figure F.21) is used to delete all imported skid and texture data. The user needs to repeat the above steps to select new data.

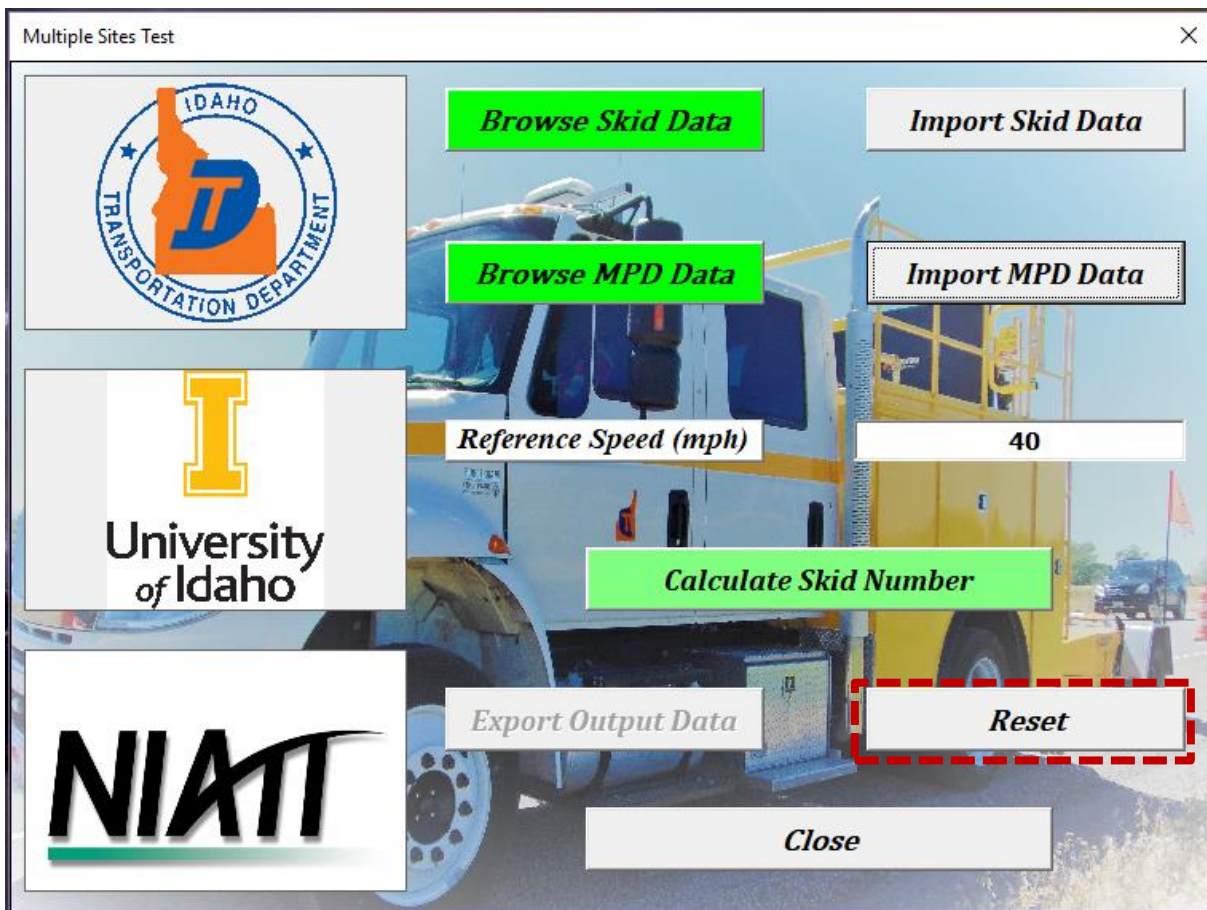


Figure F.21. Resetting the Software to Initial Conditions

11. Step 11

The user can return to the main software interface (Figure F.12) by selecting the “Close” command button as shown in Figure F.22. The user can either close the software or run the software again in different modes; Single Test Site or Multiple Test Sites.

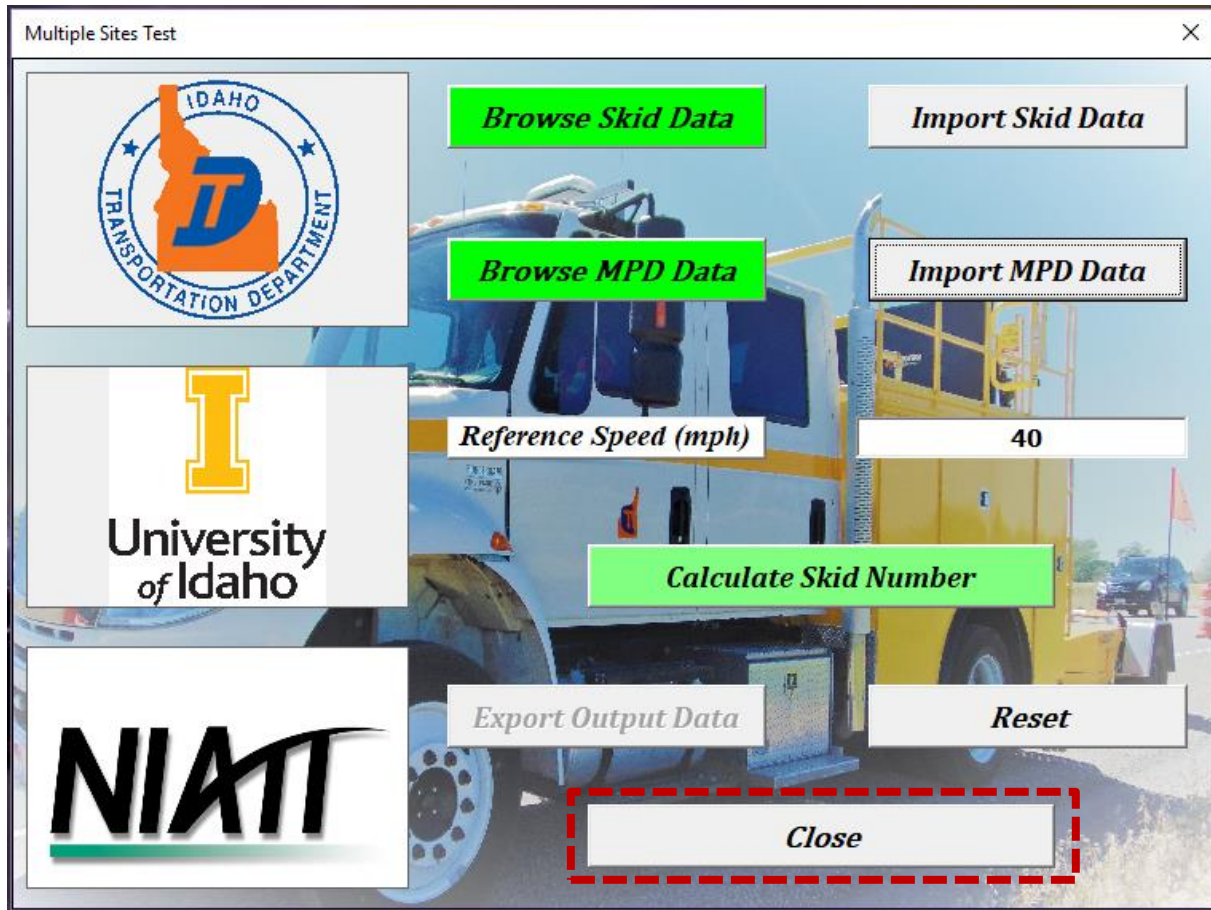


Figure F.22. Closing the Multiple Test Sites Mode